Newsletters on Stratigraphy

Conodonts in Biostratigraphy. A 300-million-years long journey through geologic time

Carlo Corradini[1]*, Charles Henderson[2], James E. Barrick[3] and Annalisa Ferretti[4]

With 14 figures and 3 plates

Abstract. Conodonts are tooth-like elements of a primitive chordate and are generally abundant in many marine sedimentary rocks deposited from the late Cambrian to the latest Triassic. For all this time interval, more than 300 million years, conodonts represent the best tool for biostratigraphic studies. Conodonts are also widely used in paleoecologic, paleogeographic, and geochemical studies, making them the most useful fossil to investigate the Earth's history during the "Conodontozoic". A summary of the present knowledge on conodonts is presented, mainly focused on their stratigraphic applications. Biozonation schemes in use are discussed and the importance of these fossils in chronostratigraphic correlation is stressed.

Key words. Conodonts, Paleozoic, Triassic, biozonation, chronostratigraphy, GSSPs

1. Introduction

Conodonts are one of the major tools for biostratigraphic studies in marine rocks from the late Cambrian to the end-Triassic, through a time interval of almost 300 million years. They are the small phosphatic "tooth-like" parts, called elements (0.5–1.0 mm average size), of an eel-like animal that are commonly preserved in carbonate rocks, but may also occur in marine shale, sandstone and chert. Identifiable elements can persist into low-grade metamorphic rocks as high as chlorite-grade green-schist facies (Rejebian et al. 1987).

For a long time after the first description of conodonts by Pander (1856), these elements were the only known parts of the organism, whose biologic affinity was hotly debated. The absence of the rest of the body resulted in many interesting hypotheses, and elements were interpreted to be associated with a variety of fossil groups, including plants (see summary in Knell 2013). Finally, preserved soft body impressions were found in the Carboniferous Granton Shrimp Beds in Scotland, where an eel-like animal carried a feeding apparatus comprising a complete set of elements (Briggs et al. 1983; Fig. 1). These Granton specimens, later supported by exceptional new material from the Upper Ordovician Soom Shale of South Africa (Aldridge & Theron 1993, Aldridge et al. 1995), provide some of the strongest evidence of chordate and vertebrate affinity of conodonts, including the presence of a notochord, chevron-shaped myomeres, paired eye structures and ray-supported caudal fins (Aldridge et al. 1995, Purnell 1995). The apparatus of generally 15 to 19 elements in the mouth of the animal could

---

Authors' addresses:
[1] Dipartimento di Matematica, Informatica e Geoscienze, Università degli Studi di Trieste, Via Weiss 2, 34128 Trieste, Italy
[2] Department of Earth, Energy and Environment, University of Calgary, Alberta, Canada T2N 1N4
[3] Department of Geosciences, Texas Tech University, Lubbock, TX 79409, USA
[4] Dipartimento di Scienze Chimiche e Geologiche, Università degli Studi di Modena e Reggio Emilia, Via Campi 103, 41125 Modena, Italy
* Corresponding author: ccorradini@units.it

DOI: 10.1127/nos/2024/0822
Borntraeger Science Publishers, Stuttgart, www.borntraeger-cramer.com

have been used for grasping and crushing/shredding prey or for filtering plankton.

Compositionally, elements are similar to vertebrate structures and histological studies reveal signs of occlusion and wear (Donoghue & Purnell 1999, Purnell & Jones 2012), suggesting that they were homologous to vertebrate teeth (Purnell 1995). Other workers, integrating microstructure analysis on earliest elements by synchrotron radiation X-ray tomographic microscopy, propose that this is the result of convergent evolution (Murdock et al. 2013). Whatever the interpretation, conodont elements and soft body strongly indicate some type of vertebrate affinity.

Over the 300 Ma interval during which they existed, conodonts represent an incredibly useful fossil group not only in biostratigraphy, but also in paleobiogeography and paleoecology (e.g., Mei & Henderson 2001). The organic-phosphatic composition of the elements has made them excellent indicators of thermal maturity of the enclosing sediment (CAI: Color Alteration Index; Epstein et al. 1977). Application of CAI has made conodonts valuable tools in basin analysis for hydrocarbon assessments and locally and regionally for mineral resource exploration and assessment. Finally, the skeletal material is resistant to diagenetic processes and has been used, with some limitations (see below), for geochemical characterization of ancient seas and oceans using mainly trace elements and oxygen, carbon, neodymium and strontium isotopes (e.g., Trotter et al. 2008, Joachimski et al. 2012).

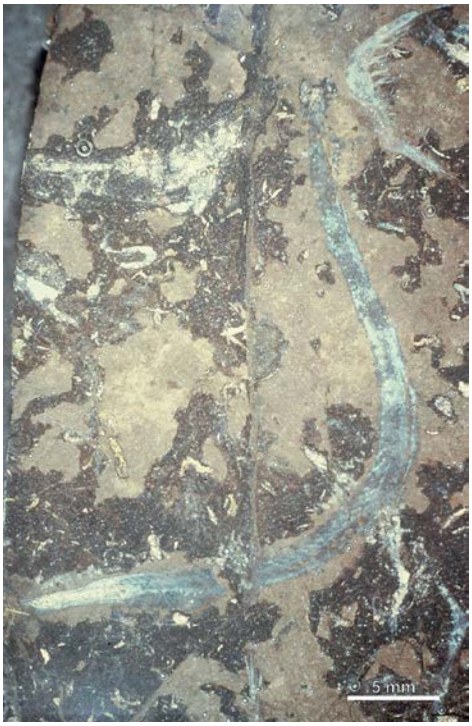

Fig. 1. The conodont animal (modified original photograph provided courtesy of Derek Briggs; this was the basis of black and white image in Briggs et al. 1983).

Conodont zonal schemes first appeared during the middle of the last century, mainly based on Ordovician to lower Carboniferous sequences in Europe and North America (e.g., Voges 1959, 1960; Ziegler 1962, 1969; Walliser 1964, Lane et al. 1970, Bergström 1971). These schemes were widely applied and continue to be improved. Zones now exist for all of the stratigraphic range of the group (the "Conodontozoic" as recently defined by Ferretti et al. 2020). In addition to the "standard" conodont subdivisions of potential global applicability, alternative regional zonations of local application have been produced in different geographic areas as discussed below. Finally, conodonts represent the most used tool for the correlation of chronostratigraphic boundaries. The main criteria used to mark the Global Stratotype Section and Point for 27 stages from the Lower Ordovician into the Upper Triassic are the First Appearance Datums (FADs) of conodont taxa (see section 7).

2. Taxonomy

Conodonts are known almost exclusively by the phosphatic "tooth-like" elements that represent the only mineralized parts of the animal. Since they are extracted mostly by acid leaching of carbonate rocks or easily disaggregated shales and sandstones, the great majority of the elements are collected as isolated components of the multi-element apparatus. For more than a century after conodonts were first described by Pander in 1856, the taxonomy was exclusively based on the morphology of single-elements (form-taxonomy). Coniform, ramiform and pectiniform elements are the three more common identified morphotypes (Fig. 2). Large pectiniforms are often named platform elements.

Now we know that several elements, usually of different morphologic types, were housed in the mouth of the conodont, forming a complex feeding apparatus. The transition from single-element form-taxonomy to multi-element taxonomy, which approximates a natural biological classification, took a long time. A few associations of elements on bedding surfaces were described early and interpreted as a natural assemblage

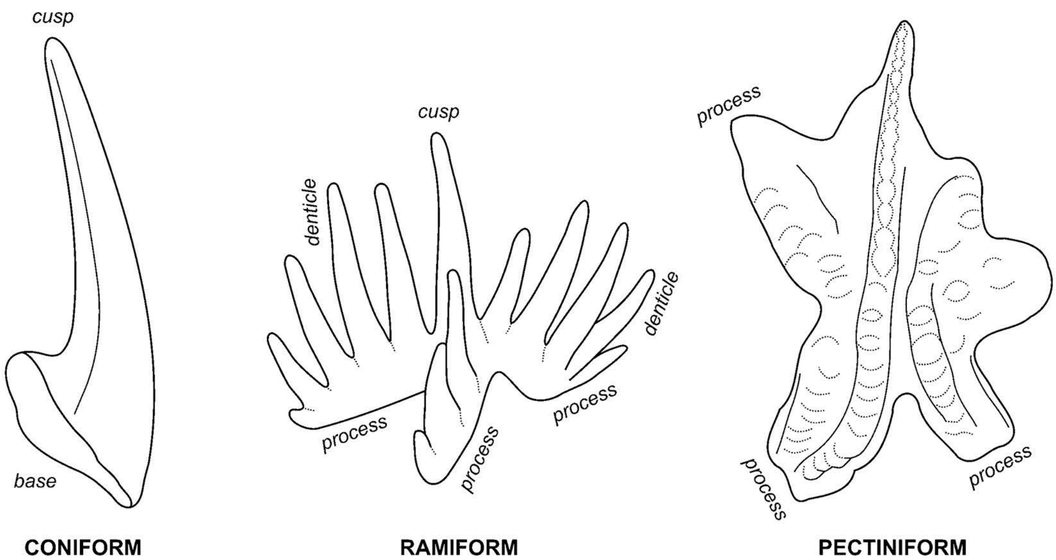

Fig. 2. General conodont element morphotypes (coniform, ramiform and pectiniform elements) and simplified morphologic terminology.

of a conodont animal (e.g., Schmidt 1934, Rhodes 1952), but the rarity of such recoveries did not affect taxonomic practice. At the beginning of the second half of the twentieth century, Huckriede (1958) and Walliser (1964) noted that the composition of recurrent groups of elements in large collections of isolated conodont elements could represent or closely approximate that of the natural assemblages. Bergström & Sweet (1966) and Webers (1966) based the species they recognized on assemblages generated empirically from their collections, starting the shift from form-element taxonomy to multi-element taxonomy. At the first international meeting of conodont workers held in Marburg, Germany, in 1971 it was decided that multi-element taxonomy was to be preferred over form-taxonomy (Lindström & Ziegler 1972, Sweet & Donoghue 2001).

Complete conodont apparatuses are known from exceptional recovery on bedding planes (e.g., Aldridge & Theron 1993, Purnell & Donoghue 1997, Liu et al. 2017) or from fused elements ("clusters") recovered in some processed samples. Others are known from "lucky samples" that are monospecific or where a few already well-known species are present, and can provide information on the apparatus composition for the one or two other species in the sample (e.g., Serpagli 1983, Corriga & Corradini 2019b). The majority of known multielement species has been reconstructed on this basis.

Rare intact natural assemblages show that the apparatus is bilaterally symmetrical and generally composed of 15 to 19 discrete elements, structurally divisible into elements occupying three positions in the apparatus, S, M and P elements (Fig. 3; Sweet 1988, Purnell et al. 2000). In the P position two pairs of pectiniform elements normally occur (P_1 and P_2; and P_3 in a few taxa) that are commonly the most robust; they are approximately mirror images of one another with the denticulated surfaces opposed. These robust elements often represent the majority of discrete conodont elements recovered, being more easily preserved than the more fragile ramiform elements that occupied other positions in the apparatus. Consequently, many species are known only by P_1 elements (platforms) and the other elements of the apparatus are considered to be similar, if not the same, to coeval species with a comparable P_1 element for which the apparatus is known. Some taxa have an apparatus formed only by coniform or coniform plus ramiform elements. These apparatuses are simpler and may lack an obvious structural division into distinct suites of elements that compare to the P, M and S divisions (Sansom et al. 1994).

Genera and species are based on the morphologic features of individual elements, most often the P_1 and M elements. A few suprageneric classifications of multielement taxa have been proposed, of which Sweet (1988) and Dzik (1991) are the more commonly used. Suprageneric groups are based on the structure of the reconstructed apparatus. Cladistic analyses of selected multielement conodont genera (Donoghue et al. 2008) produced an alternative classification that has not been

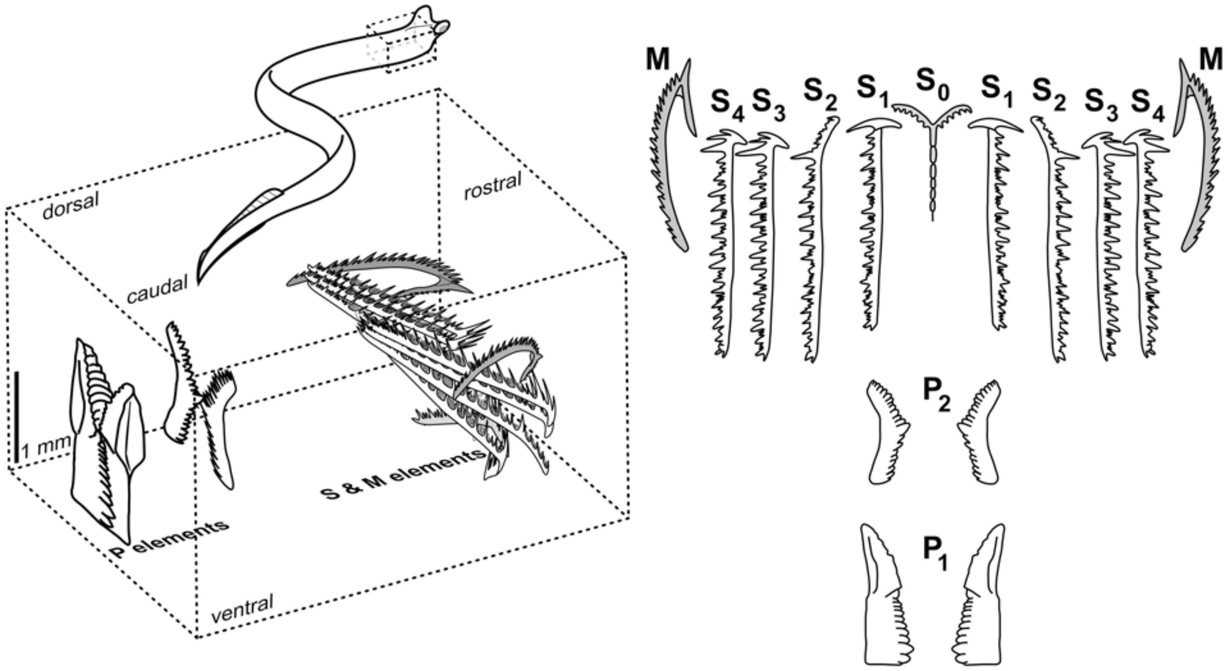

Fig. 3. Apparatus location in the conodont animal (modified after Henderson 2021 based on original artwork provided with permission by Mark Purnell) and general architecture of the 15-element apparatus of ozarkodinids (modified after Liu et al. 2017).

widely used, probably because all genera were not included.

3. Paleoecology and paleogeography

The analysis of the soft-tissue anatomy of conodonts documented a hydrodynamic silhouette provided with fins, supporting a nektic habit and an ecologic distribution of most species largely independent of conditions on the bottom (Sweet 1988). The conodont animal lived in the water column, possibly at various water depths (Seddon & Sweet 1971). The discovery of eye muscles used for eye movements suggests a general adaptation of conodonts to the photic zone (Gabbott et al. 1995, Rigo & Joachimski 2010). The presence of mineralized tooth- and jaw-like elements in the cephalic lobe indicates a predatory habit (Sweet 1988, Purnell 1995) on a wide variety of alimentary resources (Terrill et al. 2022). The food capture and processing mechanisms involved a pulley-like grasping motion, rotational kinematics of elements, and occlusion of some elements (Goudemand et al. 2011, Jones et al. 2012).

The coexistence of conodonts with only marine biota supports a marine habitat for these animals. Owing to the lack of extant biological analogues, the abundance, diversity, and spatial distributions of species have been inferred using sedimentologic features, co-occurring taxa, and geochemical trends, which are the only available proxies to formulate detailed paleoecologic and paleobiogeographic hypotheses. It is likely that conodonts responded to many hydrographic conditions that are not otherwise well-preserved in the stratigraphic record and, thus, their distribution can serve as an important proxy of paleoenvironmental change (e.g., Spiridonov et al. 2016, Lüddecke et al. 2017). However, determination of the specific controls on the distribution of taxa is not readily accomplished.

A global synthesis on conodont paleoecology and paleogeography is biased by the fact that studies are often limited to restricted stratigraphic intervals. The concept of "communities", introduced by Barnes et al. (1973) and Merrill (1973), was later replaced with that of "biofacies" to highlight preferred or limited conodont distribution in certain environments, resulting by a combination of biologic and taphonomic processes. For most intervals of geologic time, three generalized conodont biofacies can be identified. The major biofacies is the normal marine shelf biofacies, which tends to be the most diverse biofacies, and the one for which conodont zonations are most readily applicable. The combination of normal marine hydrographic conditions and an abundant food supply, as is characteristic of subtropical to tropical shelf settings, permitted the conodont animals to flourish, but the exact controls on distribution of individual genera and species across the shelf environment have been difficult to interpret. Abundance of elements is a function of biologic productivity relative to rates of sediment accumulation. The offshore and deeper water conodont biofacies occurs on shelf margins, slope, and basinal settings. Here occur species that may be pelagic, and often cosmopolitan in distribution. Diversity of the offshore species is lower than on the shelf, but the admixture of offshore species with downslope transport of shelf taxa and low sediment accumulation rates can make the resulting assemblages appear more abundant and diverse. The offshore species can serve as useful zonal indicators that allow regional to global correlation to be affected. The nearshore biofacies is characterized by low diversity and is constituted of genera and species that could tolerate the variable salinities and other restrictive environmental aspects of the marginal marine environment. Biostratigraphic correlation of this biofacies can be difficult and in many instances conodont zonations different than the standard marine zonations have been used.

The biogeographic distribution of conodont species is related to biofacies distributions, surface/deep water temperatures, and degree of geographic isolation. Endemic species appear to be more common in nearshore, probably shallow-water biofacies, while more cosmopolitan species characterize offshore, deeper-water biofacies. The most diverse conodont assemblages occur in tropical to subtropical settings, and diversity decreases into the higher latitudes and especially in areas near glacial activity. Several time frames can be referred to for illustrative examples.

The Ordovician represents a key-interval in biogeographic studies, due to the high diversification of conodonts in a period of profound geographic differentiation. The marine realm was subdivided into two major biogeographic units: the North American Midcontinent and the North Atlantic Provinces (Sweet et al. 1959). Sweet & Bergström (1984) referred the former to warm waters, largely restricted to 25–30° latitude and temperature above 15 °C, and the latter to cold waters of latitudes around 40°. They identified a Late Ordovician series of biofacies through the equator-to-pole transition to suggest that, exactly as in recent seas, warm-water faunas exhibited higher species diversity than cold-water ones, possibly also favored by exchanges triggered by equatorial currents. The succeeding integration of isotopic techniques within correlation proxies has enabled a more precise comparison among different conodont populations recovered in different areas, and a new series of paleogeographic/biofacies studies has been released. Rasmussen & Stouge (2018), based on multivariate statistical analyses, recently identified in the Middle Ordovician of the Baltoscandian platform three distinct, recurrent and laterally extensive conodont biofacies (Fig. 4). During the Dapingian Stage (early Middle Ordovician), the relatively shallow proximal and intermediate shelf settings were characterized by the *Baltoniodus–Microzarkodina* biofacies both in the transition area of Baltica to the Tornquist Sea and in that to the Iapetus Ocean. In the distal shelf, the *Protopanderodus* biofacies occupied the southern cooler waters facing the Tornquist Sea while the *Periodon* biofacies developed in the northern warmer waters towards the Iapetus Ocean. In the following Darriwilian Stage, possibly due to the onset of a cooling event, the *Gothodus–Nordiora* (GN in Fig. 4) assemblage appeared in relatively cool areas of the platform margins within both the *Protopanderodus* biofacies and *Periodon* biofacies. The two genera *Gothodus* and *Nordiora*, known from high-latitude Gondwana, probably had a nektobenthic mode of life in deep and/or cool settings (Rasmussen & Stouge 2018).

Conodont diversity declined greatly after the end-Ordovician (Hirnantian) extinction event (Fig. 5). Because taxonomic diversity at the generic level was reduced by about 50–60 %, the pattern of conodont distribution is more subdued and Llandovery conodont biofacies are not well-defined (Zhang & Barnes 2002). A series of oceanic extinction events associated with carbon isotope excursions punctuated the conodont record during the Silurian (see Calner 2008) and likely suppressed a major diversification of conodonts during this period. Coniform taxa that have little apparent biostratigraphic value dominate most faunas. Chen et al. (2017) recognized four Llandovery conodont provinces that differ significantly from the Ordovician ones, of which only about 10 % of the species were considered to be cosmopolitan. On a gentle ramp setting on Anticosti Island, Zhang & Barnes (2002) could distinguish Llandovery shallow ramp and deeper ramp biofacies. Communities occurring in Llandovery

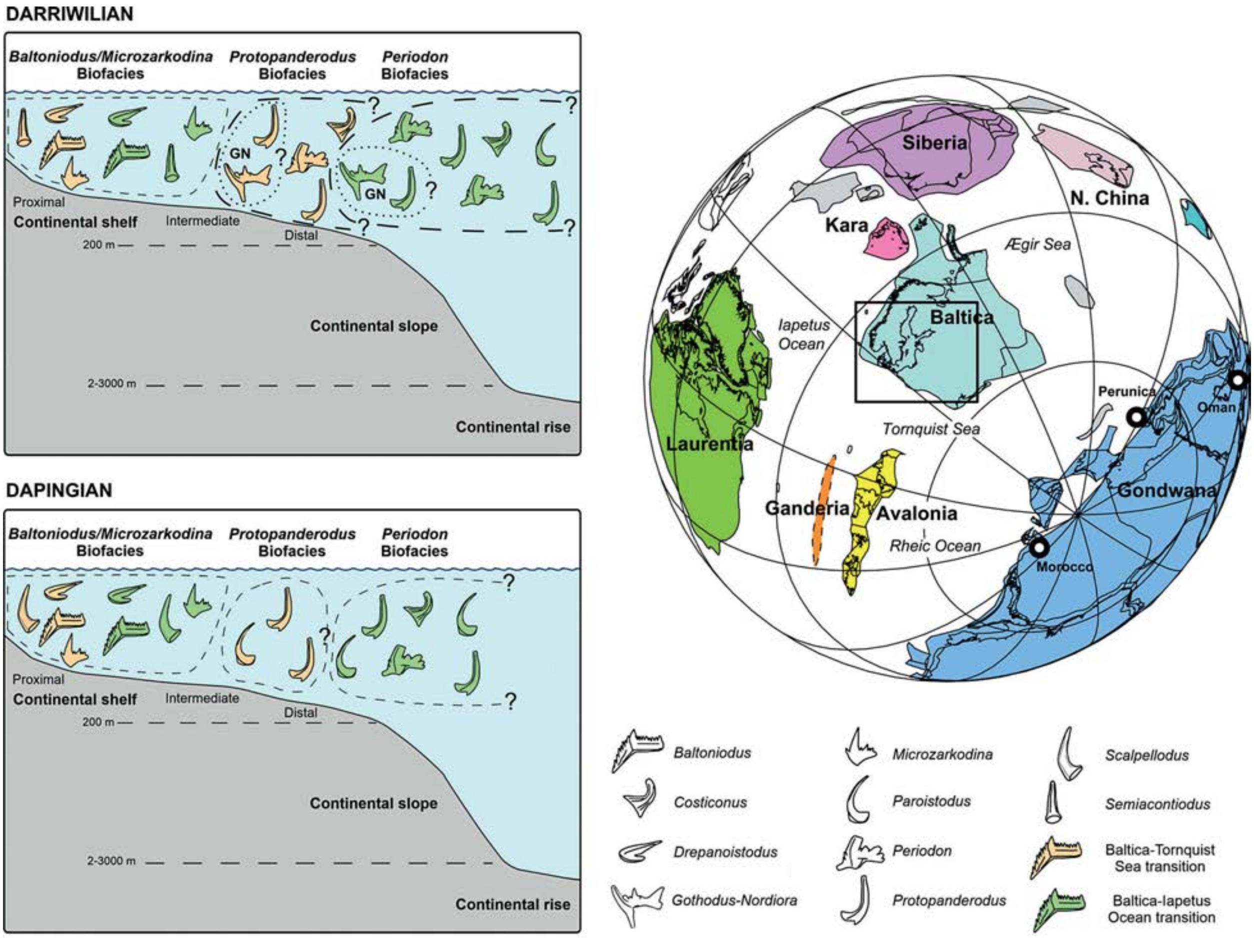

Fig. 4. Conodont biofacies in the Middle Ordovician (Dapingian and Darriwilian) of the Baltoscandian platform (modified after Rasmussen & Stouge 2018). The onset of the Darriwilian documented in the deeper and cooler parts of the platform margin the appearance of the *Gothodus–Nordiora* (GN) assemblage, triggered by a general cooling of the waters.

through Wenlock slope and basinal environments in Arctic Canada include many species with a widespread geographic distribution (Zhang et al. 2016). In the Baltic region, a distinctive diverse nearshore biofacies developed, but is restricted to that region (Jarochowska et al. 2017).

The radiation of icriodids and then polygnathids during the Early Devonian led to the development of a shallow shelf icriodid biofacies, with many endemic species, and an offshore shelf polygnathid biofacies, the species of which are common regional to global zonal indices. Endemism was high early in the Devonian and decreased later as more cosmopolitan species of polygnathids appeared and rising sea levels flooded cratonic regions (Klapper & Johnson 1980). The biofacies spectrum broadened in the Late Devonian with the appearance of palmatolepids, a rapidly evolving group that occupied the farthest offshore settings with bispathodids, and included many cosmopolitan zonal species. Across the shelf region in western North America, offshore palmatolepid-polygnathid and shallower water polygnathid-icriodid/pelekysgnathid biofacies occur (e.g., Sandberg 1976). In the shelf faunas lacking palmatolepids, separate polygnathid zonations have been proposed (e.g., Klapper & Lane 1985, Ovnatanova & Kononova 2001, 2008). The nearshore clydagnathid biofacies occupied waters of variable salinity. The model by Sandberg (1976) based on relative abundance of genera is applied all over the world, and was augmented by recognition of pelagic species of *Icriodus* (Corradini 1998, 2003) in North Gondwana.

A comparable spectrum of conodont biofacies reappeared in the early Carboniferous (Mississippian) after the extinction of *Palmatolepis* species. In the western United States, a diverse fauna of biostratigraphically important genera (e.g., *Gnathodus*, *Scaliognathus*, *Bactrognathus* and *Pseudopolygnathus*)

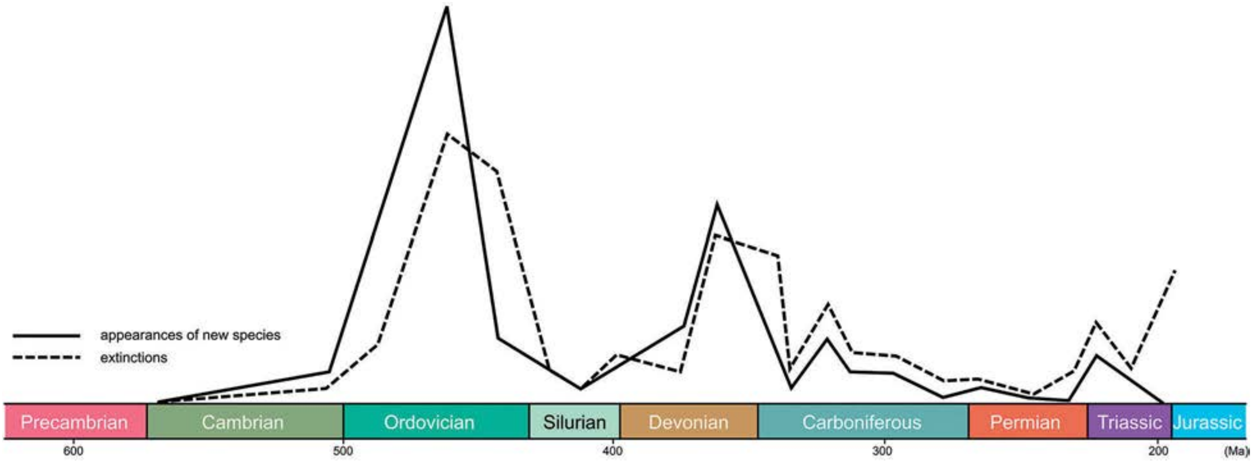

Fig. 5. Conodont diversity expressed by appearances of new species (solid line) and extinctions (dashed line). Decline of conodont diversity occurs when the appearance line is below the extinction one (modified after Knell 2012).

occupied the outermost shelf to slope setting, but in the starved basin these genera are less common and species interpreted to be pelagic, such as *Bispathodus* and *Polygnathus communis*, are more characteristic (Sandberg & Gutschick 1979). On the shallower parts of the shelf, *Eotaphrus*, *Hindeodus*, and *Pandorinellina*, all with simple blade-like pectiniform elements, dominate faunas. The *Mesognathus* biofacies, which occurs in the most restricted near-shore environment, has its own zonation, and a cosmopolitan distribution (von Bitter et al. 1986).

Several new genera of gnathodids appeared at the beginning of the late Carboniferous (Pennsylvanian) and their lineages dominated conodont faunas from the Bashkirian into the early Permian (Barrick et al. 2022, 2023). Heckel & Baesemann (1975) and Swade (1985) interpreted the distribution of some Pennsylvanian taxa in North American Midcontinent epeiric seaway cyclothems as being controlled by the position of the thermocline, and related to water temperature. The nearshore biofacies of *Adetognathus* and *Ellisonia* grades into the *Hindeodus* biofacies in shallow marine carbonates. Offshore, idiognathodids (e.g., *Idiognathodus*, *Streptognathodus* and *Neognathodus*) dominate. The interpretation of the factors controlling the distribution of the most offshore genera, *Gondolella* and *Idioprioniodus* in the black shale lithofacies has been controversial (Sweet 1988). Herrmann et al. (2015, 2019) suggested that Midcontinent Pennsylvanian conodont biofacies distributions seem to have been controlled by physicochemical properties of the water mass (e.g., temperature, salinity, nutrients, turbidity, and/or dissolved oxygen levels) that may correspond less directly to water depth. The proximity to terrestrial freshwater influx and the strength of anoxia/euxinia in the subpycnoclinal water mass may have had significant roles in the spatial distributions of conodont taxa. Two to three major biogeographic regions, each with many endemic species, existed, especially during the Moscovian and Kasimovian, and hinder global biostratigraphic correlations (Barrick et al. 2022).

Paleoecologic controls for the Permian and Triassic are mostly comparable to the Swade (1985) model with the position of the thermocline affecting distribution. Conodonts are absent from very cold water in proximity to major glaciers during the Late Paleozoic Ice Age (Nicoll 1976). During the Permian, *Ellisonia* occupied a near-shore position; it was accompanied by *Adetognathus* only in the earliest Permian and *Hindeodus* for much of the Permian. *Streptognathodus* occupied warm-water above much of the shelf during the earliest Permian Asselian Stage and was ecologically replaced by *Sweetognathus* during the early Permian Sakmarian Stage and later by descendants *Neostreptognathodus* and *Iranognathus*. The offshore setting, restricted to waters below a thermocline, was characterized by *Mesogondolella* during the early Permian. The Permian world was characterized by increasing levels of provincialism for much of the late early, middle and late Permian. Mei & Henderson (2001) described three provinces including an Equatorial Warm-water Province (EWWP), North Cool-water Province (NCWP), and peri-Gondwana Cool-water province (GCWP). *Jinogondolella* and *Clarkina* dominated an offshore biofacies below a thermocline in the EWWP during the middle and late Permian respectively. In contrast, *Mesogondolella* ranged through the entire Permian (Henderson 2018) in the NCWP in both shallow and deeper shelf because of thermocline shoaling. One explanation for this thermocline shoaling is that circulation and surface currents were cut-off from equatorial settings, for example by the closure of Uralian gateway (Beauchamp et al. 2022). *Ellisonia* and *Hindeodus* continued to occupy the very near shore setting in middle and late Permian of the NCWP, but *Sweetognathus* and descendants were absent. The offshore setting in the GCWP included some *Mesogondolella* and *Vjalovognathus* (Mei & Henderson 2001).

The paleoecologic distribution of *Hindeodus* was expanded during the Permian-Triassic boundary interval to offshore and nearshore environments (Lai et al. 2001). Conodonts were not significantly affected by the end-Permian mass extinction (Orchard 2007), but there was an important turnover in the early Induan (latest Griesbachian substage) including the extinction of *Hindeodus*. The migration of the EWWP genus *Clarkina* into the NCWP near the Permian-Triassic boundary was related to the effect of major rise in global ocean temperatures (Algeo et al. 2012, Joachimski et al. 2012). This was followed by major radiations (Orchard 2007) in the Olenekian (mid-Smithian and early Spathian substages). The degree of provincialism increased throughout the Middle Triassic, when Chen et al. (2016) distinguished two conodont domains including Tethyan and Panthalassan. Rigo & Joachimski (2010) indicated that Late Triassic conodonts, including *Carnepigondolella*, *Epigondolella*, *Parvigondolella*, *Metapolygnathus*, *Orchardella*, and *Misikella*, were nektic surface dwellers in warm water within the photic zone.

4. Taphonomy

The taxonomic combination of elements recovered from a sample processed for conodonts differs greatly from that seen in natural and complete apparatuses exposed in bedding plane assemblages. Upon decay and disintegration of soft parts, elements of different shapes and relative sizes are released as sand-sized sedimentary particles. The complex shapes of the conodont elements give them a range of hydrodynamic properties that determine their susceptibility to entrainment, transport, and sorting (Broadhead et al. 1990, McGoff 1991). Larger and more compact pectiniform elements are often over-represented relative to less compact ramiform elements (Purnell & Donoghue 2005). Helms & Over (2006) suggested that ramiform elements were preferentially destroyed when conodonts were digested as prey. Broadhead & Driese (1994) concluded that destruction by abrasion when suspended in water was unlikely. Von Bitter & Purnell (2005) found that over-representation of pectiniform elements can occur because of preferential fragmentation of ramiform elements during compaction and diagenesis. However, all elements, including platforms, may be fractured in shaly lithotypes during compaction, even at shallow depths (Johnston & Henderson 2005). In addition, the techniques used to extract conodonts from the host rock can be selectively destructive of elements. The type, concentration, and buffering of the acid used on carbonates also affect element recovery and preservation. Washing the residues through screens may increase breakage of elements, especially ramiforms, and very small fragments may be lost through the screens along with tiny elements. Other laboratory methods of separation can create additional biases (see Jeppsson 2005). Despite the potential losses associated with these techniques, many samples when carefully processed will yield exceptionally well-preserved elements in close to their natural proportions.

The number of conodonts per kilogram of rock varies greatly, from zero to thousands of elements. Conodont elements are composed of apatite and are denser (2.9 to 3.0 g/cm^3) than other sedimentary particles, such as quartz and calcite (2.7 g/cm^3), and they behave as heavy mineral particles. Sedimentary processes that sort sediment grains will also sort and concentrate conodont elements, especially larger pectiniforms, into layers of sand-sized particles. In Pennsylvanian strata in the southwest United States, selective sampling of layers of sand-sized carbonate material leads to much better recoveries of conodont elements than for carbonate muds. Conodonts do not occur evenly dispersed in basinal shale and chert deposits, but concentrate in thin sandy lag beds and lenses formed by gravity flows or bottom currents.

The durability of conodont elements allows them to be reworked into younger strata. Discolored elements may help recognize reworking, but reworked elements may be preserved identically to younger elements. In proximal sandy environments, the reworked grains may be somewhat rounded to fully rounded (Broadhead & Driese 1994). When the age differences are great, the reworked conodonts can be used to identify the age of the source beds (e.g., Spalletta & Perri 1993). If the ages are close, then the overlying strata may be incorrectly dated or conodont ranges mixed, as is the case in oolitic beds of the Devonian-Carboniferous GSSP at the La Serre section in France (Kaiser 2009). The Upper Devonian Holts Summit Sandstone of Missouri is an extreme case where thousands of well-preserved, but discolored conodonts form grey and black cross-bed laminae (Thompson 1993). Gravity flows represent a special problem because conodonts may be transported from the shelf region into the basin. The mixing of contemporaneous shallow water taxa into deeper water may be an advantage for biostratigraphy. No obvious mixing of faunas of different ages may be evident, which appears to be the case in the thick Pennsylvanian carbonate slope sections in South China (Qi et al. 2020). The presence of reworking may be less obvious and more difficult to interpret, such as the Global Stratotype Section and Point (GSSP) for the base of the Ordovician in the Green Point Formation, Newfoundland (Cooper et al. 2001). A worse case is the Lower Pennsylvanian Dimple Limestone in West Texas, where over 85 % of samples contained reworked conodonts that comprise 7 % of the conodont elements (Proctor 1991). Ordovician through Mississippian elements were recovered.

Karsting of carbonates underlying unconformities provides conduits for sediments containing elements to infiltrate as a stratigraphic leak. The leak may be confined to the upper part of the underlying unit, where if unrecognized, the top of the underlying unit may be incorrectly dated. Pervasive karsting of Silurian carbonate strata in West Texas has allowed numerous Late Devonian elements to be leaked over 100 metres downward (Barrick & Meyer 2019), likewise, again in West Texas, younger conodonts are found in infillings of karst in the Lower Ordovician (Bellian et al. 2012).

Sedimentary and biological processes during deposition can hinder the reliable resolution of species ranges. Herbers et al. (2017) showed that repeated 1 kg samples revealed large fluctuations of conodont abundance and faunal associations in Devonian pelagic micrite where recovery was 100's of specimens per kg. Even 10 kg samples were not sufficient to obtain all rare species. The impact of sequence stratigraphic architecture on ranges is well documented (Holland 1995, 2000, 2023; Barrick & Männik 2005). At a finer scale, detailed stratigraphic resolution is difficult to attain because of syndepositional reworking (Cutler & Flessa 1990) and advection by burrowing organisms (Martin 1993) that "time-average" the fauna. Studies suggest that significant advection may occur over a sediment thickness of 30–40 cm – the significance for correlation depending on depositional rate. This may create overlapping ranges of species that occur near each other in time, information that has been used to infer evolutionary events and support zonal boundaries. Despite this intense scrutiny of the various processes that affect the distribution of conodonts, they remain among the best fossils for correlation of most marine facies.

Conodont elements are composed of bioapatite, a term referring to an apatite of strictly biochemical origin. Because this bioapatite may archive sea water chemistry information, conodonts are frequently used in paleoenvironmental investigations on past ocean geodynamics and climates (e.g., Holmden et al. 1996, Trotter et al. 1999, Wenzel et al. 2000). However, different iso- and heterovalent substitutions may occur in the bioapatite framework during *in-vivo* biologically-mediated crystal growth or during *post-mortem* burial and diagenesis (LeGeros 1981). It is therefore critical to detect and filter any later effect on the primary bioapatite signal (see, among others, Trotter & Eggins 2006, Medici et al. 2020, Shohel et al. 2020). By the application of a consolidated protocol of experimental techniques (e.g., Nardelli et al. 2016, Ferretti et al. 2017, 2021a; Malferrari et al. 2019), the uptake of rare earth elements (REE) and other high field strength elements (HFSE) has been recently tested as a proxy of diagenesis overprinting (Ferretti et al. 2021b, 2023; Medici et al. 2021, Malferrari et al. 2024), but further evidence is needed to enhance the potential and reliability of conodont elements as superb geochemical tools.

5. Biostratigraphy

The distribution of conodonts in space and time has proven that they are unique biostratigraphic tools for the correlation of marine rocks from their appearance in the late Cambrian until the Triassic-Jurassic transition. The range of significant genera is summarized in Figure 6. Overall, conodonts exhibit cyclical patterns of evolutionary development throughout their history (Sweet 1988). Conodont diversity appears to have expanded during interglacial intervals and to have remained stationary or even reduced during glacial episodes. These diversity patterns can be followed at both regional and global scales and deeply influenced related biostratigraphic zonation schemes (Ferretti et

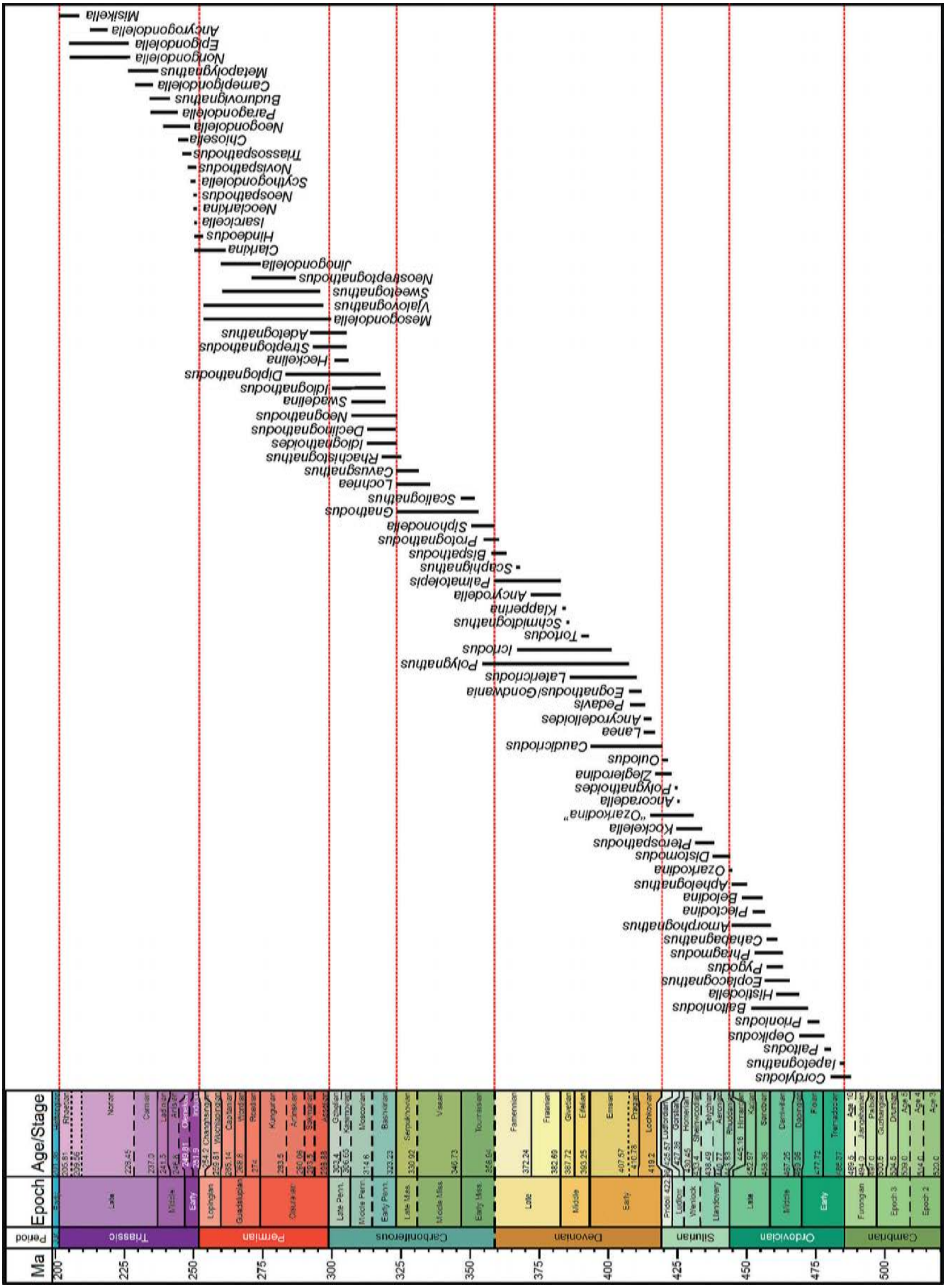
Ma
Period
Epoch
Age/Stage
200
225
250
275
300
325
350
375
400
425
450
475
500
Triassic
Permian
Carboniferous
Devonian
Silurian
Ordovician
Cambrian
Late
Middle
Early
Lopingian
Guadalupian
Cisuralian
Late Penn.
Middle Penn.
Early Penn.
Late Miss.
Middle Miss.
Early Miss.
Pridoli
Ludlow
Wenlock
Llandovery
Furongian
Epoch 3
Epoch 2
Norian
Carnian
Ladinian
Anisian
Olenekian
Induan
Changhsingian
Wuchiapingian
Capitanian
Wordian
Roadian
Kungurian
Artinskian
Sakmarian
Asselian
Gzhelian
Kasimovian
Moscovian
Bashkirian
Serpukhovian
Visean
Tournaisian
Famennian
Frasnian
Givetian
Eifelian
Emsian
Pragian
Lochkovian
Telychian
Aeronian
Rhuddanian
Hirnantian
Katian
Sandbian
Darriwilian
Dapingian
Floian
Tremadocian
Age 10
Jiangshanian
Paibian
Guzhangian
Drumian
Age 5
Age 4
Age 3
Miskiella
Ancyrogondolella
Epigondolella
Norigondolella
Metapolygnathus
Carnepigondolella
Budurovignathus
Paragondolella
Neogondolella
Chiosella
Triassospathodus
Novispathodus
Scythogondolella
Neospathodus
Neoclarkina
Isarcicella
Hindeodus
Clarkina
Jinogondolella
Neostreptognathodus
Sweetognathus
Vjalovognathus
Mesogondolella
Adetognathus
Streptognathodus
Heckelina
Diplognathodus
Idiognathodus
Swadelina
Neognathodus
Declinognathodus
Idiognathoides
Rhachistognathus
Cavusgnathus
Lochriea
Scaliognathus
Gnathodus
Siphonodella
Protognathodus
Bispathodus
Scaphignathus
Palmatolepis
Ancyrodella
Klapperina
Schmidtognathus
Tortodus
Icriodus
Polygnathus
Latericriodus
Eognathodus/Gondwania
Pedavis
Ancyrodelloides
Lanea
Caudicriodus
Oulodus
Zieglerodina
Polygnathoides
Ancoradella
"Ozarkodina"
Kockelella
Pterospathodus
Distomodus
Ozarkodina
Aphelognathus
Belodina
Plectodina
Amorphognathus
Cahabagnathus
Phragmodus
Pygodus
Eoplacognathus
Histiodella
Baltoniodus
Prioniodus
Oepikodus
Paltodus
Iapetognathus
Cordylodus

Fig. 6. Distribution of main genera used in biozonation schemes. Note that for long ranging genera only the interval with biostratigraphic value is reported.

◄

al. 2020). A number of studies recognize bioevents or biohorizons that represent stratigraphic boundaries or short intervals across which significant change in biostratigraphic character occur. They have been employed in Ordovician to Devonian studies to distinguish major changes in biodiversity, immigration, emigration, evolutionary radiation, and extinction (Zhang & Barnes 2004, Slavik & Hladil 2020). Bioevents or biohorizons that mark the most significant biostratigraphic zonal boundaries are widely applicable and correlatable, and often mark GSSPs. Conodont ranges may also be tuned to major flooding intervals associated with third-order stratigraphic sequences and some zones or subzones may be associated with higher frequency eccentricity cycles (e.g., Pennsylvanian cyclothems).

The small size of conodont elements makes them ideal index fossils to study in surface sections, subsurface core, and even in cuttings. Conodonts may be recovered from a series of closely spaced samples, providing a detailed perspective on their evolutionary changes that may be unmatched by other Paleozoic and Triassic fossil groups. Arguably conodonts represent the best biostratigraphic markers, when considering that their entire 300 million years history is subdivided into at least 240 interregional biozones (1.25 Ma/zone on average) and many additional regional zones and subzones provide even higher resolution (e.g., at least 16 zones in the 4.8 Ma Lower Triassic, representing ~300 Kyrs/zone; Henderson et al. 2018).

Most conodont biostratigraphic studies describe interval biozones representing a body of strata based on the distribution of species from closely spaced samples. The majority of these interval zones are partial taxon range lineage zones in which the first occurrence (FO) of the nominate taxon defines the zone base with the zone top being defined by the FO of a younger related species (e.g., Yuan et al. 2014 for the upper Permian). In the Silurian a few zones are range zones, the boundaries of which are discriminated by the FO and last occurrence (LO) of the nominate taxon. Two of these, the *Polygnathoides siluricus* and the “*Ozarkodina*” *crispa* zones are widely used in all Silurian zonation schemes (e.g., Walliser 1964, Corradini et al. 2015, Corradini & Corriga 2018). Conodont biostratigraphic data have been incorporated into other biostratigraphic and chronostratigraphic schemes such as graphic correlation (e.g., Sweet 1984, Klapper et al. 1995, Klapper & Kirchgasser 2016), CONOP (e.g., Sadler et al. 2009, Schmitz & Davydov 2012), and the Unitary Associations Method (e.g., Wu et al. 2020, Leu et al. 2022, Lyu et al. 2023).

6. Biozonation schemes

Conodont zonations extending from the late Cambrian to the end of the Triassic have been proposed over the last 75 years. Because conodont faunas evolved so quickly through time, workers tend to specialize on one or a few geological periods. A patchwork of regional zonations developed that were based on local faunas whose compositions were determined by a combination of paleoecologic associations and regional endemism. Composite “global” zonations that best work for offshore environments have appeared in publications such as Geologic Time Scale (GTS) 2020. Better sources for understanding the complexities of the biostratigraphic applications of conodonts are given below.

6.1. Late Cambrian

Conodonts started to diversify during the Miaolingian Series and became sufficiently common and differentiated to be useful in biostratigraphy in the Furongian Series. Prior to the Furongian, “conodonts” comprised their presumed ancestral “paraconodonts”. The “true” euconodonts appeared in the Furongian. Regional zonations were proposed in various parts of the world, such as North America (Miller et al. 2006), Australia (Shergold & Nicoll 1992, Kruse et al. 2009) and China (Dong & Zhang 2017). These schemes were mostly based on endemic taxa; however, several widely-spread taxa (e.g., species of *Proconodontus*, *Eoconodontus* and *Cordylodus*) allowed intercontinental correlations in the upper part of Stage 10 (Miller et al. 2018, Peng et al. 2020).

6.2. Ordovician

Conodonts and graptolites represent the most useful index fossils in the Ordovician, with the former dominating carbonate successions. The relevance of conodonts in Ordovician biostratigraphy is testified by

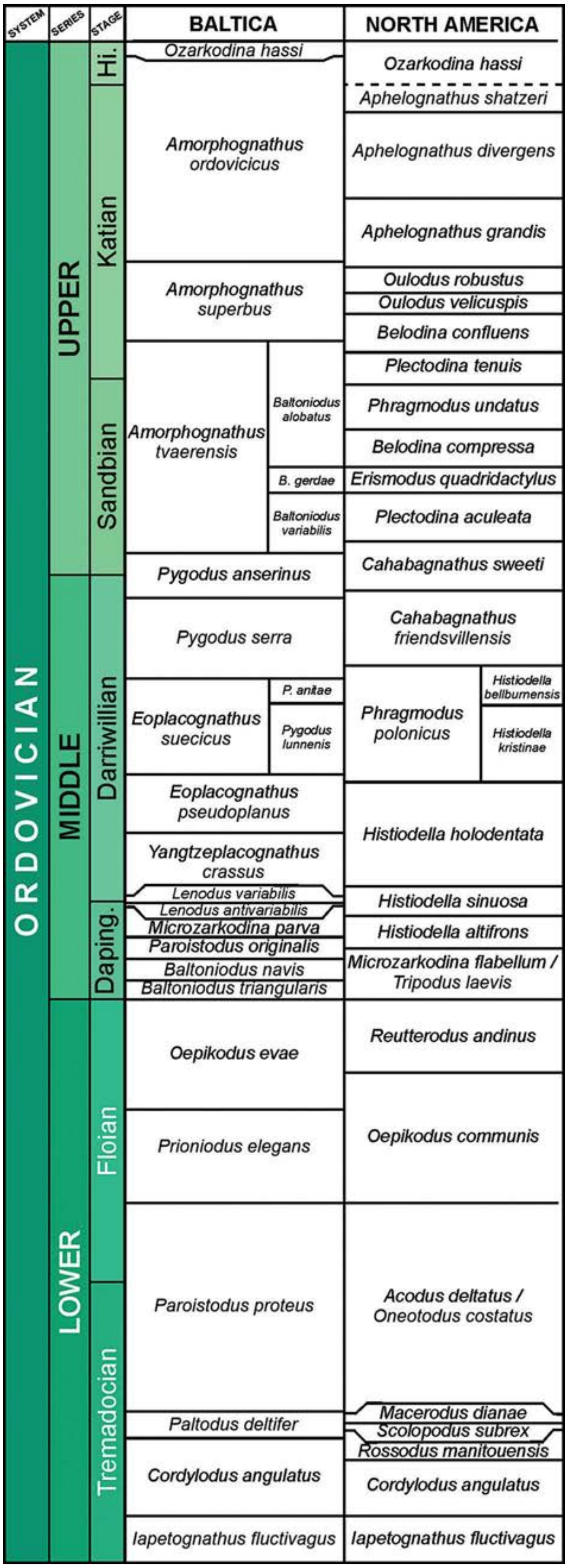

Fig. 7. Ordovician conodont zonation for Baltica and North America (adapted after Goldman et al. 2023). Abbreviations: Daping. = Dapingian; Hi. = Hirnantian; *B.* = *Baltoniodus*, *P.* = *Pygodus*.

the fact that conodonts are the tools used to mark two of the seven global stages, and seven of the 20 stage slices of the system (Bergström et al. 2009).

Lindström (1954) was the first to introduce formal conodont zones, with a biozonation scheme applied to the Lower Ordovician of Sweden and the proposal of four formal conodont zones. These zones were correlated with those recognized by Tjernvik (1952) in the same stratigraphic interval using trilobites. In the symposium volume "Symposium on Conodont Biostratigraphy" published in 1971, four papers dealt with Ordovician conodont biostratigraphy, focusing on northern Europe and North America. Lindström (1971) introduced in Baltoscandia ten named conodont zones, using multi-element taxonomy with the genera *Cordylodus*, *Paltodus*, *Paroistodus*, *Prioniodus*, *Baltoniodus*, *Microzarkodina* and *Amorphognathus*, that were correlated with graptolite zones. Ethington & Clark (1970) subdivided the Lower Ordovician succession of the North American Midcontinent and Great Basin in Utah and Nevada, and adjacent part of Canada into lettered numbered Faunas A through E, basing on the vertical ranges of 39 form species. Sweet et al. (1970) subdivided the North American Ordovician into 12 preliminary numbered faunas. Bergström (1971) introduced a subdivision of the Ordovician succession in Baltoscandia into five zones and 10 subzones, mainly by the use of platform conodonts in the rapidly evolving lineages of *Eoplacognathus*, *Pygodus*, *Polyplacognathus*, *Prioniodus* and *Amorphognathus*. Each unit had a corresponding reference section in the Siljan region of central Sweden. Later studies followed in Baltoscandia, Poland, the British Isles, Southern Europe and North Africa, Siberia, New Zealand and Australia, Argentina, Canada, USA, China and South-East Asia. Since then, the Ordovician Baltoscandic zone classification has undergone only minor changes and has been correlated, with integrations due to the pronounced provincial differentiation of the Ordovician conodont faunas, all over the world. Bergström & Ferretti (2017) and Goldman et al. (2023) reviewed the development of Ordovician conodont biostratigraphy (Fig. 7) and provided comparisons between conodont zone classifications of the Ordovician in Baltoscandia, North America, Siberia, South China, North China, and the Argentine Precordillera. Data from this the former review were not included in GTS 2020 (Goldman et al. 2020).

6.3. Silurian

The original Silurian zonation of Walliser (1964), mainly based on the Cellon section, Carnic Alps, was updated by Corradini et al. (2015), who reviewed the history of Silurian conodont zonations. Although the Cellon section is reasonably complete from the Ludlow through the Přídolí, Llandovery strata are absent and Wenlock strata are discontinuous. Chen et al. (2017) illustrated a series of Llandovery zonations from different regions and noted how difficult it was to effect precise global correlations for this time interval. The GTS 2020 chart (Melchin et al. 2020) repeats the zonation of GTS 2012 (Melchin et al. 2012) that includes the *Pterospathodus tenuis* zone. The revised zonation of Männik et al. (2015) comprises four zones that use *Distomodus* and *Aspelundia?* species for the Rhuddanian through the early Telychian, but omits the *P. tenuis* zone, which appears to work better in offshore settings (e.g., Zhang et al. 2016). Resolution of the rapid radiation of species in *Pterospathodus* during the late Telychian permitted a series of detailed zones to be recognized first in the Baltic and then to be correlated on a global scale (Männik 1998, Corradini et al. 2015, Chen et al. 2017). Jeppsson (1997) and Jeppsson et al. (2006, 2012) presented detailed zonations from the latest Llandovery to the latest Ludlow based on the succession on Gotland. Not all of these zones have widespread applicability because some reflect local environmental conditions on Gotland, some zonal markers are extremely rare, and others are endemic to the Baltic region (Corradini et al. 2015). Even some common taxa, like *Kockelella walliseri*, have diachronous first occurrences globally (Cramer et al. 2010). The smaller number of more reliable zones based on Corradini &

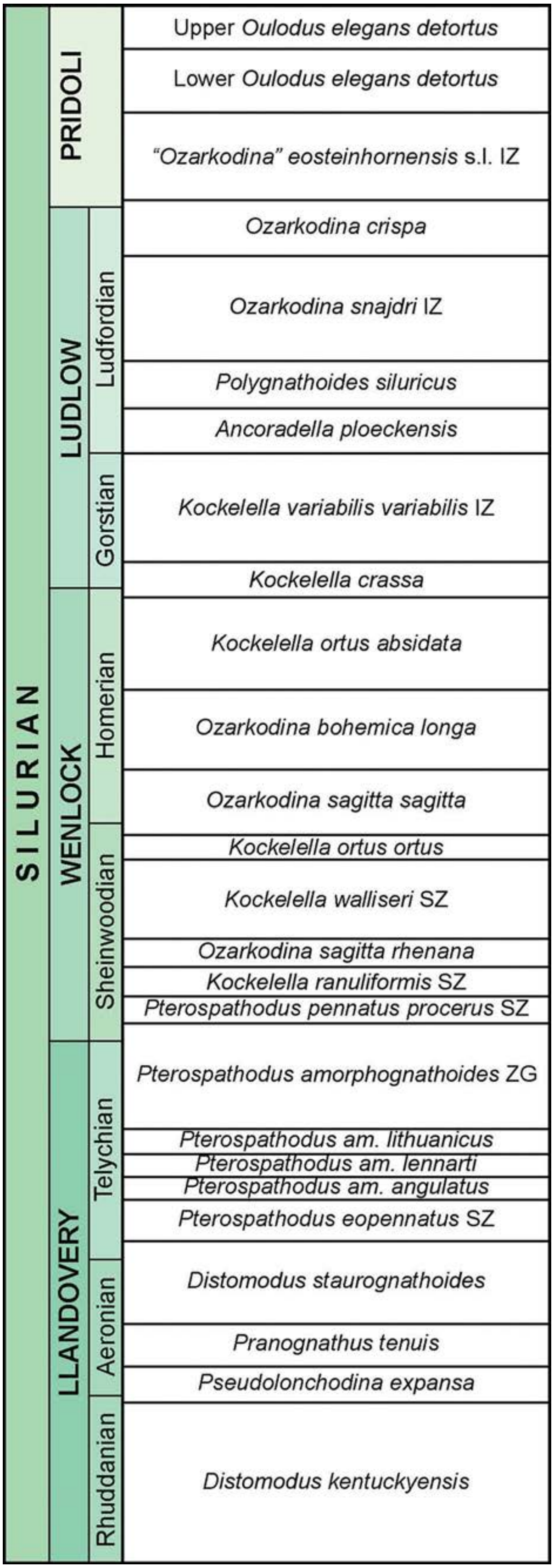

Fig. 8. Silurian conodont zonation, modified after Cramer et al. (2011), Corradini & Corriga (2012) and Melchin et al. (2020). Chronostratigraphic intervals not to scale. Abbreviations: IZ = interval Zone; SZ = superzone; ZG = Zonal Group.

Serpagli (1999) and Cramer et al. (2011), as shown in the GTS 2020, represents a better compromise for the Wenlock and most of the Ludlow (Corradini et al. 2016, Schönlaub et al. 2017). Most of the zones for the Gorstian and lower Lufordian are based on genera with large platforms, such as *Kockelella*, *Ancyrodella* and *Polygnathoides*, that did not survive the mid-Ludfordian Lau Event.

Upper Ludfordian and Přídolí zones are based on ozarkodinids and *Oulodus*. More recent work in the Carnic Alps (Corradini & Corriga 2012, Corradini et al. 2020), Sardinia (Corriga et al. 2009, Corradini & Corriga 2012), and Bohemia (Slavík et al. 2010, 2014; Slavík & Carls 2012, Vacek et al. 2018) have provided new data that modify the late Ludlow to Přídolí zones of Walliser (1964), adding more detail. However, the global applicability of these schemes is still not demonstrated and these changes were not included in GTS 2020. The Silurian biozonation scheme here proposed (Fig. 8) is an updated version of that scheme.

6.4. Devonian

Becker et al. (2020) provided a discussion of recent modifications of Devonian conodont biostratigraphy, stage by stage. The composite zonation shown on their accompanying diagrams (fig. 22.11) is largely that for deeper water successions where interregional to global correlation is possible. However, in a few cases the published scheme does not reflect any previous published zonation and the introduction of zones or combination of different schemes requires a better discussion.

The conodont zonation for the Lochkovian uses the Icriodontidae *Caudicriodus* and *Pedavis*, and genera with carminate P_1 elements (e.g., *Lanea*, *Ancyrodelloides* and *Masaraella*), but global correlations are problematic. Even if some schemes are claimed to be of global value (e.g., Valenzuela-Ríos & Murphy 1997, Corradini & Corriga 2012, Valenzuela-Ríos et al. 2015), they actually have a regional applicability due to limited geographic distribution of some taxa (Slavík et al. 2012, Murphy & Valenzuela-Ríos 2017, Corriga & Corradini 2019a). A global zonation for the Pragian does not exist, and several schemes were proposed (e.g., Lane & Ormiston 1979, Slavík 2004, Murphy 2005). However, the index taxa used have a limited geographic and/or ecologic distribution and many authors combine them variously in local works.

The conodont zones for the Emsian through Givetian are based on polygnathids and are more useful globally. Shallow water zonations using endemic species of icriodids are used regionally.

Frasnian conodont zones are based on well-studied, rapidly evolving species of *Ancryodella* and *Palmatolepis.* The MN (Montagne Noire) zonation of Klapper (1989), renamed as Frasnian Zonation (FZ, Klapper & Kirchgasser 2016) is now more widely used than the traditional Frasnian part of the “Late Devonian Standard Zonation” by Ziegler & Sandberg (1990) because it is more detailed and can be applied globally. Shallow water areas are dominated by polygnathids, but local polygnathid zones in Russia (e.g., Ovnatanova & Kononova 2001, 2008) and Alberta (Klapper & Lane 1985) are difficult to correlate with the deeper water zonation. The well documented Famennian global deeper water conodont zonation is mostly based on *Palmatolepis* species following Ziegler (1962, 1969) and updated by Ziegler & Sandberg (1984, 1990). Spalletta et al. (2017) recommended a simplified and slightly revised zonal scheme emphasizing FADs for the Famennian that was mostly adopted for the GTS 2020. Detailed range charts for species were included. The latest Famennian part was updated by Corradini et al. (2021) and Spalletta et al. (2021). Regional zonations for endemic shallow-water faunas using polygnathids have been proposed (Becker et al. 2020), and an alternative Frasnian-Famennian zonation for very shallow water strata based on icriodids exists (Sandberg & Dreesen 1984). The Devonian biozonation scheme here proposed (Fig. 9) is widely applicable.

6.5. Carboniferous

No single global zonation for the Mississippian Subsystem exists (Fig. 10). Barrick et al. (2022) showed that four major regional zonations are in use: the European deep-water zonation, the standard Russian zonation, the South China zonation and the North American Midcontinent zonation. The taxa used in these zonations are essentially the same, but in each region the succession of species and reported ranges differ slightly, which has led to different zonations. Versions of the European deep-water zonation and the Midcontinent zonations are shown in GTS 2020 (Aretz et al. 2020), and the assertion that a detailed global zonation exists is misleading. Global correlations can be made at the substage boundary level, but exact biostratigraphic correlation is possible at only a few

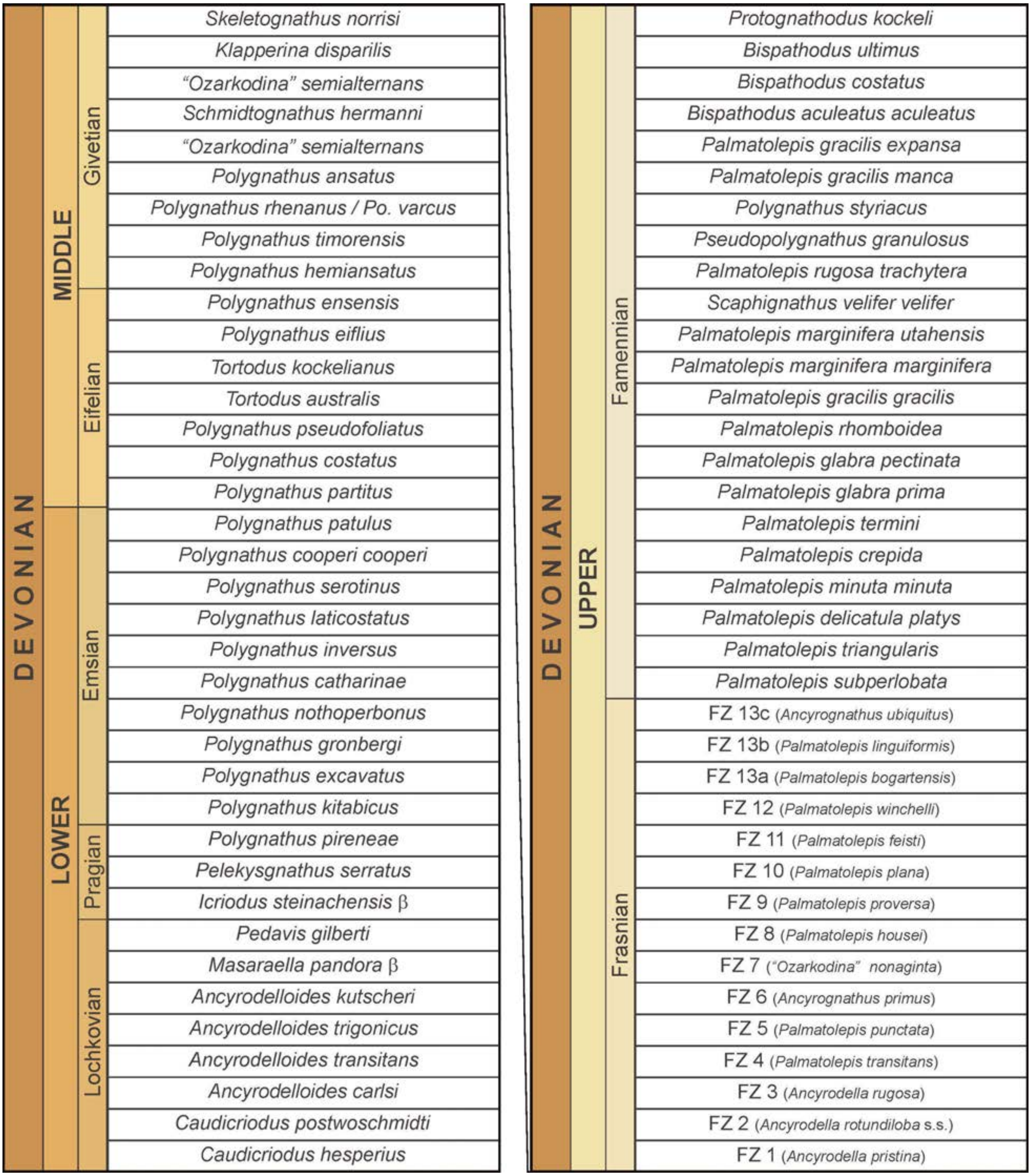

DEVONIAN	MIDDLE	Givetian	*Skeletognathus norrisi*
			Klapperina disparilis
			"Ozarkodina" semialternans
			Schmidtognathus hermanni
			"Ozarkodina" semialternans
			Polygnathus ansatus
			Polygnathus rhenanus / Po. varcus
			Polygnathus timorensis
			Polygnathus hemiansatus
		Eifelian	*Polygnathus ensensis*
			Polygnathus eiflius
			Tortodus kockelianus
			Tortodus australis
			Polygnathus pseudofoliatus
			Polygnathus costatus
			Polygnathus partitus
	LOWER	Emsian	*Polygnathus patulus*
			Polygnathus cooperi cooperi
			Polygnathus serotinus
			Polygnathus laticostatus
			Polygnathus inversus
			Polygnathus catharinae
			Polygnathus nothoperbonus
			Polygnathus gronbergi
			Polygnathus excavatus
			Polygnathus kitabicus
		Pragian	*Polygnathus pireneae*
			Pelekysgnathus serratus
			Icriodus steinachensis β
		Lochkovian	*Pedavis gilberti*
			Masaraella pandora β
			Ancyrodelloides kutscheri
			Ancyrodelloides trigonicus
			Ancyrodelloides transitans
			Ancyrodelloides carlsi
			Caudicriodus postwoschmidti
			Caudicriodus hesperius

DEVONIAN	UPPER	Famennian	*Protognathodus kockeli*
			Bispathodus ultimus
			Bispathodus costatus
			Bispathodus aculeatus aculeatus
			Palmatolepis gracilis expansa
			Palmatolepis gracilis manca
			Polygnathus styriacus
			Pseudopolygnathus granulosus
			Palmatolepis rugosa trachytera
			Scaphignathus velifer velifer
			Palmatolepis marginifera utahensis
			Palmatolepis marginifera marginifera
			Palmatolepis gracilis gracilis
			Palmatolepis rhomboidea
			Palmatolepis glabra pectinata
			Palmatolepis glabra prima
			Palmatolepis termini
			Palmatolepis crepida
			Palmatolepis minuta minuta
			Palmatolepis delicatula platys
			Palmatolepis triangularis
			Palmatolepis subperlobata
		Frasnian	FZ 13c (*Ancyrognathus ubiquitus*)
			FZ 13b (*Palmatolepis linguiformis*)
			FZ 13a (*Palmatolepis bogartensis*)
			FZ 12 (*Palmatolepis winchelli*)
			FZ 11 (*Palmatolepis feisti*)
			FZ 10 (*Palmatolepis plana*)
			FZ 9 (*Palmatolepis proversa*)
			FZ 8 (*Palmatolepis housei*)
			FZ 7 (*"Ozarkodina" nonaginta*)
			FZ 6 (*Ancyrognathus primus*)
			FZ 5 (*Palmatolepis punctata*)
			FZ 4 (*Palmatolepis transitans*)
			FZ 3 (*Ancyrodella rugosa*)
			FZ 2 (*Ancyrodella rotundiloba* s.s.)
			FZ 1 (*Ancyrodella pristina*)

Fig. 9. Devonian conodont zonation compiled with some variations after (in stratigraphic order) Corradini & Corriga (2012), Valenzuela-Ríos et al. (2015), Slavík (2004), Becker et al. (2020), Klapper & Kirchgasser (2016) and Spalletta et al. (2017). Chronostratigraphic intervals not to scale. Abbreviation: *Po.* = *Polygnathus*.

levels. The lowermost Mississippian is zoned by widely distributed *Siphonodella* species, except in shallow-water facies, where other polygnathids and siphonodellids are used. However, owing to work connected with the redefinition of the base of Carboniferous System and taxonomic problems of some siphonodellids, the classical lower-middle Tournaisian scheme by Sandberg et al. (1978) has been revised into

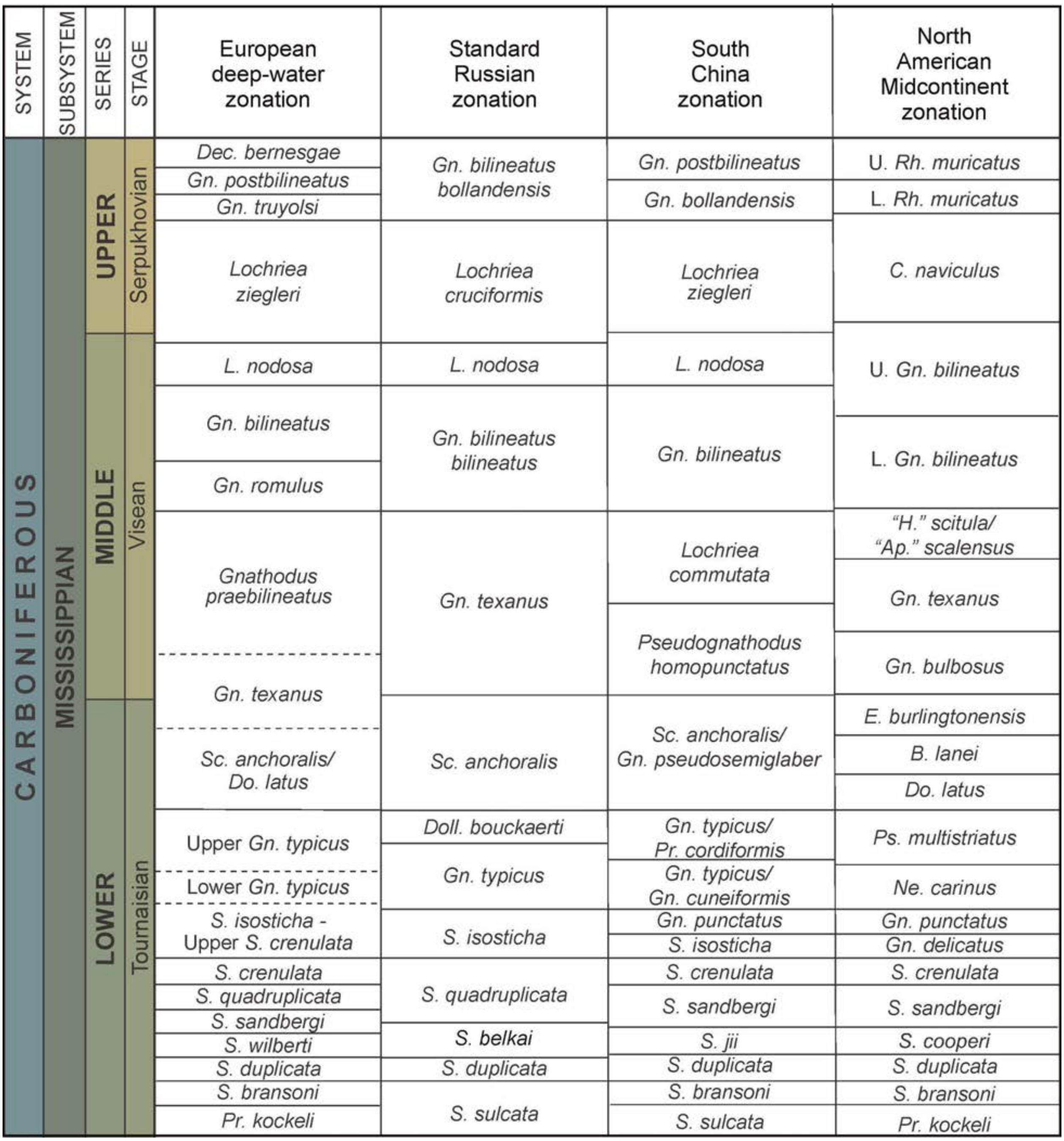

SYSTEM	SUBSYSTEM	SERIES	STAGE	European deep-water zonation	Standard Russian zonation	South China zonation	North American Midcontinent zonation
CARBONIFEROUS	MISSISSIPPIAN	UPPER	Serpukhovian	*Dec. bernesgae*	*Gn. bilineatus bollandensis*	*Gn. postbilineatus*	U. *Rh. muricatus*
				Gn. postbilineatus			
						Gn. bollandensis	L. *Rh. muricatus*
				Gn. truyolsi			
				Lochriea ziegleri	*Lochriea cruciformis*	*Lochriea ziegleri*	*C. naviculus*
							U. *Gn. bilineatus*
		MIDDLE	Visean	*L. nodosa*	*L. nodosa*	*L. nodosa*	
				Gn. bilineatus	*Gn. bilineatus bilineatus*	*Gn. bilineatus*	
							L. *Gn. bilineatus*
				Gn. romulus			
				Gnathodus praebilineatus	*Gn. texanus*	*Lochriea commutata*	*"H." scitula/ "Ap." scalensus*
							Gn. texanus
						Pseudognathodus homopunctatus	
							Gn. bulbosus
				Gn. texanus			
		LOWER	Tournaisian		*Sc. anchoralis*	*Sc. anchoralis/ Gn. pseudosemiglaber*	*E. burlingtonensis*
				Sc. anchoralis/ Do. latus			*B. lanei*
							Do. latus
				Upper *Gn. typicus*	*Doll. bouckaerti*	*Gn. typicus/ Pr. cordiformis*	*Ps. multistriatus*
					Gn. typicus		
				Lower *Gn. typicus*		*Gn. typicus/ Gn. cuneiformis*	*Ne. carinus*
				S. isosticha - Upper *S. crenulata*	*S. isosticha*	*Gn. punctatus*	*Gn. punctatus*
						S. isosticha	*Gn. delicatus*
				S. crenulata	*S. quadruplicata*	*S. crenulata*	*S. crenulata*
				S. quadruplicata		*S. sandbergi*	*S. sandbergi*
				S. sandbergi			
				S. wilberti	*S. belkai*	*S. jii*	*S. cooperi*
				S. duplicata	*S. duplicata*	*S. duplicata*	*S. duplicata*
				S. bransoni	*S. sulcata*	*S. bransoni*	*S. bransoni*
				Pr. kockeli		*S. sulcata*	*Pr. kockeli*

Fig. 10. Correlation of regional conodont zonations for the Mississippian Subsystem (lower Carboniferous). Chart simplified from Barrick et al. (2022, fig. 13) where descriptions of the regional zonations and interregional correlations can be found. Genus abbreviations: *Ap.* = *Apatognathus*; *B.* = *Bactrognathus*; *C.* = *Cauvusgnathus*; *Dec.* = *Declinognathodus*; *Do.* = *Doliognathus*; *Doll.* = *Dollymae*; *Gn.* = *Gnathodus*; *H.* = *Hindeodus*; *L.* = *Lochriea*; *Pr.* = *Protognathodus*; *Ps.* = *Pseudopolygnathus*; *Rh.* = *Rhachistognathus*; *S.* = *Siphonodella*; Sc. = *Scaliognathus.*

slightly different zonations (e.g., Kaiser et al. 2009, Becker et al. 2016, Corradini et al. 2017, Hogancamp et al. 2019, Zhuravlev et al. 2021). The extinction of siphonodellids was followed by a middle Tournaisian radiation of *Gnathodus* species, which define some zones to the end of the Mississippian, but the species-level taxonomy of *Gnathodus* is still unsettled. A short late Tournaisian maximum in diversity, characterized by several short-lived genera, such as *Scaliognathus*, allows for easy correlation of this interval. Low

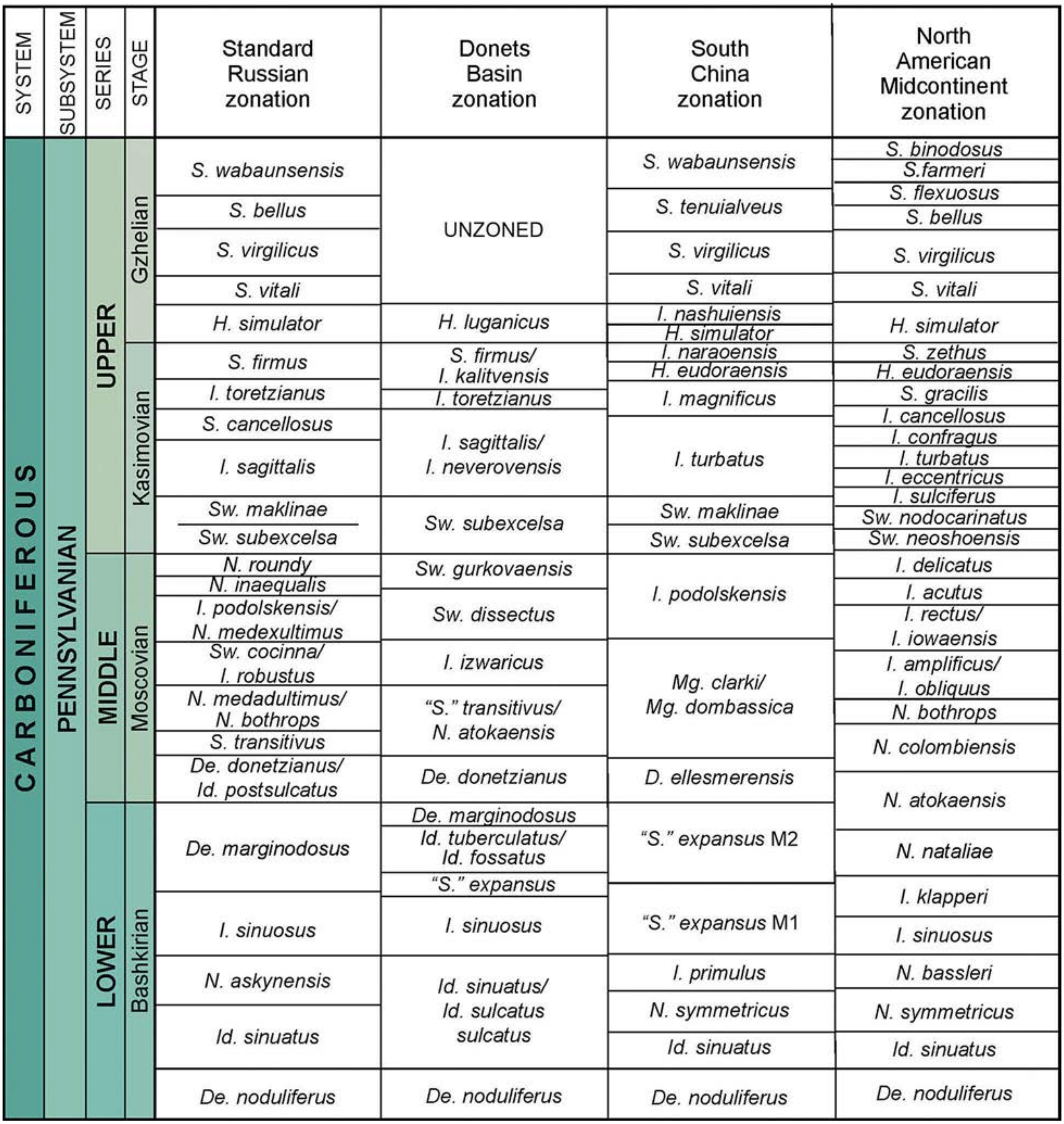

Fig. 11. Correlation of regional conodont zonations for the Pennsylvanian Subsystem (upper Carboniferous). Chart simplified from Barrick et al. (2022, fig. 14) where descriptions of the regional zonations and interregional correlations can be found. The base of the Kasimovian is shown at the traditional level whereas the proposed alternative level lies at the base of the *Idiognathodus eccentricus* zone in North America. Genus abbreviations: *D.* = *Diplognathodus*; *De.* = *Declinognathodus*; *I.* = *Idiognathodus*; *Id.* = *Idiognathoides*; *H.* = *Heckelina*; *Mg.* = *Mesogondolella*; *N.* = *Neognathodus*; *S.* = *Streptognathodus*; *Sw.* = *Swadelina*.

diversity faunas of *Gnathodus* species and carminate species continue through the Visean into the Serpukhovian. In the late Visean and Serpukhovian, a burst of diversification in *Lochriea* provides biostratigraphic resolution in offshore facies. Local shallow-water zonations based on *Taphrognathus, Cavusgnathus* and *Mestognathus* are difficult to correlate to offshore zonations (e.g., von Bitter et al. 1986).

During the Pennsylvanian differences in regional zonations increased because of expanding endemism.

Four major regional zonations are in use (Fig. 11): the Russian standard zonation, the Donets Basin zonation, the South China zonation, and the North American Midcontinent zonation (Barrick et al. 2022). The "European" zonation shown in GTS 2020 seems to be a rough composite of the Russian and Donets Basin zonations, but no explanation was provided. Near the base of the Pennsylvanian, the extinction of typical Mississippian taxa was followed by a major radiation of new gnathodid genera. These new genera characterize Bashkirian and early Moscovian zonations: *Rhachistognathus*, *Declinognathodus*, *Neognathodus*, *Idiognathoides*, and *Idiognathodus*. By the middle of the Moscovian, fewer useful genera remained, *Idiognathodus*, *Neognathodus*, and *Swadelina*, and the increasing number of endemic species makes global correlation difficult. During the early Kasimovian, the end-Desmoinesian extinction event reduced diversity sharply and subsequent early Kasimovian radiations in idiognathodids occurred largely independently in North America, Eurasia, and South China (Barrick et al. 2023). As *Idiognathodus* species declined in diversity during the Kasimovian, groups of grooved and troughed idiognathodids diversified and dominated faunas. These forms have traditionally been included in *Streptognathodus*, a North American Kasimovian clade, but comprise a series of clades unrelated to *Streptognathodus* (Barrick et al. 2023). During the Gzhelian, *Heckelina* and "*Streptognathodus*" species become cosmopolitan in distribution and similar, but long ranging zones are used (Barrick et al. 2022). Near the end of the Gzhelian, rapid diversification of a group of "*Streptognathodus*" species extended into the early Cisuralian.

The distribution of species first and last appearances during the Middle and Late Pennsylvanian reflects the cyclicity imposed by the eustatic events that produced the corresponding stratigraphic sequences. This is best seen in the North America Midcontinent region where zones are confined to one or a few sequences (cyclothems; Heckel 2013). Correlation often involves using conodonts to recognize age-equivalent cycles, or sequence biostratigraphy, such in the western United States (Ritter et al. 2002, 2022). On a global scale, cyclostratigraphy has been used to correlate endemic Middle and Upper Pennsylvanian conodont faunas (Heckel et al. 2007). Schmitz & Davydov (2012) used a combination of conodont range events in a CONOP9 composite, cyclostratigraphy and high-precision U-Pb zircon ages to develop a ca. 0.4-Myr resolution model for the Middle Pennsylvanian to early Permian (Cisuralian).

6.6. Permian

Henderson (2018) summarized Permian conodont biostratigraphy and described 40 international zones and 35 additional regional zones for the nine stages and 47 million years of the Permian. An updated version is here presented (Fig. 12). Henderson & Shen (2020) showed the distribution of 44 zones throughout the Permian. Almost all of the zones are defined as partial range lineage zones. Earlier biozonal schemes were discussed by Clark & Behnken (1970) and Kozur (1978). The Cisuralian Series (lower Permian) consists of the Asselian, Sakmarian, Artinskian, and Kungurian stages. The Asselian is zoned on the basis of rapid evolution of species of "*Streptognathodus*", which is a holdover taxon from the Carboniferous and may represent more than one lineage. The base of the Permian is recognized by the evolution of "*Streptognathodus*" *isolatus* with the GSSP set at the Aidaralash section in Kazakhstan (Davydov et al. 1998, Henderson & Shen 2020). "*Streptognathodus*" becomes extinct at or near the Asselian-Sakmarian boundary and is ecologically replaced by the genus *Sweetognathus* (Chernykh 2005, 2006). These changes represent an event marking the end of the main phase of the late Paleozoic Ice Age. *Sweetognathus* and an evolutionary descendant *Neostreptognathodus* provide the basis for international zonal schemes for most of the remaining lower Permian. At least two lineages exhibiting parallel evolution are currently attributed to *Sweetognathus* (Petryshen et al. 2020) and this has complicated biostratigraphic correlation. Biostratigraphic zonal resolution will be enhanced when these lineages are fully developed and described (see Chernykh et al. 2023 for progress). Chernykh (2005, 2006) demonstrated a zonation based on *Mesogondolella* for middle Asselian and Sakmarian from slope successions in the Urals, but few studies elsewhere yielded these taxa until recently. The taxon is presumably controlled by position below a thermocline and is usually found in more offshore settings. Now the base-Sakmarian is recognized by the FAD of *Mesogondolella monstra* at the Usolka section and comparisons were made with Nevada and Arctic Canada (Chernykh et al. 2020, Beauchamp et al. 2022). The base-Artinskian is recognized by the FAD of *Sweetognathus asymmetricus* at the Dal'ny Tulkas section in the Urals (Chernykh et al. 2023). Based on the recognition of two parallel lineages of *Sweetognathus*, cyclothems in Kansas (Boardman et al. 2009) that were for a long time correlated as lower Artinskian are now correlated with the upper Asselian (see Henderson 2018 for ca. 0.4 Myr astronomical tuning). The base Sakmarian and base Artinskian are both defined within transgressive facies at or near the maximum flooding surface, which is generally the case when boundaries are defined by pelagic conodonts. The upper Artinskian is correlated with the near cosmopolitan taxon *Neostreptognathodus pequopensis*. This level nearly coincides with the Wolfcampian-Leonardian boundary in the USA, which is based on the first occurrence of the fusulinid *Schwagerina crassitectoria*. The offset between the American zonation and International can be explained by differences in environmental preferences of conodonts *versus* fusulinids. The base-Kungurian is recognized by the FAD of *Neostreptognathodus pnevi* at Mechetlino in the Urals and Rockland in Nevada (Henderson et al. 2012). Additional Kungurian zones are correlated by the evolution of *Neostreptognathodus* species. Cisuralian zones are typically cosmopolitan and are broadly correlated in many regions. In contrast, distinct provincialism develops (Mei & Henderson 2001) within the middle Permian or Guadalupian Series and upper Permian or Lopingian Series. The recognition of geographic clines assists correlation (Henderson & Mei 2007) at these levels.

The middle Permian is zoned mostly using species of a serrated gondolellid called *Jinogondolella*. *Sweetognathus* continues to be available for zonation in shallow, warm-water platform environments within the Equatorial Warm-water Province (Mei & Henderson 2001, Mei et al. 2002). The zonation of *Jinogondolella* species is well correlated between South China and the Delaware Basin in West Texas. The FADs of *Jinogondolella nankingensis*, *J. aserrata*, and *J. postserrata* are used to recognize the base-Roadian, base-Wordian, and base-Capitanian respectively. The GSSPs are all located in the Guadalupe Mts of West Texas (Lambert et al. 2000, Wardlaw 2000). The

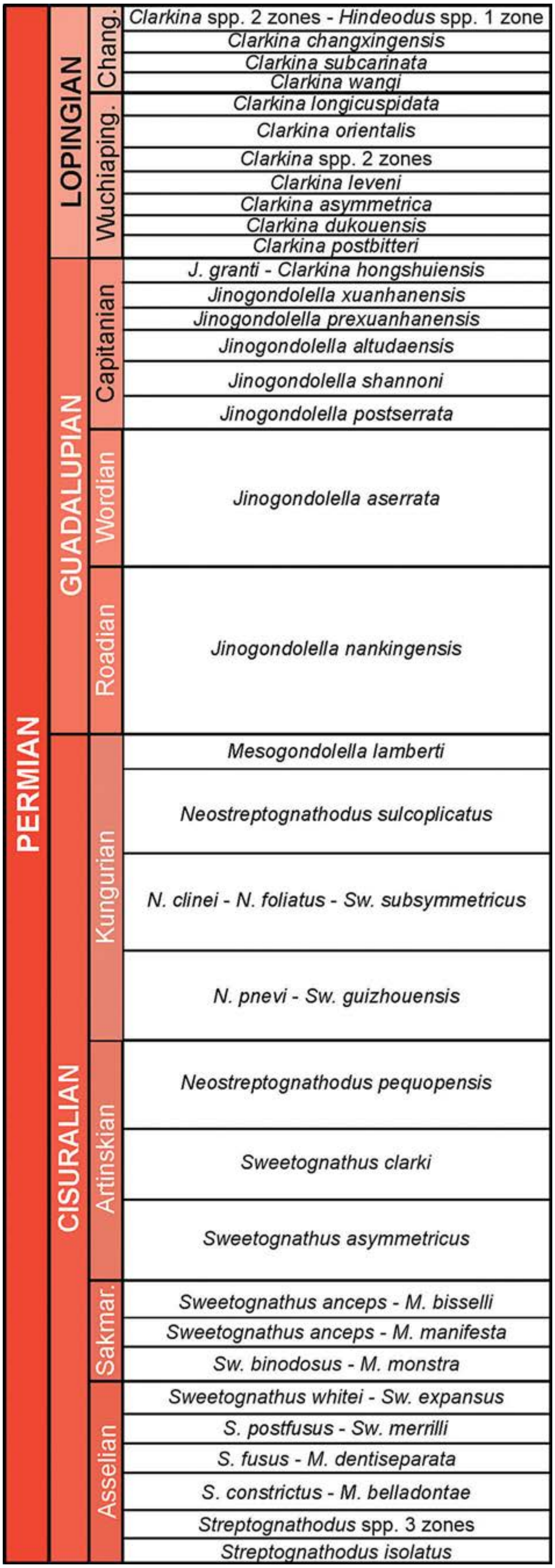

PERMIAN	LOPINGIAN	Chang.	*Clarkina* spp. 2 zones - *Hindeodus* spp. 1 zone
			Clarkina changxingensis
			Clarkina subcarinata
			Clarkina wangi
		Wuchiaping.	*Clarkina longicuspidata*
			Clarkina orientalis
			Clarkina spp. 2 zones
			Clarkina leveni
			Clarkina asymmetrica
			Clarkina dukouensis
			Clarkina postbitteri
	GUADALUPIAN	Capitanian	*J. granti - Clarkina hongshuiensis*
			Jinogondolella xuanhanensis
			Jinogondolella prexuanhanensis
			Jinogondolella altudaensis
			Jinogondolella shannoni
			Jinogondolella postserrata
		Wordian	*Jinogondolella aserrata*
		Roadian	*Jinogondolella nankingensis*
	CISURALIAN	Kungurian	*Mesogondolella lamberti*
			Neostreptognathodus sulcoplicatus
			N. clinei - N. foliatus - Sw. subsymmetricus
			N. pnevi - Sw. guizhouensis
		Artinskian	*Neostreptognathodus pequopensis*
			Sweetognathus clarki
			Sweetognathus asymmetricus
		Sakmar.	*Sweetognathus anceps - M. bisselli*
			Sweetognathus anceps - M. manifesta
			Sw. binodosus - M. monstra
		Asselian	*Sweetognathus whitei - Sw. expansus*
			S. postfusus - Sw. merrilli
			S. fusus - M. dentiseparata
			S. constrictus - M. belladontae
			Streptognathodus spp. 3 zones
			Streptognathodus isolatus

Fig. 12. Permian conodont zonation (modified from Henderson 2018). The three *Streptognathodus* zones in the Asselian include in ascending order *S. glenisteri*, *S. cristellaris*, and *S. sigmoidalis*. The two *Clarkina* zones in the Wuchiapingian include in ascending order *C. guangyuanensis* and *C. transcaucasica*. The two *Clarkina* zones in the upper Changhsingian include *C. yini* and *C. meishanensi* – *C. zhejiangensis*. The *Hindeodus* Zone is *H. praeparvus* – *H. changxingensis*. Abbreviations: *J.* = *Jinogondolella*; *M* = *Mesogondolella*; *N* = *Neostreptognathodus*; *S* = *Streptognathodus*; *Sw* = *Sweetognathus*; Sakmar. = Sakmarian; Wuchiaping. = Wuchiapingian; Chang. = Changhsingian.

zonation is not applicable to cool-water provinces, except a brief interval allowing correlation of the base-Guadalupian as shown by a geographic cline (Henderson & Mei 2007). Above this level the cool-water provinces are typified by longer ranging species of *Mesogondolella* and endemic *Vjalovognathus* in the peri-Gondwana cool-water province. The latest Guadalupian is associated with the most significant lowstand of sea-level during the Phanerozoic. In fact, the Delaware Basin became evaporative and isolated. This lowstand would have isolated populations and adaptive pressure led to the evolution of a new gondolellid called *Clarkina*.

The upper Permian or Lopingian Series is zoned on the basis of species of *Clarkina*, but in shallow, warm-water environments species of *Iranognathus*, which evolved from *Sweetognathus*, have been used. The zonation has been described in detail in many papers (Shen & Mei 2010, Yuan et al. 2014, 2017). All of these taxa are typical of the Equatorial Warm-water Province and especially in the region from West Texas to South China. In cool-water provinces long-ranging species of *Mesogondolella* continued to evolve (Beauchamp et al. 2009). Integration of these two zonal schemes is poorly constrained (Henderson 2018). Near the very end of the Permian a runaway greenhouse led to Earth's greatest mass extinction event, but conodonts were only slightly affected. *Clarkina* migrated and appears in the Canadian Arctic about 300 Kyrs before the close of the Permian (Algeo et al. 2012). Species of *Clarkina* are used for zonation of part of the Lower Triassic and the zonal taxa were again more cosmopolitan.

6.7. Triassic

Conodonts continued to evolve through the Triassic, but ultimately became extinct at the end of Triassic closing their 300 Myr evolutionary record. Orchard (2010) provided a summary of the role of conodonts in stage boundary definitions for the entire Triassic. Ogg & Chen (2020) showed the distribution of 46 Tethyan zones for the 50.5 million years of the Triassic; they also showed more generalized regional zones for the Arctic/Panthalassan and South China regions. A generalized zonation based on these schemes is provided in Figure 13. The base of the Triassic is recognized by *Hindeodus parvus* and *Clarkina* (formerly *Neogondolella*) *taylorae*, which represent holdover taxa from the Permian; both became extinct within the short Induan Stage (Orchard 2010). Intense study of the Permian-Triassic boundary interval has resulted in the recognition of many species of *Hindeodus* and its derivative *Isarcicella* as well as *Clarkina* and its derivative *Neoclarkina* that offer high-resolution biostratigraphic control over a wide region of the globe (Henderson et al. 2018). The upper Induan and Olenekian stages are dominated by pedomorphic gondolellids demonstrating an evolutionary radiation in which they have lost the platform or only bear remnants, including *Neospathodus*, *Novispathodus*, *Discretella*, *Sweetospathodus*, and others with a platform, including *Borinella*, *Neogondolella*, and *Columbitella*. The base-Olenekian is recognized by the FAD of *Novispathodus waageni*, but *Neospathodus posterolongatus* and an ornate *Eurygnathodus costatus* provide support.

The Middle Triassic includes the Anisian and Ladinian stages. The Olenekian-Anisian boundary interval and lower Anisian is represented by a major transgressive succession in which *Triassospathodus* dominated faunas, especially *T. homeri*, give way to *Chiosella*; *C. timorensis* may be used to mark the base-Anisian, but it is still debated how well this correlates with the traditional ammonoid boundary. Species of *Magnigondolella* and *Neogondolella* are used to correlate the upper Olenekian and Anisian (Golding & Orchard 2016, 2018). Conodonts are important index fossils for the remainder of the Triassic, but ammonoid and bivalve evolution are playing the main role as defining taxa. The base of the Ladinian is recognized by the FAD of the ammonoid *Eoprotrachyceras curionii*, but species of *Neogondolella*, *Paragondolella*, and *Budurovignathus* constrain many zone level correlations. The FAD of *Budurovignathus praehungaricus* was considered as a candidate for the base-Ladinian.

The Upper Triassic includes the stages Carnian, Norian, and Rhaetian. The base-Carnian is recognized by the FAD of the ammonoid *Daxatina canadensis*, but species of *Carnepigondolella*, *Metapolygnathus*, *Paragondolella*, *Parapetella*, and *Quadraella* constrain many correlations; the FAD of *Quadraella polygnathiformis* was a candidate to recognize the boundary. The base-Norian is recognized by the FAD of the bivalve *Halobia austriaca*, but species of *Ancyrogondolella*, *Carniepigondolella*, *Epigondolella*, *Metapolygnathus*, *Mockina*, *Norigondolella*, and *Orchardella* constrain many zone level correlations; the FAD of *Metapolygnathus parvus* was a candidate to recognize the boundary. The base of the Rhaetian is not defined yet and species of *Parvigondolella* and *Misikella* constrain many zone level correlations. The FAD of *Misikella posthernsteini* is under consideration to mark the base-Rhaetian boundary. The tragic end-

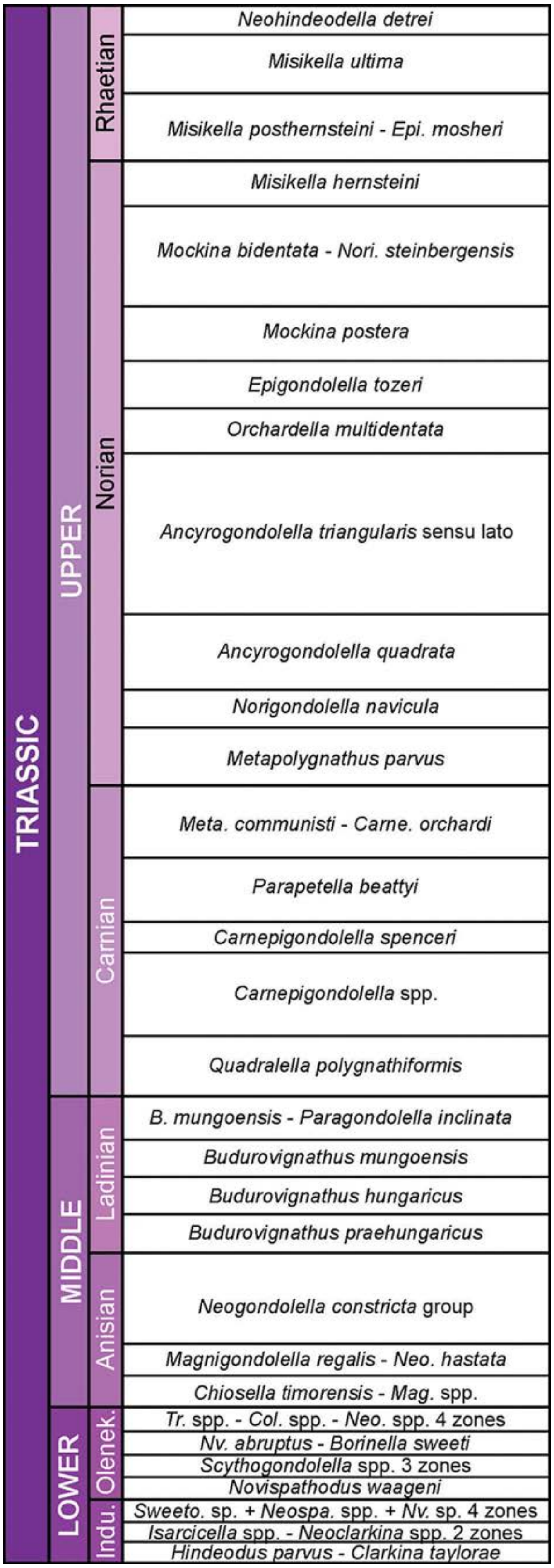

TRIASSIC	UPPER	Rhaetian	*Neohindeodella detrei*
			Misikella ultima
			Misikella posthernsteini - Epi. mosheri
		Norian	*Misikella hernsteini*
			Mockina bidentata - Nori. steinbergensis
			Mockina postera
			Epigondolella tozeri
			Orchardella multidentata
			Ancyrogondolella triangularis sensu lato
			Ancyrogondolella quadrata
			Norigondolella navicula
			Metapolygnathus parvus
		Carnian	*Meta. communisti - Carne. orchardi*
			Parapetella beattyi
			Carnepigondolella spenceri
			Carnepigondolella spp.
			Quadralella polygnathiformis
	MIDDLE	Ladinian	*B. mungoensis - Paragondolella inclinata*
			Budurovignathus mungoensis
			Budurovignathus hungaricus
			Budurovignathus praehungaricus
		Anisian	*Neogondolella constricta* group
			Magnigondolella regalis - Neo. hastata
			Chiosella timorensis - Mag. spp.
	LOWER	Olenek.	*Tr.* spp. - *Col.* spp. - *Neo.* spp. 4 zones
			Nv. abruptus - Borinella sweeti
			Scythogondolella spp. 3 zones
			Novispathodus waageni
		Indu.	*Sweeto.* sp. + *Neospa.* spp. + *Nv.* sp. 4 zones
			Isarcicella spp. - *Neoclarkina* spp. 2 zones
			Hindeodus parvus - Clarkina taylorae

Fig. 13. Triassic conodont zonation. The Lower Triassic zonation is modified from Henderson et al. (2018). The Middle and Upper Triassic is modified from several sources including primarily from Ogg & Chen (in GTS 2020), and also from Orchard (2010), Mazza et al. (2012), Golding & Orchard (2018), 2020), and Orchard & Golding (2023). There is no single standard zonation for Middle and Upper Triassic and the generic assignments are in a state of flux. The two Induan *Isarcicella* – *Neoclarkina* zones include in ascending order *I. staeschei* – *N. krystyni* and *I. isarcica* – *N. discreta*. The four *Sweeto*. – *Neospa*. – *Nv.* zones include in ascending order *Sweetospathodus kummeli*, *Neospathodus dieneri*, *Neospathodus cristagalli*, and *Novispathodus pakistanensis* zones. The three Olenekian *Scythogondolella* spp. zones include in ascending order *Scy. lachrymiformis*, *Scy. mosheri*, and *Scy. milleri*. The Olenekian *Tr.* – *Col.* – *Neo*. spp. zones include in ascending, but overlapping order, *Triassospathodus symmetricus*, *Columbitella* spp., *Neogondolella* spp., *Tr. homeri*, and *Neogondolella bucheri*. Abbreviations: Indu. = Induan; Olenek. = Olenekian. Neo = *Neogondolella*; Mag = *Magnigondolella*; Nori = *Norigondolella*; Epi = *Epigondolella*.

Triassic mass extinction involves the final demise of conodonts, but recently conodonts have been recovered from the earliest Jurassic of Japan (Du et al. 2020, 2023) suggesting that the extinction may be "diachronous".

7. Correlation and integration

Conodont biostratigraphy is the basis for age constraint of any kind of study in the Paleozoic and in the Triassic. Chronostratigraphic boundaries are often defined on the basis of the First Appearance Datum of conodont taxa, or are aligned with the base of conodont zones, and the position of geochemical peaks is often referred to conodont biostratigraphy.

7.1. Chronostratigraphy

Conodonts are the most used fossil group in the formal definition of chronostratigraphic boundaries. Twenty-seven stage boundaries are marked by the FAD of conodont taxa (Fig. 14, Plates 1–3), and many others are tied with the base of a conodont zone. To better underline the significance of conodonts in chronostratigraphy, the two other more used fossil groups are cephalopods and graptolites that mark 17 and 13 boundaries, respectively (data from GST 2020). However, it should be noted that these numbers may change,

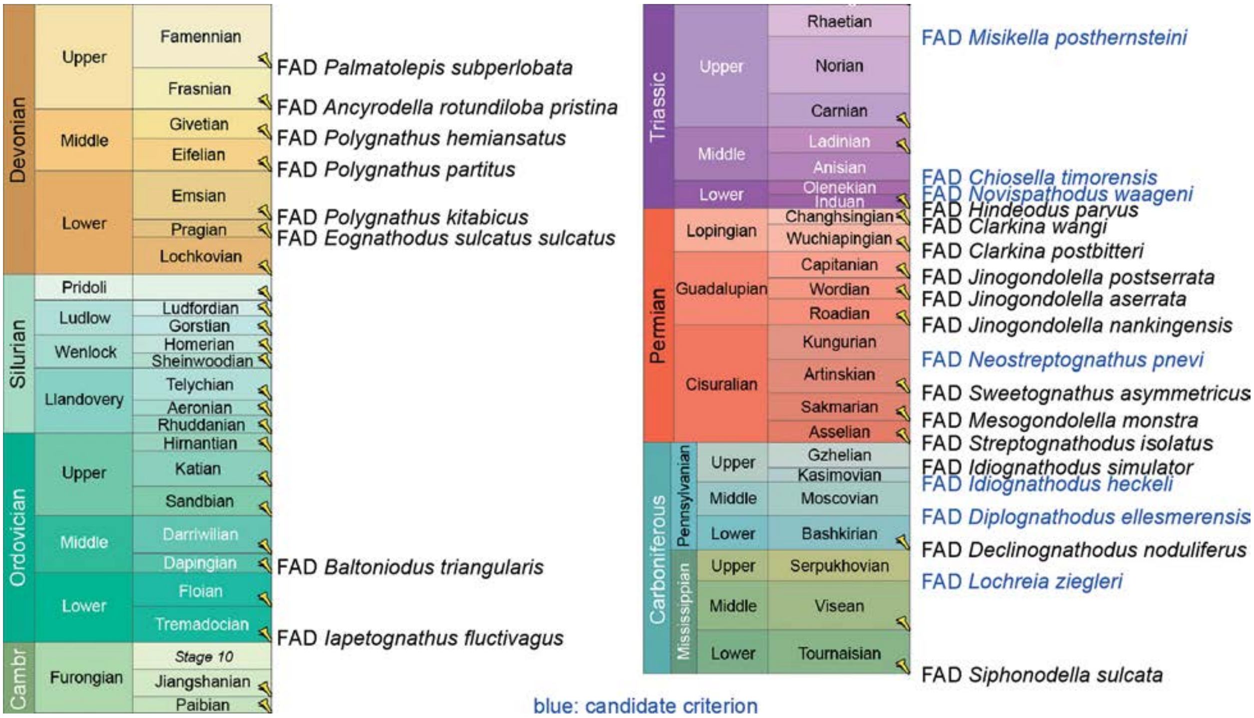

Fig. 14. Chronostratigraphic boundaries defined by FAD of conodont taxa.

Plate 1. Selected Ordovician, Silurian and Devonian conodonts important in stratigraphy. All scale bars = 200 µm. **1.** *Palmatolepis subperlobata* Branson & Mehl, 1934, index for the base of the Famennian, upper view of P_1 element (refigured after Klapper et al. 2004). **2.** *Ancyrodella pristina* Khalymbadzha & Chernysheva, 1970, index for the base of the Frasnian, lower (2a) and upper (2b) views of P_1 element (refigured after Klapper 2021). **3.** *Polygnathus hemiansatus* Bultynck, 1987, index for the base of the Givetian, lower (3a) and upper (3b) views of P_1 element (refigured after Gouwy et al. 2013). **4.** *Polygnathus partitus* Klapper, Ziegler & Mashkova, 1978, index for the base of the base of the Eifelian, upper view of P_1 element (refigured after Berkyová 2007). **5.** *Polygnathus kitabicus* Yolkin, Weddige, Izokh & Erina, 1994, index for the base of the Emsian, lower (5a) and upper (5b) views of P_1 element (refigured after Yolkin et al. 1994). **6.** *Eognathodus sulcatus* Philip, 1965, index for the base of the Pragian, upper view of P_1 element (refigured after Slavík & Hladil 2004). **7.** *Latericriodus hesperius* (Klapper & Murphy, 1975), conodont marker for the base of the Devonian, upper view of P_1 element (refigured after Corradini et al. 2016). **8.** *Zieglerodina zellmeri* Carls, Slavík & Valenzuela-Ríos, 2007, conodont marker for the base of the Přídolí, lateral view of P_1 element (refigured after Carls et al. 2007). **9.** *Polygnathoides siluricus* Branson & Mehl, 1933, the most stable conodont index taxon of the Silurian, upper-lateral view of P_1 element (refigured after Corradini et al. 1998). **10.** *Ancoradella ploeckensis* Walliser, 1964, conodont marker for the base of the Ludfordian, lower (10a) and upper (10b) views of P_1 element (refigured after Corriga et al. 2021). **11.** *Kockelella crassa* (Walliser, 1964), conodont marker for the base of the Gorstian, upper (10a) and lower (10b) views of P_1 element (refigured after Serpagli & Corradini, 1999). **12.** *Distomodus kentuckyensis* (Branson & Branson, 1947), conodont marker for the base of the Silurian, upper view of P_1 element (refigured after Danielsen & Over 2016). **13.** *Amorphognathus ordovicicus* Branson & Mehl, 1933, index taxon for the base of the Katian Ka3 stage slice, posterior view of M element (refigured after Ferretti et al. 2014). **14.** *Pygodus anserinus* Lamont & Lindström, 1957, index of the Zone approximating the base of the Sandbian, upper view of P_1 element (refigured after Bergström & Ferretti 2018). **15.** *Baltoniodus triangularis* Lindström, 1954, index for the base of the Dapingian, lateral view of M element, photo courtesy of S. Stouge. **16.** *Eoplacognathus lindstroemi* (Hamar, 1964), upper view of the Pa element (refigured after Ferretti & Bergström 2022). Several species of the genus *Eoplacognathus* mark the subzones of the Darriwilian. **17.** *Iapetognathus fluctivagus* Nicoll et al., 1999, index for the base of the Ordovician System and of the Tremadocian Stage, lateral (17a) and upper (17b) views of Pa element (refigured after Nicoll et al. 1999).

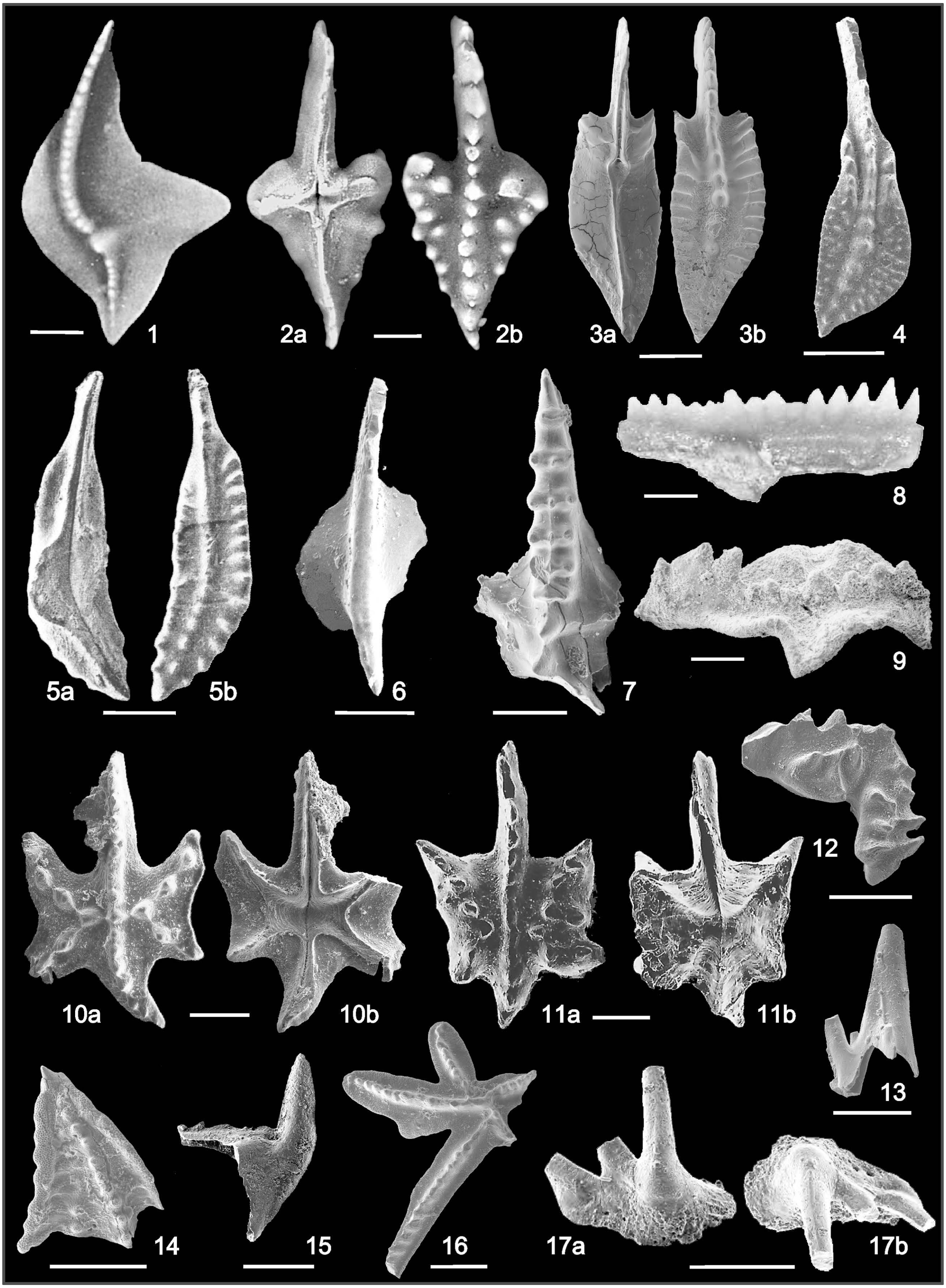
1
2a
2b
3a
3b
4
5a
5b
6
7
8
9
10a
10b
11a
11b
12
13
14
15
16
17a
17b

as some boundaries are not already formally defined by placing a GSSP, and others are under revision.

7.1.1. Ordovician

The Ordovician System is subdivided into 3 series and 7 stages. Conodonts and graptolites represent the most useful index fossils in the Ordovician, and all the stage boundaries are defined by these groups. The base of the Tremadocian (= base of Ordovician System, = base of the Lower Ordovician Series), and the base of the Dapingian (= base of the Middle Ordovician Series) are marked by FAD of the conodonts *Iapetognathus fluctivagus* and *Baltoniodus triangularis*, respectively (Fig. 14). Also, seven of the 20 stage slices of the system (Bergström et al. 2009) are defined by conodonts.

7.1.2. Silurian

The Silurian System is subdivided into 4 series and 8 stages. All but two of the chronostratigraphic subdivisions of the Silurian System were defined on the basis of graptolite faunas. Some are now under revision, because of the imprecise definition and/or problems in the GSSPs, ratified more than 40 years ago. Graptolites are abundant in pelitic facies represented by black shales and rare or absent in calcareous facies, whilst conodonts are abundant in the limestone and very rare in the shales. It results that a precise time equivalence of events based on these groups is difficult due to the limited co-occurrence of these fossils in the same rocks, even though some attempts have been made (e.g., Melchin et al. 2004, 2012, 2020; Corradini et al. 2009, Cramer et al. 2011).

The base of the Rhuddanian (= base of the Llandovery Series, = base of the Silurian System) is aligned with the base of the *D. kentuckyensis* zone, and the base of the Ludfordian is tentatively tied with the base of the *A. ploeckensis* zone (Cramer et al. 2011). All the other stage boundaries fall within conodont zones, although at places the FAD of some species can precisely approximate these levels. As example, the base of the Přídolí Series can be discriminated by the FAD of *Zieglerodina zellmeri* (Slavík & Carls 2012, Vacek et al. 2018). Five of the 24 stage slices of the Silurian (Cramer et al. 2011) are defined by the base of conodont zones.

7.1.3. Devonian

The Devonian System is subdivided into 3 series and 7 stages. Its chronostratigraphy is based mainly on conodonts. Beside the base of the system, defined by the graptolite *Uncinatograptus uniformis* (Prybil), all the other six stage boundaries are defined by FAD of conodont taxa (Fig. 14).

The conodont species FAD that best approximate the base of the Devonian is *Caudicriodus hesperius* (Carls et al. 2007, Corradini & Corriga 2012, Corriga et al. 2016), and recently Ferretti et al. (2022) discussed the Silurian/Devonian boundary from a conodont perspective, highlighting a series of first and last occurrences of species that help to recognize the boundary in many parts of the world.

The base of the Pragian is marked by the FAD of *Eognahodus sulcatus* ssp., the base of the Emsian by *Polygnathus kitabicus*, the base of the Eifelian by *Po. partitus*, the base of the Givetian by *Po. hemiansatus*, the base of the Frasnian by *Ancyrodella*

Plate 2. Selected Carboniferous conodonts important in stratigraphy. All scale bars = 200 μm.
1–2. *Heckelina simulator* (Ellison, 1941), index for base of Gzhelian Stage; upper views of P_1 elements (refigured after Hogancamp et al. 2016). **3–4.** *Idiognathodus heckeli* (Rosscoe & Barrick, 2013), proposed index for base of Kasimovian Stage; upper views of P_1 elements (refigured after Rosscoe & Barrick 2013). **5–6.** *Swadelina subexcelsus* (Alekseev & Goreva, 2001), index for traditional base of Kasimovian Stage; upper views of P_1 elements (refigured after Goreva et al. 2009). **7–8.** *Diplognathodus ellesmerensis* Bender, 1980, proposed index for the base of the Moscovian Stage; lateral views of P_1 elements (refigured after Hu et al. 2020). **9.** *Declinognathodus donetzianus* Nemrovskaya, 1990, proposed index for the base of the Moscovian Stage; upper views of P_1 elements (refigured after Nemyrovska & Hu 2018). **10–11.** *Declinognathodus noduliferous* (Ellison & Graves, 1941), index for the base of the Pennsylvanian Subsystem and of the Bashkirian Stage; upper views of P_1 elements (refigured after Lane et al. 2019). **12–13.** *Lochriea ziegleri* Nemirovskaya, Perret-Mirouse & Meischner, 1994, index for the base of the Serpukovian Stage; upper views of P_1 elements (12: refigured after Qi et al. 2014; 13: refigured after Qi et al. 2018). **14–15.** *Protognathodus kockeli* (Bischoff, 1957), index of the zone that correlates better the newly proposed base of the Carboniferous System; upper views of P_1 elements (refigured after Corradini et al. 2011). **16–17.** *Siphonodella sulcata* (Huddle, 1934), current index for the base of the Carboniferous System; upper (a) and lower (b) views of P_1 elements (refigured after Bahrami et al. 2011).

rotundiloba and the base of the Famennian by *Palmatolepis subperlobata*. However, the base of the Emsian is under revision, but it has been already decided that the new marker will be a conodont.

In the last years the Subcommission on Devonian Stratigraphy subdivided the stages into substages, not already formally ratified by the International Commission on Stratigraphy (for a summary refer to Becker et al. 2020). These subdivisions mostly reflect the classical European regional stages used in Bohemia, Germany, and Belgium. Conodonts are taken to discriminate the base of most substages.

7.1.4. Carboniferous

The Carboniferous System is subdivided into 2 subsystems, 6 series and 7 stages. Only three stages (Tournaisian, Visean, and Bashkirian) are formally

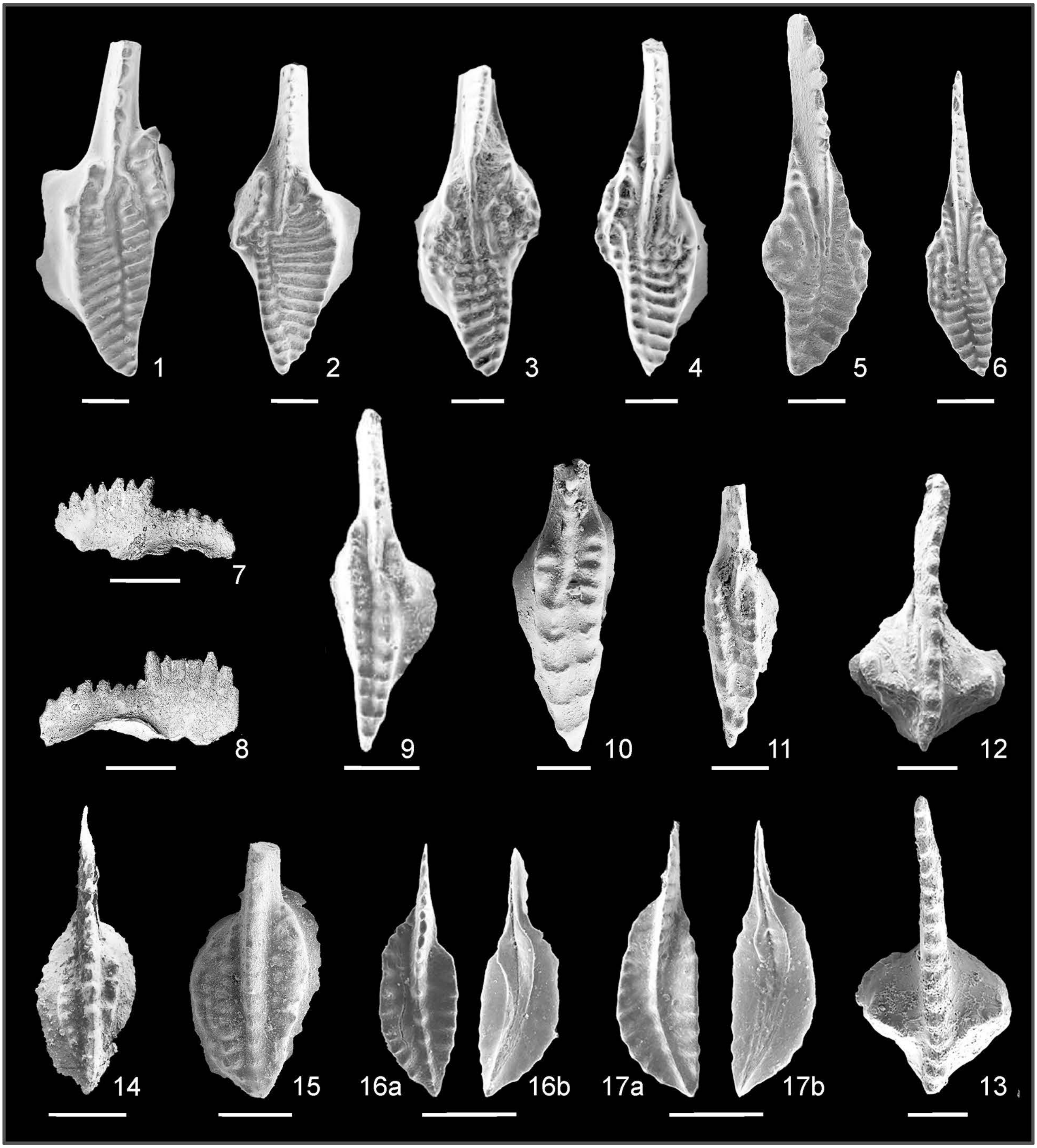

defined with a ratified GSSP. Two are marked by the FAD of conodonts (Fig. 14), while the Visean is marked by the FAD of the foraminifer *Eoparastaffella simplex*. For the other four stages a candidate criterion to discriminate the base has been proposed, and it is always a conodont (Aretz et al. 2020). Barrick et al. (2022) discussed the applicability of conodonts to recognize Carboniferous chronostratigraphic boundaries.

The base of the Carboniferous System (base of Mississippian Subsystem; base of Tournaisian Stage) is marked by the FAD of the conodont *Siphonodella sulcata*. However, due to problems with the GSSP (Kaiser 2009) and the index taxon (Kaiser & Corradini 2011), the ICS established a Working Group with the goal of defining a new criterion for the boundary definition and a new GSSP. Work is still in progress, but the new criterion will be based on a timeline that can be discriminated by different criteria, which should increase the potential of placing the boundary in different facies realms and provinces, and increase the practicability of global correlations. One of these primary criteria is the base of the *Protognathodus kockeli* conodont zone (Aretz & Corradini 2019, 2021). The GSSP for the base of the Serpukhovian Stage will likely use the conodont *Lochriea ziegleri* as the index taxon, but this has not yet been resolved (Nikolaeva et al. 2020).

The GSSP for the mid-Carboniferous boundary (base of the Pennsylvanian Subsystem; base of Bashkirian Stage) was defined to lie at the FO of *Declinognathodus noduliferus sensu lato* within the lower Bird Spring Formation at Arrow Canyon, Nevada (Lane et al. 1999). However, specimens originally identified as *D. noduliferus* at Arrow Canyon are better assigned to *D. inaequalis*, according to recent taxonomic revisions (Hu et al. 2019, Lane et al. 2019). Regardless of the correct name, this *Declinognathodus* species has provided reliable identification of the base of the Pennsylvanian globally. The approximate level for the base of the Moscovian Stage is generally agreed upon and the FO of either the conodont species *Declinognathodus donetzianus* or *Diplognathodus ellemerensis* will be used to place the GSSP (see Hu et al. 2020). Two different levels have been proposed for the base of the Kasimovian (see Barrick et al. 2022) and, depending on which is chosen, either S*wadelina subexcelsus* or an *Idiognathodus* species will be used at the GSSP. *Heckelina simulator* has been selected to indicate the base of the Gzhelian Stage (Heckel et al. 2008), but no stratotype section has been selected.

→

Plate 3. Selected Permian and Triassic conodonts important in stratigraphy. All scale bars = 200 µm.
1. *Misikella ultima* (Kozur & Mock, 1991), a late Rhaetian species; lateral view of P_1 element (refigured after Mazza et al. 2012). **2.** *Misikella posthernsteini* (Kozur & Mock, 1974), potential index for base of the Rhaetian Stage; lateral (a) and lower (b) views of P_1 element (refigured after Mazza et al. 2012). **3.** *Novispathodus waageni eowaageni* (Zhao & Orchard in Zhao et al. 2005), potential index for the base of the Olenekian Stage; lateral view of P_1 element (refigured after Lyu et al. 2018). **4–5.** *Novispathodus waageni waageni* (Sweet, 1970), (4. holotype), potential index for the base of the Olenekian Stage; upper views of P_1 elements (refigured after Lyu et al. 2018). **6.** *Chiosella timorensis* (Nogami, 1968), potential index for the base of the Anisian Stage; lateral (a), lower (b) and upper (c) views P_1 elements (refigured after Golding et al. 2015). **7–8.** *Hindeodus parvus* (Kozur & Pjatakova, 1976), index for the base of the Induan Stage and Triassic System; lateral (7, 8a) and upper (8b) views of P_1 element (refigured after Chen et al. 2009). **9–10.** *Clarkina postbitteri* Mei & Wardlaw in Mei et al. 1994, index for the base of the Wuchiapingian Stage; upper (9b) and upper-lateral (9a, 10) views of P_1 element (refigured after Shen et al. 2024). **11–12.** *Clarkina wangi* (Zhang, 1987), index for the base of the Changhsingian Stage; upper (11a, 12a) and upper-lateral (11b, 12b) views of P_1 element (refigured after Mei et al. 2004). **13–14.** *Neostreptognathodus pnevi* Kozur & Movschovitsch in Movschovitsch et al. 1979, proposed index for the base of the Kungurian Stage; upper views of P_1 elements (refigured after Chernykh et al. 2020a). **15.** *Jinogondolella nankingensis* (Ching (Jin), Y., 1960), index for the base of Roadian Stage; upper view of P_1 element (refigured after Henderson & Shen 2020). **16–17.** *Jinogondolella aserrata* (Clark & Behnken, 1979), index for the base of the Wordian Stage; upper views of P_1 elements (16: refigured after Henderson & Shen 2020; 17: refigured after Wardlaw 2000). **18–19.** *Jinogondolella postserrata* (Behnken, 1975), index for the base of the Capitanian Stage; upper views of P_1 elements (18: refigured after Wardlaw 2000; 19: refigured after Henderson & Shen 2020). **20–21.** "*Streptognathodus" isolatus* Chernykh et al., 1997, index for base of Asselian Stage and Permian System; upper views of P_1 elements (refigured after Henderson & Shen 2020). **22–24.** *Mesogondolella monstra* Chernykh, 2005, index for base of Sakmarian Stage; upper views of P_1 elements (refigured after Chernykh et al. 2020). **25.** *Sweetognathus binododus* Chernykh, 2005, (holotype), supplementary index for base of Sakmarian Stage; upper view of P_1 element (refigured after Chernykh et al. 2020). **26–27.** *Sweetognathus asymmetricus* Sun & Lai *in* Sun et al. 2017, index for the base of the Artinskian Stage; upper views of P_1 elements (refigured after Chernykh et al. 2023).

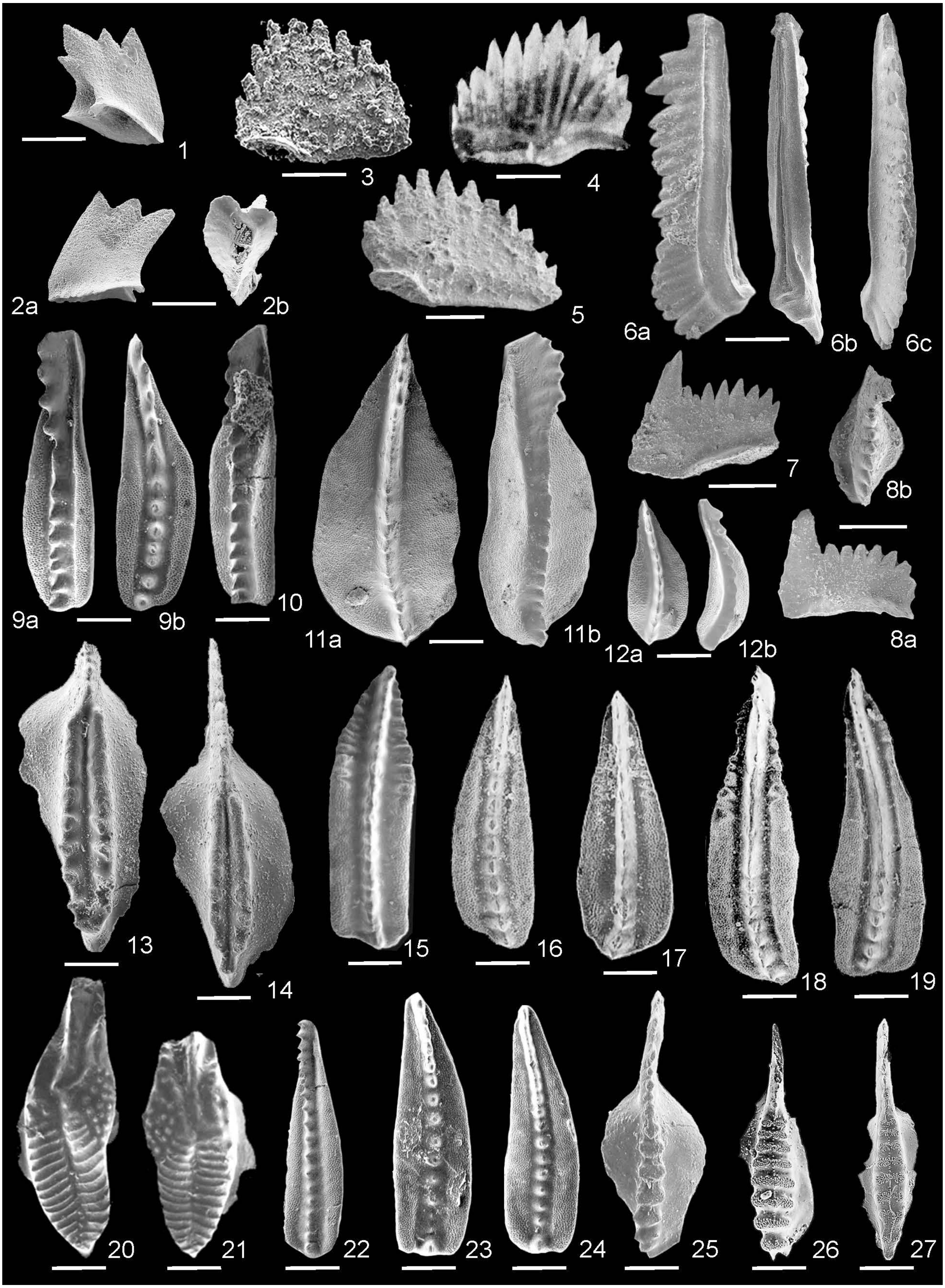
1
3
4
2a
2b
5
6a
6b
6c
9a
9b
10
11a
11b
7
8b
12a
12b
8a
13
14
15
16
17
18
19
20
21
22
23
24
25
26
27

7.1.5. Permian

The Permian System is subdivided into 3 series and 9 stages. All of the stage boundary GSSPs are marked by the FAD of conodont species (Fig. 14; Henderson & Shen 2020). These include the base-Asselian (Carboniferous-Permian boundary) by "*Streptognathodus*" *isolatus* (Davydov et al. 1998), the base-Sakmarian by *Mesogondolella monstra* (Chernykh et al. 2020b), the base-Artinskian by *Sweetognathus asymmetricus* (Chernykh et al. 2023), the base-Kungurian is proposed using *Neostreptognathodus pnevi* as the marker, the base-Roadian by *Jinogondolella nankingensis*, the base-Wordian by *J. aserrata*, the base-Capitanian by *J. postserrata* (Shen et al. 2022), the base-Wuchiapingian by *Clarkina postbitteri* (Jin et al. 2006a), and the base-Changhsingian by *C. wangi* (Jin et al. 2006b). The GSSP for the Kungurian is not yet defined, but there is a general consensus on the stratotype and the criterion, and it is expected to be ratified soon.

7.1.6. Triassic

The Triassic System is subdivided into 3 series and 7 stages. Among those, only three GSSPs are ratified, and only the base of the Induan Stage (= base of the Triassic System) is recognized by a conodont (Fig. 14) – this position is marked by the FAD of *Hindeodus parvus* at the Meishan section in South China (Yin et al. 2001). The FAD of *Novispathodus waageni* is a strong candidate to mark the base-Olenekian Stage. The FAD of *Chiosella timorensis* is a candidate to mark the base-Anisian. Finally, the FAD of *Misikella posthernsteini* is a candidate for the base-Rhaetian. Other stages are a work in progress, as summarized by Ogg & Chen (2020) and the International Commission on Stratigraphy website.

7.2. "Events" and Chemostratigraphy

Event is the name used to indicate a perturbation of the Earth System which often is brought to an extinction. Several biotic and abiotic events have been discriminated in history of the Earth. The severity, regional expression and controlling factors of many of those events are still disputed. They are related to various factors, which can include rapid sea-level changes, volcanism, meteorite impacts, intense continental weathering, the evolution of land plants and soils, chemical changes of the ocean water (e.g., pH, salinity, oxygen content), climate changes, and paleogeography. Many of these events are associated with organic-rich deposits, often black shales (Negri et al. 2009a, b; Hedhli et al. 2023). It is often questionable how these events interrupted the "normal" ups and downs of biodiversity through time (taxonomic severity) and how the structure of ecosystems changed before and after the crises (ecological severity). However, these events have become important time markers and are always related to biostratigraphy.

Since biozonation schemes based on conodonts are the reference and most used schemes for the Ordovician, Devonian, Carboniferous, Permian, and Triassic works, the precise timing of events is referred to conodont zones.

The same apply to chemostratigraphy: the timing of isotopic excursions in these periods is calibrated to conodont zonation schemes.

8. Conclusions

Conodonts represent the best tool for biostratigraphic studies for over 300 million of years of Earth history from the late Cambrian to the Triassic. Rapid evolution and global distribution make these fossils perfect index fossils, and global zonation schemes are widely used to correlate rocks, from all over the world. Conodonts are also the most used tool to correlate the GSSPs, as 27 of them are defined by the FAD of a conodont species. Beside stratigraphy, conodonts are also widely used in Paleoecologic, paleogeographic, and geochemical studies, making them the most useful fossil to study the history of the Earth.

Acknowledgments. Thomas Becker, Derek Briggs, Mark Purnell, John Repetski and Sven Stouge kindly provided material for the preparation of figures and are deeply acknowledged. The comments by three anonymous reviewers helped to improve the manuscript. This research was undertaken within the framework and with the financial support of the European Community – Next Generation EU, Italian Ministry of University and Research, Project P2022K9BE8, PRIN-PNRR 2022 "OCEANS" (AF), Project 2022MAM9ZB, PRIN-2022 "BIOVERTICES" (AF) and Project 2022ZH5RWP, PRIN 2022 "DEEP PAST" (CC). CMH acknowledges support from a NSERC Discovery Grant in Canada. This paper is a contribution to the IGCP Projects n. 735 "Rocks and the Rise of Ordovician Life: Filling knowledge gaps in the Early Palaeozoic Biodiversification" and n. 652 "Reading geologic time in Paleozoic sedimentary rocks".

References

Aldridge, R. J., & Theron, J. N. (1993). Conodonts with preserved soft tissue from a new Ordovician *Konservat-Lagerstätte. Journal of Micropalaeontology*, *12*(1), 113–117. https://doi.org/10.1144/jm.12.1.113

Aldridge, R. J., Purnell, M. A., Gabbott, S. E., & Theron, J. N. (1995). The apparatus architecture and function of *Promissum pulchrum* Kovács-Endrödy (Conodonta, Upper Ordovician) and the prioniodontid plan. *Philosophical Transactions of the Royal Society of London. Series B, Biological Sciences*, *347*(1321), 275–291. https://doi.org/10.1098/rstb.1995.0027

Algeo, T., Henderson, C. M., Ellwood, B., Rowe, H., Elswick, E., Bates, S., … Freeman, K. H. (2012). Evidence for a diachronous Late Permian marine crisis from the Canadian Arctic region. *Geological Society of America Bulletin*, *124*(9-10), 1424–1448. https://doi.org/10.1130/B30505.1

Aretz, M., & Corradini, C. (2019). The redefinition of the Devonian-Carboniferous Boundary: state of the art. In S. Hartenfels, H.-G. Herbig, M. R. W. Amler, & M. Aretz (Eds.), 19*th* International Congress on the Carboniferous and Permian, Cologne July 29–August 2, 2019, Abstracts. *Kölner Forum für Geologie und Paläontologie*, *23*, 31–32.

Aretz, M., & Corradini, C. (2021). Global review of the Devonian-Carboniferous Boundary: An introduction. *Palaeobiodiversity and Palaeoenvironments*, *101*(2), 285–293. https://doi.org/10.1007/s12549-021-00499-8

Aretz, M., Herbig, H. G., & Wang, X. D. (2020). The Carboniferous Period. In F. M. Gradstein, J. G. Ogg, M. D. Schmitz, & G. M. Ogg (Eds.)*, Geologic Time Scale 2020* (pp. 811–874). Amsterdam: Elsevier. https://doi.org/10.1016/B978-0-12-824360-2.00023-1

Bahrami, A., Corradini, C., & Yazdi, M. (2011). Upper Devonian-Lower Carboniferous conodont biostratigraphy in the Shotori Range, Tabas area, Central-East Iran Microplate. *Bollettino della Società Paleontologica Italiana*, *50*, 35–53.

Barnes, C. R., Rexroad, C. B., & Miller, J. F. (1973). Lower Paleozoic provincialism. In F. H. T. Rhodes (Ed.)*, Conodont paleozoology* (pp. 156–190). Boulder: Geological Society of America.

Barrick, J. E., & Männik, P. (2005). Silurian conodont biostratigraphy and palaeobiology in stratigraphic sequences. *Special Papers in Palaeontology*, *73*, 103–116.

Barrick, J. E., & Meyer, B. D. (2019). Silurian-Devonian conodont biostratigraphy in the southern Midcontinent region of North America. *American Association of Petroleum Geologists, Memoir*, *118*(1), 137–165.

Barrick, J. E., Alekseev, A. S., Blanco-Ferrera, S., Goreva, N. V., Hu, K., Lambert, L. L., & Sanz-Lopez, J. (2022). Carboniferous conodont biostratigraphy. In S. G. Lucas, J. W. Schneider, X. Wang, & S. Nikolaeva (Eds.)*, The Carboniferous Timescale* (pp. 695–768). London: Geological Society. https://doi.org/10.1144/SP512-2020-38

Barrick, J. E., Hogancamp, N. J., & Rosscoe, S. J. (2023). Evolutionary patterns in Late Pennsylvanian conodonts. In S. G. Lucas, W. A. DiMichele, S. Oplustil, & X. Wang (Eds.)*, Ices Ages, Climate Dynamics and Biotic Events* (pp. 383–408). London: Geological Society. https://doi.org/10.1144/SP535-2022-139

Beauchamp, B., Henderson, C. M., Grasby, S. E., Gates, L. T., Beatty, T. W., Utting, J., & James, N. P. (2009). Late Permian sedimentation in the Sverdrup Basin, Canadian Arctic: The Lindström and Black Stripe Formations. *Bulletin of Canadian Petroleum Geology*, *57*(2), 167–191. https://doi.org/10.2113/gscpgbull.57.2.167

Beauchamp, B., Henderson, C. M., Dehari, E., Waldbott von Bassenheim, D., Elliot, S., & Calvo Gonzalez, D. (2022). Carbonate sedimentology and conodont biostratigraphy of Late Pennsylvanian-Early Permian stratigraphic sequences, Carlin Canyon, Nevada: new insights into the tectonic and oceanographic significance of an iconic succession of the basin and range. In C. M. Henderson, W. S. Snyder, & S. Ritter (Eds.), *Late Paleozoic and early Mesozoic tectonostratigraphy and biostratigraphy of western Pangea* (pp. 34–71). Claremore: Society for Sedimentary Geology.

Becker, R. T., Kaiser, S. I., & Aretz, M. (2016). Review of chrono-, litho- and biostratigraphy across the global Hangenberg Crisis and Devonian–Carboniferous Boundary. In R. T. Becker, P. Königshof, & C. E. Brett (Eds.)*, Devonian Climate, Sea Level and Evolutionary Events* (pp. 355–386). London: Geological Society. https://doi.org/10.1144/SP423.10

Becker, R. T., Marshall, J. E. A., & Da Silva, A.-C. (2020). The Devonian Period. In F. M. Gradstein, J. G. Ogg, M. D. Schmitz, & G. M. Ogg (Eds.)*, Geologic Time Scale 2020* (pp. 733–810). Amsterdam: Elsevier. https://doi.org/10.1016/B978-0-12-824360-2.00022-X

Behnken, F. H. (1975). Leonardian and Guadalupian (Permian) conodont biostratigraphy in western and southwestern United States. *Journal of Paleontology*, *49*, 284–315.

Bellian, J. A., Kerans, C., & Repetski, J. E. (2012). Digital outcrop model of stratigraphy and breccias of the southern Franklin Mountains, El Paso, Texas. *American Association of Petroleum Geologists Memoir*, *98*, 909–939. https://doi.org/10.1306/13331521M983516

Bergström, S. M. (1971). Conodont biostratigraphy of the Middle and Upper Ordovician of Europe and eastern North America. In W. C. Sweet, & S. M. Bergström (Eds.), *Symposium on conodont biostratigraphy* (pp. 83–157). Boulder: Geological Society of America.

Bergström, S. M., & Ferretti, A. (2017). Conodonts in Ordovician biostratigraphy. *Lethaia*, *50*(3), 424–439. https://doi.org/10.1111/let.12191

Bergström, S. M., & Ferretti, A. (2018). Deciphering the geology of some Darriwilian–Sandbian (Ordovician) 'ghost' formations in the UK and North America using olistoliths in marine debris flows. *Geological Magazine*, *155*(7), 1507–1522. https://doi.org/10.1017/S0016756817000383

Bergström, S. M., & Sweet, W. C. (1966). Conodonts from the Lexington Limestone (Middle Ordovician) of Kentucky and its lateral equivalents in Ohio and Indiana. *Bulletins of American Paleontology*, *50*, 271–441.

Bergström, S. M., Chen, X., Gutiérrez-Marco, J. C., & Dronov, A. (2009). The new chronostratigraphic classification of the Ordovician System and its relations to major regional series and stages and to δ^{13}C chemostratigraphy. *Lethaia*, *42*(1), 97–107. https://doi.org/10.1111/j.1502-3931.2008.00136.x

Berkyová, S. (2009). Lower-Middle Devonian (upper Emsian-Eifelian, *serotinus-kockelianus* zones) conodont faunas from the Prague Basin, the Czech Republic. *Bulletin of Geosciences*, *84*, 667–686. https://doi.org/10.3140/bull.geosci.1153

Boardman, D. R., Wardlaw, B. R., & Nestell, M. K. (2009). Stratigraphy and conodont biostratigraphy of the Upper Carboniferous and Lower Permian from the North American midcontinent. *Kansas Geological Survey Bulletin*, *255*, 1–253.

Branson, E. B., & Branson, C. C. (1947). Lower Silurian conodonts from Kentucky. *Journal of Paleontology*, *21*, 549–556.

Branson, E. B., & Mehl, M. G. (1933). Conodonts from the Bainbridge (Silurian) of Missouri. *University of Missouri Studies*, *8*, 39–52.

Branson, E. B., & Mehl, M. G. (1934). Conodonts from the Grassy Creek shale of Missouri. *University of Missouri Studies*, *8*, 171–259.

Briggs, D. E. G., Clarkson, E. N. K., & Aldridge, R. J. (1983). The conodont animal. *Lethaia*, *16*(1), 1–14. https://doi.org/10.1111/j.1502-3931.1983.tb01993.x

Broadhead, T. W., & Driese, S. G. (1994). Experimental and natural abrasion of conodont in marine and eolian environments. *Palaios*, *9*(6), 546–560. https://doi.org/10.2307/3515127

Broadhead, T. W., Driese, S. G., & Harvey, J. L. (1990). Gravitational settling of conodont elements, implications for paleoecologic interpretations of conodont assemblages. *Geology*, *18*(9), 850–853. https://doi.org/10.1130/0091-7613(1990)018<0850:GSOCEI>2.3.CO;2

Bultynck, P. (1987). Pelagic and neritic conodont successions from the Givetian of pre-Sahara Morocco and the Ardennes. *Bulletin de l'Institut Royal des Sciences Naturelles de Belgique Sciences de la Terre*, *57*, 149–181.

Calner, M. (2008). Silurian global events – at the tipping point of climate change. In A. M. T. Elewa (Ed.), *Mass extinction* (pp. 21–57). Berlin: Springer. https://doi.org/10.1007/978-3-540-75916-4_4

Carls, P., Slavík, L., & Valenzuela-Ríos, J. I. (2007). Revisions of conodont biostratigraphy across the Silurian-Devonian boundary. *Bulletin of Geosciences*, *82*, 145–164. https://doi.org/10.3140/bull.geosci.2007.02.145

Chen, J., Beatty, T. W., Henderson, C. M., & Rowe, H. (2009). Conodont biostratigraphy across the Permian-Triassic Boundary at the Dawen section, Great Bank of Guizhou, Guizhou Province, South China: Implications for the Late Permian extinction and correlation with Meishan. *Journal of Asian Earth Sciences*, *36*(6), 442–458. https://doi.org/10.1016/j.jseaes.2008.08.002

Chen, Y. L., Krystyn, L., Orchard, M. J., Lai, X. L., & Richoz, S. (2016). A review of the evolution, biostratigraphy, provincialism and diversity of Middle and early Late Triassic conodonts. *Papers in Palaeontology*, *2*(2), 235–263. https://doi.org/10.1002/spp2.1038

Chen, Z., Männik, P., & Fan, J. (2017). Llandovery (Silurian) conodont provincialism: An update based on quantitative analysis. *Palaeogeography, Palaeoclimatology, Palaeoecology*, *485*, 661–672. https://doi.org/10.1016/j.palaeo.2017.07.023

Chernykh, V. V. (2005). *Zonal method in biostratigraphy. Zonal conodont scale of the Lower Permian in the Urals*. Ekaterinburg: Russian Academy of Science. [in Russian]

Chernykh, V. V. (2006). *Lower Permian conodonts of the Urals*. Ekaterinburg: Russian Academy of Science. [in Russian]

Chernykh, V. V. (2012). *Conodonts of the Gzhelian Stage*. Ekaterinburg: Russian Academy of Science. [in Russian]

Chernykh, V. V., Ritter, S. M., & Wardlaw, B. R. (1997). *Streptognathodus isolatus* new species (conodont): Proposed index for the Carboniferous-Permian boundary. *Journal of Paleontology*, *71*(1), 162–164. https://doi.org/10.1017/S0022336000039068

Chernykh, V. V., Kotlyar, G. V., Chuvashov, B. I., Kutygin, R. V., Filimonova, T. V., Sungatullina, G. M., … Batalin, G. A. (2020a). Multidisciplinary study of the Mechetlino Quarry section (Southern Urals, Russia) – the GSSP candidate for the base of the Kungurian Stage (Lower Permian). *Palaeoworld (Amsterdam)*, *29*(2), 325–352. https://doi.org/10.1016/j.palwor.2019.05.012

Chernykh, V. V., Chuvashov, B. I., Shen, S.-Z., Henderson, C. M., Yuan, D.-X., & Stephenson, M. H. (2020b). The Global Stratotype Section and Point (GSSP) for the base-Sakmarian Stage (Cisuralian, Lower Permian). *Episodes*, *43*(4), 961–979. https://doi.org/10.18814/epiiugs/2020/020059

Chernykh, V. V., Henderson, C. M., Kutygin, R. V., Filimonova, T. V., Sungatullina, G. M., Afanasieva, M. S., … Chuvashov, B. I. (2023). Global Stratotype Section and Point (GSSP) for the base-Artinskian Stage (Lower Permian). *Episodes*, *46*(4), 623–651. https://doi.org/10.18814/epiiugs/2023/023015

Ching, Y. K. (1960). Conodonts from the Kufeng Suite (Formation) of Lungtan, Nanking. *Acta Palaeontologica Sinica*, *8*(3), 242–248.

Clark, D. L., & Behnken, F. H. (1970). Conodonts and biostratigraphy of the Permian. *Geological Society of America*, *127*, 415–440. https://doi.org/10.1130/MEM127-p415

Clark, D. L., & Behnken, F. H. (1979). Evolution and taxonomy of the North American Upper Permian *Neogondolella serrata* complex. *Journal of Paleontology*, *53*, 263–275.

Cooper, R. A., Nowlan, G. S., & Williams, S. H. (2001). Global stratotype section and point for base of the Ordovician System. *Episodes*, *24*(1), 19–28. https://doi.org/10.18814/epiiugs/2001/v24i1/005

Corradini, C. (1998). Famennian conodonts from two sections near Villasalto. *Giornale di Geologia*, *60*, 122–135.

Corradini, C. (2003). Late Devonian (Famennian) conodonts from the Corona Mizziu Sections near Villasalto (Sardinia, Italy). *Palaeontographia Italica*, *98*, 65–116.

Corradini, C., & Corriga, M. G. (2012). A Přídolí-Lochkovian conodont zonation in Sardinia and the Carnic Alps: Implications for a global zonation scheme. *Bulletin of Geosciences*, *87*, 635–650. https://doi.org/10.3140/bull.geosci.1304

Corradini, C., & Corriga, M. G. (2018). The new genus *Walliserognathus* and the origin of *Polygnathoides siluricus* (Conodonta, Silurian). *Estonian Journal of Earth Sciences*, *67*(2), 113–121. https://doi.org/10.3176/earth.2018.08

Corradini, C., & Serpagli, E. (1999). A Silurian conodont zonation from late Llandovery to end Přídolí in Sardinia. *Bollettino della Società Paleontologica Italiana*, *38*, 255–273.

Corradini, C., Ferretti, A., Serpagli, E., & Barca, S. (1998). The Ludlow-Přídolí Section "Genna Ciuerciu" west of Silius. *Giornale di Geologia*, *60*, 112–118.

Corradini, C., Ferretti, A., & Storch, P. (2009). The Silurian of Sardinia: Introduction to the field trip. *Rendiconti della Società Paleontologica Italiana*, *3*, 171–176.

Corradini, C., Kaiser, S. I., Perri, M. C., & Spalletta, C. (2011). *Protognathodus* (Conodonta) and its potential as a tool for defining the Devonian/Carboniferous boundary. *Rivista Italiana di Paleontologia e Stratigrafia*, *117*, 12–28.

Corradini, C., Corriga, M. G., Männik, P., & Schönlaub, H. P. (2015). Revised conodont stratigraphy of the Cellon section (Silurian, Carnic Alps). *Lethaia*, *48*(1), 56–71. https://doi.org/10.1111/let.12087

Corradini, C., Pondrelli, M., Simonetto, L., Corriga, M. G., Spalletta, C., Suttner, T. J., … Serventi, P. (2016). Stratigraphy of the La Valute area (Mt. Zermula massif, Carnic Alps, Italy). *Bollettino della Società Paleontologica Italiana*, *55*(1), 55–78. https://doi.org/10.4435/BSPI.2019.14

Corradini, C., Spalletta, C., Mossoni, A., Matyja, H., & Over, D. J. (2017). Conodonts across the Devonian/Carboniferous boundary: A review and implication for the redefinition of the boundary and proposal of an updated conodont zonation. *Geological Magazine*, *154*(4), 888–902. https://doi.org/10.1017/S001675681600039X

Corradini, C., Corriga, M. G., Pondrelli, M., & Suttner, T. J. (2020). Conodonts across the Silurian/Devonian boundary in the Carnic Alps (Austria and Italy). *Palaeogeography, Palaeoclimatology, Palaeoecology*, *549*, 109097. https://doi.org/10.1016/j.palaeo.2019.02.023

Corradini, C., Mossoni, A., Corriga, M. G., & Spalletta, C. (2021). The Devonian/Carboniferous Boundary in Sardinia (Italy). *Palaeobiodiversity and Palaeoenvironments*, *101*(2), 507–514. https://doi.org/10.1007/s12549-019-00411-5

Corriga, M. G., & Corradini, C. (2019a). Ontogeny of *Ancyrodelloides carlsi* (Boersma) and comments on its generic attribution (Conodonta, Lower Devonian). *Geobios*, *57*, 25–32. https://doi.org/10.1016/j.geobios.2019.10.002

Corriga, M. G., & Corradini, C. (2019b). The conodont apparatus of *Zieglerodina eladioi* (Valenzuela-Ríos, 1994). *Bollettino della Società Paleontologica Italiana*, *58*(2), 181–185. https://doi.org/10.4435/BSPI.2019.14

Corriga, M. G., Corradini, C., & Ferretti, A. (2009). Silurian conodonts from Sardinia: An overview. *Rendiconti della Società Paleontologica Italiana*, *3*, 95–107.

Corriga, M. G., Corradini, C., Pondrelli, M., Schönlaub, H. P., Nozzi, L., Todesco, R., & Ferretti, A. (2021). Uppermost Ordovician to lowermost Devonian conodonts from the Valentintörl section and comments on the post Hirnantian hiatus in the Carnic Alps. *Newsletters on Stratigraphy*, *54*(2), 183–207. https://doi.org/10.1127/nos/2020/0614

Cramer, B. D., Kleffner, M. A., Brett, C. E., McLaughlin, P. I., Jeppsson, L., Munnecke, A., & Samtleben, C. (2010). Paleobiogeography, high resolution stratigraphy, and the future of Paleozoic biostratigraphy: Fine-scale diachroneity of the Wenlock (Silurian) conodont *Kockelella walliseri. Palaeogeography, Palaeoclimatology, Palaeoecology*, *294*(3-4), 232–241. https://doi.org/10.1016/j.palaeo.2010.01.002

Cramer, B. D., Brett, C. E., Melchin, M. J., Männik, P., Kleffner, M. A., McLaughlin, P. I., … Saltzman, M. R. (2011). Revised correlation of Silurian Provincial series of North America with global and regional chronostratigraphic units and $\delta^{13}C_{carb}$ chemostratigraphy. *Lethaia*, *44* (2), 185–202. https://doi.org/10.1111/j.1502-3931.2010.00234.x

Cutler, A. H., & Flessa, K. W. (1990). Fossils out of sequence: Computer simulations and strategies for dealing with stratigraphic disorder. *Palaios*, *5*(3), 227–235. https://doi.org/10.2307/3514941

Danielsen, E. M., & Over, D. J. (2016). Lower Silurian conodonts from the Shine Jinst region, southwestern Mongolia. *Journal of Paleontology*, *90*(1), 78–91. https://doi.org/10.1017/jpa.2016.18

Davydov, V. I., Glenister, B. F., Spinosa, C., Ritter, S. M., Chernykh, V. V., Wardlaw, B. R., & Snyder, W. S. (1998). Proposal of Aidaralash as Global Stratotype Section and Point (GSSP) for base of the Permian System. *Episodes*, *21*(1), 11–18. https://doi.org/10.18814/epiiugs/1998/v21i1/003

Dong, X. P., & Zhang, H. (2017). Middle Cambrian through lowermost Ordovician conodonts from Hunan, South China. *Journal of Paleontology*, *91*(S73), 1–89. https://doi.org/10.1017/jpa.2015.43

Donoghue, P. C. J., & Purnell, M. A. (1999). Growth, function and the conodont fossil record. *Geology*, *27*(3), 251–254. https://doi.org/10.1130/0091-7613(1999)027<0251:GFATCF>2.3.CO;2

Donoghue, P. C. J., Purnell, M. A., Aldridge, R. J., & Zhang, S. (2008). The interrelationships of 'complex' conodonts (Vertebrata). *Journal of Systematic Palaeontology*, *6*(2), 119–153. https://doi.org/10.1017/S1477201907002234

Du, Y., Chiari, M., Karádi, V., Nicora, A., Onoue, T., Pálfy, J., … Rigo, M. (2020). The asynchronous disappearance of conodonts: New constraints from Triassic-Jurassic boundary sections in the Tethys and Panthalassa. *Earth-Science Reviews*, *203*, 103176. https://doi.org/10.1016/j.earscirev.2020.103176

Du, Y., Onoue, T., Tomimatsu, Y., Wu, Q., & Rigo, M. (2023). Lower Jurassic conodonts from the Inuyama area of Japan: Implications for conodont extinction. *Frontiers in Ecology and Evolution*, *11*, 1135789. https://doi.org/10.3389/fevo.2023.1135789

Dzik, J. (1991). Evolution of the oral apparatuses in the conodont chordates. *Acta Palaeontologica Polonica*, *36*, 265–323.

Epstein, A. G., Epstein, J. B., & Harris, L. D. (1977). Conodont color alteration – An index of organic metamorphism. *U. S. Geological Survey Professional Paper*, *995*, 1–27.

Ethington, R. L., & Clark, D. L. (1970). Lower Ordovician conodonts in North America. *Geological Society of America Memoirs*, *127*, 63–82. https://doi.org/10.1130/MEM127-p63

Ferretti, A., Messori, A., & Bergström, S. M. (2014). Composition and significance of the Katian (Upper Ordovician) conodont fauna of the Vaux Limestone (Calcaire des Vaux) in Normandy, France. *Estonian Journal of Earth Sciences*, *63*(4), 214–219. https://doi.org/10.3176/earth.2014.21

Ferretti, A., Malferrari, D., Medici, L., & Savioli, M. (2017). Diagenesis does not invent anything new: Precise replication of conodont structures by secondary apatite. *Scientific Reports*, *7*(1), 1624. https://doi.org/10.1038/s41598-017-01694-4

Ferretti, A., Bancroft, A. M., & Repetski, J. E. (2020). GECkO: Global events impacting COnodont evolution. *Palaeogeography, Palaeoclimatology, Palaeoecology*, *549*, 109677. https://doi.org/10.1016/j.palaeo.2020.109677

Ferretti, A., Malferrari, D., Savioli, M., Siepe, T., & Medici, L. (2021a). 'Conodont pearls' do not belong to conodonts. *Lethaia*, *54*(3), 300–313. https://doi.org/10.1111/let.12403

Ferretti, A., Medici, L., Savioli, M., Mascia, M. T., & Malferrari, D. (2021b). Dead, fossil or alive: Bioapatite diagenesis and fossilization. *Palaeogeography, Palaeoclimatology, Palaeoecology*, *579*, 110608. https://doi.org/10.1016/j.palaeo.2021.110608

Ferretti, A., Corriga, M. G., Slavik, L., & Corradini, C. (2022). Running across the Silurian/Devonian boundary along northern Gondwana: A conodont perspective. *Geosciences*, *12*(1), 43. https://doi.org/10.3390/geosciences12010043

Ferretti, A., Corradini, C., Fakir, S., Malferrari, D., & Medici, L. (2023). To be or not to be a conodont. The controversial story of *Pseudooneotodus* and *Eurytholia. Marine Micropaleontology*, *182*, 102258. https://doi.org/10.1016/j.marmicro.2023.102258

Gabbott, S. E., Aldridge, R. J., & Theron, J. N. (1995). A giant conodont with preserved muscle tissue from the Upper Ordovician of South Africa. *Nature*, *374*(6525), 800–803. https://doi.org/10.1038/374800a0

Golding, M. L., & Orchard, M. J. (2016). New species of the conodont *Neogondolella* from the Anisian (Middle Triassic) of northeastern British Columbia, Canada, and their importance for regional correlation. *Journal of Paleontology*, *90*(6), 1197–1211. https://doi.org/10.1017/jpa.2016.119

Golding, M. L., & Orchard, M. J. (2018). *Magnigondolella*, a new conodont genus from the Triassic of North America. *Journal of Paleontology*, *92*(2), 207–220. https://doi.org/10.1017/jpa.2017.123

Golding, M. L., Orchard, M. J., Zonneveld, J.-P., Wilson, N. S. F., & Reinson, G. (2015). Determining the age and depositional model of the Doig Phosphate Zone in northeastern British Columbia using conodont biostratigraphy. *Bulletin of Canadian Petroleum Geology*, *63*(2), 143–170. https://doi.org/10.2113/gscpgbull.63.2.143

Goldman, D., Sadler, P. M., & Leslie, S. A. (2020). The Ordovician Period. In F. M. Gradstein, J. G. Ogg, M. D. Schmitz, & G. M. Ogg (Eds.), *Geologic Time Scale 2020* (pp. 631–694). Amsterdam: Elsevier. https://doi.org/10.1016/B978-0-12-824360-2.00020-6

Goldman, D., Leslie, S. A., Liang, Y., & Bergström, S. M. (2023). Ordovician biostratigraphy: index fossils, biozones and correlation. In D. A. T. Harper, B. Lefebvre, I. G. Percival, & T. Servais (Eds.), *A Global Synthesis of the Ordovician System: Part 1* (pp. 31–62). London: Geological Society. https://doi.org/10.1144/SP532-2022-49

Goreva, N., Alekseev, A., Isakova, T., & Kossovaya, O. (2009). Biostratigraphical analysis of the Moscovian–Kasimovian transition at the neostratotype of Kasimovian Stage (Afanasievo section, Moscow Basin, Russia). *Palaeoworld (Amsterdam)*, *18*(2-3), 102–113. https://doi.org/10.1016/j.palwor.2009.04.008

Goudemand, N., Orchard, M. J., Urdy, S., Bucher, H., & Tafforeau, P. (2011). Synchrotron-aided reconstruction of the conodont feeding apparatus and implications for the mouth of the first vertebrates. *Proceedings of the National Academy of Sciences of the United States of America*, *108* (21), 8720–8724. https://doi.org/10.1073/pnas.1101754108

Gouwy, S., Liao, J.-C., & Valenzuela-Ríos, J. I. (2013). Eifelian (Middle Devonian) to Lower Frasnian (Upper Devonian) conodont biostratigraphy in the Villech section (Spanish Central Pyrenees). *Bulletin of Geosciences*, *88*, 315–338. https://doi.org/10.3140/bull.geosci.1341

Hamar, G. (1964). The Middle Ordovician of the Oslo region, Norway. 17. Conodonts from the lower Middle Ordovician of Ringerike. *Norsk Geologisk Tidsskrift*, *44*, 243–292.

Heckel, P. H. (2013). Pennsylvanian stratigraphy of Northern Midcontinent Shelf and biostratigraphic correlation of cyclothems. *Stratigraphy*, *10*(1-2), 3–40. https://doi.org/10.29041/strat.10.1.02

Heckel, P. H., & Baesemann, J. F. (1975). Environmental interpretation of conodont distribution in Upper Pennsylvanian (Missourian) megacyclothems in Eastern Kansas. *The American Association of Petroleum Geologists Bulletin*, *59*, 486–509.

Heckel, P. H., Alekseev, A. S., Barrick, J. E., Boardman, D. R., Goreva, N. V., Nemyrovska, T. I., … Work, D. M. (2007). Cyclothem ["digital"] correlation and biostratigraphy across the global Moscovian–Kasimovian–Gzhelian stage boundary interval (Middle–Upper Pennsylvanian) in North America and eastern Europe. *Geology*, *35* (7), 607–610. https://doi.org/10.1130/G23564A.1

Heckel, P. H., Alekseev, A. S., Barrick, J. E., Boardman, D. R., Goreva, N. V., Isakova, T. N., … Work, D. M. (2008). Choice of conodont *Idiognathodus simulator* (*sensu stricto*) as the event marker for the base of the global Gzhelian Stage (Upper Pennsylvanian Series, Carboniferous System). *Episodes*, *31*(3), 319–325. https://doi.org/10.18814/epiiugs/2008/v31i3/006

Hedhli, M., Grasby, S. E., Henderson, C. M., & Davis, B. J. (2023). Multiple diachronous Black Seas mimic global ocean anoxia during the latest Devonian. *Geology*, *51*(10), 973–977. https://doi.org/10.1130/G51394.1

Helms, J. J., & Over, D. J. (2006). Conodont taphonomy traveling through the alimentary canal of modern fish. *Geological Society of America Abstracts with Programs*, *38*(2), 4.

Henderson, C. M. (2018). Permian conodont biostratigraphy. In S. G. Lucas, & S. Z. Shen (Eds.), *The Permian Timescale* (pp. 119–142). London: Geological Society.

Henderson, C. M. (2021). Conodonts. In D. Alderton, & S. A. Elias (Eds.), *Encyclopedia of Geology* (pp. 435–445). Amsterdam: Elsevier.

Henderson, C. M., & Mei, S. L. (2007). Geographical clines in Permian and Lower Triassic gondolellids and its role in taxonomy. *Palaeoworld (Amsterdam)*, *16*(1-3), 190–201. https://doi.org/10.1016/j.palwor.2007.05.014

Henderson, C. M., & Shen, S. Z. (2020). The Permian Period. In F. M. Gradstein, J. G. Ogg, M. D. Schmitz, & G. M. Ogg (Eds.), *Geologic Time Scale 2020* (pp. 875–902). Amsterdam: Elsevier. https://doi.org/10.1016/B978-0-12-824360-2.00024-3

Henderson, C. M., Davydov, V. I., & Wardlaw, B. R. (2012). The Permian Period. In F. M. Gradstein, J. G. Ogg, M. D. Schmitz, & G. M. Ogg (Eds.), *Geologic Time Scale 2012* (pp. 653–679). Amsterdam: Elsevier. https://doi.org/10.1016/B978-0-444-59425-9.00024-X

Henderson, C. M., Golding, M. L., & Orchard, M. J. (2018). Conodont sequence biostratigraphy of the Lower Triassic Montney Formation. *Bulletin of Canadian Petroleum Geology*, *66*, 7–22.

Herbers, P., Becker, R. T., & Hartenfels, S. (2017). The impact of re-sampling on conodont abundance, palaeodiversity, biofacies, and stratigraphic analysis – two Famennian case studies. In J.-C. Liao, & J. I. Valenzuela-Ríos (Eds.), *Fourth International Conodont Symposium. ICOS IV. "Progress on Conodont Investigation"* (pp. 343–346). Madrid: Instituto Geologico y Minero de Espana.

Herrmann, A. D., Barrick, J. E., & Algeo, T. J. (2015). The relationship of conodont biofacies to spatially variable water mass properties in the Late Pennsylvanian Midcontinent Sea. *Paleoceanography*, *30*(3), 269–283. https://doi.org/10.1002/2014PA002725

Herrmann, A. D., Barrick, J., Algeo, T. J., & Peng, Y. (2019). Conodont biofacies and watermass structure of the Middle Pennsylvanian North American Midcontinent Sea. *Palaeogeography, Palaeoclimatology, Palaeoecology*, *531*, 109235. https://doi.org/10.1016/j.palaeo.2019.109235

Hogancamp, N. J., Barrick, J. E., & Strauss, R. E. (2016). Geometric morphometric analysis and taxonomic revision of the Gzhelian (Late Pennsylvanian) conodont *Idiognathodus simulator* from North America. *Acta Palaeontologica Polonica*, *61*, 477–502. https://doi.org/10.4202/app.00198.2015

Hogancamp, N. J., Stolfus, B. M., Cramer, B. D., & Day, J. E. (2019). A revised conodont zonation of the Tournaisian (Kinderhookian to Lower Osagean) and implications for stratigraphic correlations in North America. *Iowa Geological Survey Guidebook*, *30*, 11–17.

Holland, S. M. (1995). Sequence stratigraphy, facies control, and their effects on the stratigraphic distribution of fossils. In B. U. Haq (Ed.), *Sequence stratigraphy and depositional response to eustatic, tectonic, and climatic forcing* (pp. 1–23). Amsterdam: Kluwer. https://doi.org/10.1007/978-94-015-8583-5_1

Holland, S. M. (2000). The quality of the fossil record: A sequence stratigraphic perspective. *Paleobiology*, *26* (sp4), 148–168. https://doi.org/10.1666/0094-8373(2000)26[148:TQOTFR]2.0.CO;2

Holland, S. M. (2023). The contrasting controls on the occurrence of fossils in marine and nonmarine systems. *Bollettino della Società Paleontologica Italiana*, *62*(1), 1–25. https://doi.org/10.4435/BSPI.2023.02

Holmden, C., Creaser, R. A., Muehlenbachs, K., Bergström, S. M., & Leslie, S. A. (1996). Isotopic and elemental systematics of Sr and Nd in 454 Ma biogenic apatites: Implications for paleoseawater studies. *Earth and Planetary Science Letters*, *142*(3-4), 425–437. https://doi.org/10.1016/0012-821X(96)00119-7

Hu, K., Qi, Y., & Nemyrovska, T. I. (2019). Mid-Carboniferous conodonts and their evolution: New evidence from Guizhou, South China. *Journal of Systematic Palaeontology*, *17*(6), 451–489. https://doi.org/10.1080/14772019.2018.1440255

Hu, K., Hogancamp, N., Lambert, L. L., Qi, Y., & Chen, J. (2020). Evolution of the conodont *Diplognathodus ellesmerensis* from D. *benderi* sp. nov. at the Bashkirian–Moscovian (lower–middle Pennsylvanian) boundary in South China. *Papers in Palaeontology*, *6*(4), 627–649. https://doi.org/10.1002/spp2.1309

Huckriede, R. (1958). Die Conodonten der Mediterranen Trias und ihr stratigraphischer Wert. *Paläontologische Zeitschrift*, *32*(3-4), 141–175. https://doi.org/10.1007/BF02989028

Jarochowska, E., Viira, V., Einasto, R., Nawrot, R., Bremer, O., Männik, P., & Munnecke, A. (2017). Conodonts in Silurian hypersaline environments: Specialized and unexpectedly diverse. *Geology*, *45*(1), 3–6. https://doi.org/10.1130/G38492.1

Jeppsson, L. (1997). A new latest Telychian, Sheinwoodian and Early Homerian (Early Silurian) standard conodont zonations. *Transactions of the Royal Society of Edinburgh. Earth Sciences*, *88*(2), 91–114. https://doi.org/10.1017/S0263593300006854

Jeppsson, L. (2005). Bias in the recovery and interpretation of micropalaeontological data. *Special Papers in Palaeontology*, *73*, 57–71.

Jeppsson, L., Eriksson, M. E., & Calner, M. (2006). A latest Llandovery to latest Ludlow high-resolution biostratigraphy based on the Silurian of Gotland – a summary. *GFF*, *128*(2), 109–114. https://doi.org/10.1080/11035890601282109

Jeppsson, L., Talent, J. A., Mawson, R., Andrew, A., Corradini, C., Simpson, A. J., … Schönlaub, H. P. (2012). Late Ludfordian correlations and the Lau Event. In J. A. Talent (Ed.), *Earth and Life, International Year of Planet Earth* (pp. 653–675). Berlin: Springer. https://doi.org/10.1007/978-90-481-3428-1_21

Jin, Y. G., Shen, S. Z., Henderson, C. M., Wang, X. D., Wang, W., Wang, Y., … Shang, Q. H. (2006a). The Global Stratotype Section and Point (GSSP) for the boundary between the Capitanian and Wuchiapingian stage (Permian). *Episodes*, *29*(4), 253–262. https://doi.org/10.18814/epiiugs/2006/v29i4/003

Jin, Y. G., Wang, Y., Henderson, C. M., Wardlaw, B. R., Shen, S. Z., & Cao, C. Q. (2006b). The Global Boundary Stratotype Section and Point (GSSP) for the base of Changhsingian Stage (Upper Permian). *Episodes*, *29*(3), 175–182. https://doi.org/10.18814/epiiugs/2006/v29i3/003

Joachimski, M. M., Lai, X., Shen, S., Jiang, H., Luo, G., Chen, B., … Sun, Y. (2012). Climate warming in the latest Permian and the Permian-Triassic mass extinction. *Geology*, *40*(3), 195–198. https://doi.org/10.1130/G32707.1

Johnston, D. I., & Henderson, C. M. (2005). Disrupted conodont bedding plane assemblages, Upper Bakken Formation (Lower Mississippian) from the subsurface of Western Canada. *Journal of Paleontology*, *79*(4), 774–789. https://doi.org/10.1666/0022-3360(2005)079[0774:DCBPAU]2.0.CO;2

Jones, D., Evans, A. R., Siu, K. K. W., Rayfield, E. J., & Donoghue, P. C. J. (2012). The sharpest tools in the box? Quantitative analysis of conodont element functional morphology. *Proceedings. Biological Sciences*, *279*(1739), 2849–2854. https://doi.org/10.1098/rspb.2012.0147

Kaiser, S. I. (2009). The Devonian/Carboniferous boundary stratotype section (La Serre, France) revisited. *Newsletters on Stratigraphy*, *43*(2), 195–205. https://doi.org/10.1127/0078-0421/2009/0043-0195

Kaiser, S. I., & Corradini, C. (2011). The early siphonodellids (Conodonta, Late Devonian-Early Carboniferous): overview and taxonomic state. *Neues Jahrbuch für Geologie und Paläontologie Abhandlungen*, *261*(1), 19–35. https://doi.org/10.1127/0077-7749/2011/0144

Kaiser, S. I., Becker, R. T., Spalletta, C., & Steuber, T. (2009). High-resolution conodont stratigraphy, biofacies and extinctions around the Hangenberg Event in pelagic successions from Austria, Italy and France. *Palaeontographica Americana*, *63*, 97–139.

Khalymbadzha, V. G., & Chernysheva, N. G. (1970). Konodonty v. *Ancyrodella* is devonskikh otlozheniy volgo-kamskogo kraia i ikh stratigrahicheskoe znachenie. In V. I. Ulianova-Lenina (Ed.), *Biostratigrafia i paleontologia paleozoiskikh otloszheniy vostoka russkoj platformia i zapadnogo priuralia* (pp. 81–103). Kazan: Kazanskiy Universitet.

Klapper, G. (1989). The Montagne Noire Frasnian (Upper Devonian) conodont succession. *Canadian Society of Petroleum Geology Memoir*, *14*, 449–468.

Klapper, G. (2021). Revision of the Late Devonian conodont genus *Ancyrodella. Bulletin of Geosciences*, *96*, 295–325. https://doi.org/10.3140/bull.geosci.1828

Klapper, G., & Johnson, J. G. (1980). Endemism and dispersal of Devonian conodonts. *Journal of Paleontology*, *54*, 400–455.

Klapper, G., & Kirchgasser, W. T. (2016). Frasnian Late Devonian conodont biostratigraphy in New York: Graphic correlation and taxonomy. *Journal of Paleontology*, *90*(3), 525–554. https://doi.org/10.1017/jpa.2015.70

Klapper, G., & Lane, H. R. (1985). Upper Devonian (Frasnian) conodonts of the *Polygnathus* biofacies, N. W. T., Canada. *Journal of Paleontology*, *59*, 904–951.

Klapper, G., & Murphy, M. A. (1975). Silurian–Lower Devonian conodont sequence in the Roberts Mountains Formation of central Nevada. *University of California Publications in Geological Sciences*, *111*, 1–62.

Klapper, G., Ziegler, W., & Mashkova, T. V. (1978). Conodonts and classification of Lower-Middle Devonian boundary beds in the Barrandian area of Czechoslovakia. *Geologica et Paleontologica*, *12*, 103–115.

Klapper, G., Kirchgasser, W. T., & Baesemann, J. F. (1995). Graphic correlation of a Frasnian (Upper Devonian) Composite Standard. *Society for Sedimentary Geology Special Publication*, *53*, 177–184. https://doi.org/10.2110/pec.95.53.0177

Klapper, G., Uyeno, T. T., Armstrong, D. K., & Telford, P. G. (2004). Conodonts of the Williams Island and Long Rapids Formations (Upper Devonian, Frasnian-Famennian) of the Onakawana B drillhole, Moose River Basin, Northern Ontario, with a revision of Lower Famennian species. *Journal of Paleontology*, *78*(2), 371–387. https://doi.org/10.1666/0022-3360(2004)078<0371:COTWIA>2.0.CO;2

Knell, S. J. (2012). *The Great Fossil Enigma: The Search for the Conodont Animal*. Bloomington: Indiana University Press.

Kozur, H. (1978). Beiträge zur Stratigraphie des Perms; Teil II, Die Conodontenchronologie des Perms. *Freiberger Forschungshefte*, C 334, 85–161.

Kozur, H., & Mock, R. (1974). *Misikella posthernsteini* n. sp., die jüngste Conodontenart der tethyalen Trias. *Časopis pro mineralogii a geologii*, 19(3), 245–250.

Kozur, H., & Mock, R. (1991). New Middle Carnian and Rhaetian conodonts from Hungary and the Alps. Stratigraphic importance and tectonic implications for the Buda Mountains and adjacent areas. *Jahrbuch der Geologischen Bundesanstalt*, *134*(2), 271–297.

Kozur, H., & Pjatakova, M. (1976). Die Conodontenart *Archignathodus parvus* n.sp., eine wichtige Leitform der basalen Trias. *Koninklijke Nederlandse Akademie van Wetenschappen Proceedings*, *79*(2), 123–128.

Kruse, P. D., Jago, J. B., & Laurie, J. R. (2009). Recent developments in Australian Cambrian biostratigraphy. *Dicengxue Zazhi*, *33*, 35–47.

Lai, X. L., Wignall, P., & Zhang, K. X. (2001). Palaeoecology of the conodonts *Hindeodus* and *Clarkina* during the Permian-Triassic transitional period. *Palaeogeography, Palaeoclimatology, Palaeoecology*, *171*(1-2), 63–72. https://doi.org/10.1016/S0031-0182(01)00269-3

Lambert, L. L., Lehrmann, D. J., & Harris, M. T. (2000). Correlation of the Road Canyon and Cutoff formations, West Texas, and its relevance to establishing and International Middle Permian (Guadalupian) Series. *Smithsonian Contributions to the Earth Sciences*, *22*, 37–87.

Lamont, A., & Lindström, M. (1957). Arenigian and Llandeilian cherts identified in the Southern Uplands of Scotland by means of conodonts. *Transactions of the Edinburgh Geological Society*, *17*(1), 60–70. https://doi.org/10.1144/transed.17.1.60

Lane, H. R., & Ormiston, A. R. (1979). Siluro-Devonian biostratigraphy of the Salmontrout River area, east-central Alaska. *Geologica et Palaeontologica*, *13*, 39–70.

Lane, H. R., Merrill, G. K., Straka, J. J., II,, & Webster, G. D. (1970). North American Pennsylvanian conodont biostratigraphy. *Geological Society of America Memoirs*, *127*, 395–414. https://doi.org/10.1130/MEM127-p395

Lane, H. R., Qi, Y., Wang, Z., Nemyrovska, T. I., Richards, B. C., & Hu, K. (2019). Conodonts from the mid-Carboniferous boundary GSSP at Arrow Canyon, Nevada, USA. *Micropaleontology*, *65*(2), 77–104. https://doi.org/10.47894/mpal.65.2.01

LeGeros, R. Z. (1981). Apatites in biological systems. *Progress in Crystal Growth and Characterization*, *4*(1-2), 1–45. https://doi.org/10.1016/0146-3535(81)90046-0

Leu, M., Bucher, H., Vennemann, T., Bagherpour, B., Ji, C., Brosse, M., & Goudemand, N. (2022). A Unitary Association-based conodont biozonation of the Smithian-Spathian boundary (Early Triassic) and associated biotic crisis from South China. *Swiss Journal of Palaeontology*, *141*(1), 19. https://doi.org/10.1186/s13358-022-00259-x

Lindström, M. (1954). Conodonts from the lowermost Ordovician strata in south-central Sweden. *Geologiska Föreningens i Stockholm Förhandlingar*, *76*(4), 517–604. https://doi.org/10.1080/11035895409453581

Lindström, M. (1970). Lower Ordovician conodonts of Europe. *Geological Society of America Memoirs*, *127*, 21–61. https://doi.org/10.1130/MEM127-p21

Lindström, M., & Ziegler, Z. (Eds.)(1972). *Symposium on conodont taxonomy. Geologica et Palaeontologica, 1*, 1–158.

Liu, H. P., Bergström, S. M., Witzke, B. J., Briggs, D. E. G., McKay, R. M., & Ferretti, A. (2017). Exceptionally preserved conodont apparatuses with giant elements from the Middle Ordovician Winneshiek Konservat-Lagerstätte, Iowa, USA. *Journal of Paleontology*, *91*(3), 493–511. https://doi.org/10.1017/jpa.2016.155

Lüddecke, F., Hartenfels, S., & Becker, R. T. (2017). Conodont biofacies of a monotonous middle Famennian pelagic carbonate succession (Upper Ballberg Quarry, northern Rhenish Massif). *Palaeobiodiversity and Palaeoenvironments*, *97*(3), 591–613. https://doi.org/10.1007/s12549-017-0288-x

Lyu, Z., Orchard, M. J., Chen, Z. Q., Zhao, L., Zhang, L., & Zhang, X. M. (2018). A taxonomic re-assessment of the *Novispathodus waageni* Group and its role in defining the base of the Olenekian (Lower Triassic). *Journal of Earth Science*, *29*(4), 824–836. https://doi.org/10.1007/s12583-018-0795-3

Lyu, Z., Henderson, C. M., Chen, Z. Q., Tong, J., Zhao, L., Han, C., & Wu, S. (2023). High-resolution conodont unitary association zonations (UAZs) across the Induan-Olenekian boundary (Lower Triassic): A global correlation. *Palaeogeography, Palaeoclimatology, Palaeoecology*, *627*, 111721. https://doi.org/10.1016/j.palaeo.2023.111721

Malferrari, D., Ferretti, A., Mascia, M. T., Savioli, M., & Medici, L. (2019). How much can we trust major element quantification in bioapatite investigation? *ACS Omega*, *4* (18), 17814–17822. https://doi.org/10.1021/acsomega.9b02426

Malferrari, D., Ferretti, A., & Medici, L. (2024). The origin and significance of euhedral bioapatite crystals on conodonts. *Marine Micropaleontology*, *186*, 102308. https://doi.org/10.1016/j.marmicro.2023.102308

Männik, P. (1998). Evolution and taxonomy of the Silurian genus *Pterospathodus*. *Palaeontology*, *41*, 1001–1050.

Männik, P., Loydell, D. K., Nestor, V., & Nolvak, J. (2015). Integrated Upper Ordovician–lower Silurian biostratigraphy of the Grötlingbo-1 core section, Sweden. *GFF*, *137* (3), 226–244. https://doi.org/10.1080/11035897.2015.1042032

Martin, R. E. (1993). Time and taphonomy: actualistic evidence for time-averaging of benthic foraminiferal assemblages. In S. M. Kidwell, & A. K. Behrensmeyer (Eds.)*, Taphonomic approaches to time resolution in fossil assemblages* (pp. 34–56). Knoxville, Tennessee: The Paleontological Society.

Mazza, M., Rigo, M., & Gullo, M. (2012). Taxonomy and biostratigraphic record of the Upper Triassic conodonts of the Pizzo Mondello Section (western Sicily, Italy), GSSP candidate for the base of the Norian. *Rivista Italiana di Paleontologia e Stratigrafia*, *118*, 85–130.

McGoff, H. J. (1991). The hydrodynamics of conodont elements. *Lethaia*, *24*(3), 235–247. https://doi.org/10.1111/j.1502-3931.1991.tb01472.x

Medici, L., Malferrari, D., Savioli, M., & Ferretti, A. (2020). Mineralogy and crystallization patterns in conodont bioapatite from first occurrence (Cambrian) to extinction (end-Triassic). *Palaeogeography, Palaeoclimatology, Palaeoecology*, *549*, 109098. https://doi.org/10.1016/j.palaeo.2019.02.024

Medici, L., Savioli, M., Ferretti, A., & Malferrari, D. (2021). Zooming in REE and other trace elements on conodonts: Does taxonomy guide diagenesis? *Journal of Earth Science*, *32*(3), 501–511. https://doi.org/10.1007/s12583-020-1094-3

Mei, S., & Henderson, C. M. (2001). Evolution of Permian conodont provincialism and its significance in global correlation and paleoclimate implication. *Palaeogeography, Palaeoclimatology, Palaeoecology*, *170*(3-4), 237–260. https://doi.org/10.1016/S0031-0182(01)00258-9

Mei, S., Jin, Y. G., & Wardlaw, B. R. (1994). Zonation of conodonts from the Maokouan-Wuchiapingian boundary strata, South China. *Palaeoworld*, *4*, 225–233.

Mei, S., Henderson, C. M., & Wardlaw, B. (2002). Evolution and distribution of the conodonts *Sweetognathus* and *Iranognathus* and related genera during the Permian, and their implications for climate change. *Palaeogeography, Palaeoclimatology, Palaeoecology*, *180*(1-3), 57–91. https://doi.org/10.1016/S0031-0182(01)00423-0

Mei, S., Henderson, C. M., & Cao, C. Q. (2004). Conodont sample-population approach to defining the base of the Changhsingian Stage, Lopingian Series, Upper Permian. *Geological Society of London Special Publications*, *230*, 105–121. https://doi.org/10.1144/GSL.SP.2004.230.01.06

Melchin, M. J., Cooper, R. A., & Sadler, P. M. (2004). The Silurian Period. In F. M. Gradstein, J. G. Ogg, & A. G. Smith (Eds.), *A Geological Time Scale 2004* (pp. 188–201). Cambridge: University Press.

Melchin, M. J., Sadler, P. M., & Cramer, B. D. (2012). The Silurian Period. In F. M. Gradstein, J. G. Ogg, & A. G. Smith (Eds.), *A Geologic Time Scale 2012* (pp. 525–558). Amsterdam: Elsevier. https://doi.org/10.1016/B978-0-444-59425-9.00021-4

Melchin, M. J., Sadler, P. M., & Cramer, B. D. (2020). The Silurian Period. In F. M. Gradstein, J. G. Ogg, M. D. Schmitz, & G. M. Ogg (Eds.), *Geologic Time Scale 2020* (pp. 695–732). Amsterdam: Elsevier. https://doi.org/10.1016/B978-0-12-824360-2.00021-8

Merrill, G. M. (1973). Pennsylvanian conodont paleoecology. *Geological Society of America. Special Paper*, *141*, 239–274.

Miller, J. F., Ethington, R. L., & Rosé, R. (2006). Stratigraphic implications of lower Ordovician conodonts from the munising and au train formations at pictured rocks National Lakeshore, Upper Peninsula of Michigan. *Palaios*, *21*(3), 227–237. https://doi.org/10.2110/palo.2004.p04-50

Miller, J. F., Evans, K. R., Freeman, R. L., Loch, J. D., Ripperdan, R. L., & Taylor, J. F. (2018). Combining biostratigraphy, carbon isotope stratigraphy and sequence stratigraphy to define the base of Cambrian Stage 10. *Australasian Palaeontological Memoirs*, *51*, 19–64.

Movschovitsch, V. E., Kozur, H., Pavlov, A. M., Pnev, V. P., Polozova, A. N., Chuvashov, B. I., & Bogoslovskaya, M. F. (1979). Conodont complexes of the Lower Permian pre-Urals region and the problem of the Lower Permian deposits correlation. In G. N. Papulov, & V. N. Puchkov (Eds.), *The Urals conodonts and their stratigraphic significance* (pp. 94–134). Sverdlovsk: Akademii Nauk SSSR.

Murdock, D. J. E., Dong, X., Repetski, J. E., Marone, F., Stampanoni, M., & Donoghue, P. C. J. (2013). Origin of conodonts and of vertebrate mineralized skeletons. *Nature*, *502*(7472), 546–549. https://doi.org/10.1038/nature12645

Murphy, M. A. (2005). Pragian conodont classification in Nevada, Western North America. *Revista Española de Paleontología*, *20*, 177–206.

Murphy, M. A., & Valenzuela-Ríos, J. I. (2017). Reconstruction of the skeletal apparatus of *Flajsella* Valenzuela-Ríos and Murphy 1997 (Devonian conodont). *Stratigraphy*, *14* (1-4), 285–297. https://doi.org/10.29041/strat.14.1-4.285-297

Nardelli, M. P., Malferrari, D., Ferretti, A., Bartolini, A., Sabbatini, A., & Negri, A. (2016). Zinc incorporation in the miliolid foraminifer *Pseudotriloculina rotunda* under laboratory conditions. *Marine Micropaleontology*, *126*, 42–49. https://doi.org/10.1016/j.marmicro.2016.06.001

Negri, A., Ferretti, A., Wagner, T., & Meyers, P. A. (2009a). Organic-carbon-rich sediments through the Phanerozoic: Processes, progress, and perspectives. *Palaeogeography, Palaeoclimatology, Palaeoecology*, *273*(3-4), 213–217. https://doi.org/10.1016/j.palaeo.2008.11.016

Negri, A., Ferretti, A., Wagner, T., & Meyers, P. A. (2009b). Phanerozoic organic-carbon-rich marine sediments: Overview and future research challenges. *Palaeogeography, Palaeoclimatology, Palaeoecology*, *273*(3-4), 218–227. https://doi.org/10.1016/j.palaeo.2008.10.002

Nemyrovska, T. I., & Hu, K. (2018). Conodont association of the Bashkirian-Moscovian boundary interval of the Donets Basin, Ukraine. *Spanish Journal of Palaeontology*, *33*(1), 105–128. https://doi.org/10.7203/sjp.33.1.13245

Nicoll, R. S. (1976). The effect of Late Carboniferous-Early Permian glaciation on the distribution of conodonts in Australia. *Geological Association of Canada Special Paper*, *15*, 273–278.

Nicoll, R. S., Miller, J. F., Nowlan, G. S., Repetski, J. E., & Ethington, R. L. (1999). *Iapetonudus* (N. gen.) and *Iapetognathus* Landing, unusual earliest Ordovician multielement conodont taxa and their utility for biostratigraphy. *Geology Studies*, *44*, 27–101.

Nikolaeva, S. V., Alekseev, A. S., Kulagina, E. I., Gatovsky, Y. A., Ponomareva, G. Y., & Gibshman, N. B. (2020). An evaluation of biostratigraphic markers across multiple geological sections in the search for the GSSP of the base of the Serpukhovian Stage (Mississippian). *Palaeoworld (Amsterdam)*, *29*(2), 270–302. https://doi.org/10.1016/j.palwor.2019.01.006

Nogami, Y. (1968). Trias-Conodonten von Timor, Malaysien und Japan. Paleontological study of Portuguese Timor, 5. *Memoirs of the Faculty of Science, Kyoto University, Series of Geology and Mineralogy*, *34*(2), 115–136.

Ogg, J. G., & Chen, Z. (2020). The Triassic Period. In F. M. Gradstein, J. G. Ogg, M. D. Schmitz, & G. M. Ogg (Eds.), *Geologic Time Scale 2020* (pp. 903–953). Amsterdam: Elsevier. https://doi.org/10.1016/B978-0-12-824360-2.00025-5

Orchard, M. J. (2007). Conodont diversity and evolution through the latest Permian and Early Triassic upheavals. *Palaeogeography, Palaeoclimatology, Palaeoecology*, *252*(1-2), 93–117. https://doi.org/10.1016/j.palaeo.2006.11.037

Orchard, M. J. (2010). Triassic conodonts and their role in stage boundary definitions. *Geological Society of London Special Publications*, *334*(1), 139–161. https://doi.org/10.1144/SP334.7

Orchard, M. J., & Golding, M. L. (2023). The *Neogondolella constricta* (Mosher and Clark, 1965) group in the Middle Triassic of North America: Speciation and distribution. *Journal of Paleontology*, *97*(6), 1161–1191. https://doi.org/10.1017/jpa.2023.52

Ovnatanova, N. S., & Kononova, L. I. (2001). Conodonts and Upper Devonian (Frasnian) biostratigraphy of central regions of Russian Platform. *Courier Forschungsinstitut Senckenberg*, *233*, 1–115.

Ovnatanova, N. S., & Kononova, L. I. (2008). Frasnian conodonts from the eastern Russian Platform. *Paleontological Journal*, *42*(10), 997–1166. https://doi.org/10.1134/S0031030108100018

Pander, C. H. (1856). *Monographie der fossilen Fische des Silurischen Systems der Russisch-Baltischen Gouvernements* (pp. 1–91). St. Petersburg: Buchdruckerei der Kaiserlichen Akademie der Wissenschaften.

Peng, S. C., Babcock, L. E., & Ahlberg, P. (2020). The Cambrian Period. In F. M. Gradstein, J. G. Ogg, M. D. Schmitz, & G. M. Ogg (Eds.), *Geologic Time Scale 2020* (pp. 565–628). Amsterdam: Elsevier. https://doi.org/10.1016/B978-0-12-824360-2.00019-X

Petryshen, W., Henderson, C. M., de Baets, K., & Jarochowska, E. (2020). Evidence of parallel evolution in the dental elements of *Sweetognathus* conodonts. *Proceedings. Biological Sciences*, *287*(1939), 20201922. https://doi.org/10.1098/rspb.2020.1922

Philip, G. M. (1965). Lower Devonian conodonts from the Tyers area, Gippsland, Victoria. *Proceedings of the Royal Society of Victoria*, *79*, 95–117.

Proctor, D. D. (1991). Conodont faunas of the Dimple Limestone (Late Morrowan–Early Atokan, Early Pennsylvanian), in the Marathon Basin, Texas. PhD Thesis, Texas Tech University, Lubbock.

Purnell, M. A. (1995). Large eyes and vision in conodonts. *Lethaia*, *28*(2), 187–188. https://doi.org/10.1111/j.1502-3931.1995.tb01612.x

Purnell, M. A., & Donoghue, P. C. J. (1997). Architecture and functional morphology of the skeletal apparatus of ozarkodinid conodonts. *Philosophical Transactions of the Royal Society of London Series B, Biological Sciences*, *352*, 1545–1564. https://doi.org/10.1098/rstb.1997.0141

Purnell, M., & Donoghue, P. C. J. (2005). Between death and data: Biases in interpretation of the fossil record of conodonts. *Special Papers in Palaeontology*, *73*, 7–25.

Purnell, M. A., & Jones, D. (2012). Quantitative analysis of conodont tooth wear and damage as a test of ecological and functional hypotheses. *Paleobiology*, *38*(4), 605–626. https://doi.org/10.1666/09070.1

Purnell, M. A., Donoghue, P. C. J., & Aldridge, R. J. (2000). Orientation and anatomical notation in conodonts. *Journal of Paleontology*, *74*(1), 113–122. https://doi.org/10.1666/0022-3360(2000)074<0113:OAANIC>2.0.CO;2

Qi, Y., Nemyrovska, T. I., Wang, X., Chen, J., Wang, Z., Lane, H. R., … Wang, Q. (2014). Late Visean – early Serpukhovian conodont succession at the Naqing (Nashui) section in Guizhou, South China. *Geological Magazine*, *151*(2), 254–268. https://doi.org/10.1017/S001675681300071X

Qi, Y., Nemyrovska, T. I., Wang, Q., Hu, K., Wang, X., & Lane, H. R. (2018). Conodonts of the genus *Lochriea* near the Visean–Serpukhovian boundary (Mississippian) at the Naqing section, Guizhou Province, South China. *Palaeoworld (Amsterdam)*, *27*(4), 423–437. https://doi.org/10.1016/j.palwor.2018.09.001

Qi, Y., Barrick, J. E., Hogancamp, N. J., Chen, J., Hu, K., Wang, Q., & Wang, X. (2020). Conodont faunas across the Kasimovian-Gzhelian boundary (Late Pennsylvanian) in South China and implications for the selection of the stratotype for the base of the global Gzhelian stage. *Papers in Palaeontology*, *6*(3), 439–484. https://doi.org/10.1002/spp2.1301

Rasmussen, J. A., & Stouge, S. (2018). Baltoscandian conodont biofacies fluctuations and their link to Middle Ordovician (Darriwilian) global cooling. *Palaeontology*, *61*(3), 391–416. https://doi.org/10.1111/pala.12348

Rejebian, V. A., Harris, A. G., & Huebner, J. S. (1987). Conodont color and textural alteration: An index to regional metamorphism, contact metamorphism, and hydrothermal alteration. *Geological Society of America Bulletin*, *99*(4), 471–479. https://doi.org/10.1130/0016-7606(1987)99<471:CCATAA>2.0.CO;2

Rhodes, F. H. T. (1952). A classification of Pennsylvanian conodont assemblages. *Journal of Paleontology*, *26*, 886–901.

Rigo, M., & Joachimski, M. M. (2010). Palaeoecology of Late Triassic conodonts: Constraints from oxygen isotopes in biogenic apatite. *Acta Palaeontologica Polonica*, *55*(3), 471–478. https://doi.org/10.4202/app.2009.0100

Ritter, S. M., Barrick, J. E., & Skinner, M. R. (2002). Conodont sequence biostratigraphy of the Hermosa Group (Pennsylvanian) at Honaker Trail, Paradox basin, Utah. *Journal of Paleontology*, *76*(3), 495–517. https://doi.org/10.1666/0022-3360(2002)076<0495:CSBOTH>2.0.CO;2

Ritter, S. M., Meibos, J. K., & Robinson, T. S. (2022). Sequence biostratigraphy of Carboniferous–Permian boundary strata in Western Utah: Deciphering eustatic and tectonic controls on sedimentation in the Antler–Sonoma Distal Foreland Basin. *SEPM Special Publication*, *113*. https://doi.org/https://doi.org/10.2110/sepmsp.113.07

Rosscoe, S. J., & Barrick, J. E. (2013). North American species of the conodont genus *Idiognathodus* from the Moscovian-Kasimovian boundary composite sequence and correlation of the Moscovian-Kasimovian boundary. *New Mexico Museum of Natural History Bulletin*, *60*, 354–371.

Sadler, P. M., Cooper, R. A., & Melchin, M. J. (2009). High-resolution, early Paleozoic (Ordovician-Silurian) time scales. *Geological Society of America Bulletin*, *121*(5-6), 887–906. https://doi.org/10.1130/B26357.1

Sandberg, C. A. (1976). Conodont biofacies of Late Devonian *Polygnathus styriacus* Zone in western United States. *Geological Association of Canada Special Paper*, *15*, 171–186.

Sandberg, C. A., & Dreesen, R. (1984). Late Devonian icriodontid biofacies models and alternate shallow-water conodont zonation. *Geological Society of America. Special Paper*, *196*, 143–178.

Sandberg, C. A., & Gutschick, R. C. (1979). Guide to conodont biostratigraphy of Upper Devonian and Mississippian rocks along the Wasatch Front and Cordilleran Hingeline, Utah. *Brigham Young University Studies*, *26*, 107–134.

Sandberg, C. A., Ziegler, W., Leuteritz, K., & Brill, S. M. (1978). Phylogeny, speciation and zonation of *Siphonodella* (Conodonta, Upper Devonian and Lower Carboniferous). *Newsletters on Stratigraphy*, *7*(2), 102–120. https://doi.org/10.1127/nos/7/1978/102

Sansom, I. J., Armstrong, H. A., & Smith, M. P. (1994). The apparatus architecture of *Panderodus* and its implications for coniform conodont classification. *Palaeontology*, *37*, 781–799.

Schmidt, H. (1934). Conodonten-Funde in ursprünglichem Zusammenhang. *Paläontologische Zeitschrift*, *16*(1-2), 76–85. https://doi.org/10.1007/BF03041668

Schmitz, M., & Davydov, V. I. (2012). Quantitative radiometric and biostratigraphic calibration of the Pennsylvanian-Early Permian (Cisuralian) time scale and pan-Euramerican chronostratigraphic correlation. *Geological Society of America Bulletin*, *124*(3-4), 549–577. https://doi.org/10.1130/B30385.1

Schönlaub, H. P., Corradini, C., Corriga, M. G., & Ferretti, A. (2017). Chrono-, litho- and conodont bio-stratigraphy of the Rauchkofel Boden Section (Upper Ordovician–Lower Devonian), Carnic Alps, Austria. *Newsletters on Stratigraphy*, *50*(4), 445–469. https://doi.org/10.1127/nos/2017/0391

Seddon, G., & Sweet, W. C. (1971). An ecological model for conodonts. *Journal of Paleontology*, *45*, 869–880.

Serpagli, E. (1983). The conodont apparatus of *Icriodus woschmidti woschmidti* Ziegler. *Fossils and Strata*, *15*, 155–161. https://doi.org/10.18261/8200067378-1983-14

Serpagli, E., & Corradini, C. (1999). Taxonomy and evolution of *Kockelella* (Conodonta) from Silurian of Sardinia. *Bollettino della Società Paleontologica Italiana*, *38*, 275–298.

Shen, S. Z., & Mei, S. L. (2010). Lopingian (Late Permian) high-resolution conodont biostratigraphy in Iran with comparison to South China zonation. *Geological Journal*, *45*(2-3), 135–161. https://doi.org/10.1002/gj.1231

Shen, S. Z., Henderson, C. M., Bowring, S. A., Cao, C. Q., Wang, Y., Wang, W., … Mu, L. (2010). High-resolution Lopingian (Late Permian) timescale of South China. *Geological Journal*, *45*(2-3), 122–134. https://doi.org/10.1002/gj.1232

Shen, S. Z., Yuan, D. X., Henderson, C. M., Lambert, L. L., Zhang, Y. C., Erwin, D. H., … Wardlaw, B. R. (2022). The Global Stratotype Section and Point (GSSP) for the base of the Capitanian Stage (Guadalupian, Middle Permian). *Episodes*, *45*(3), 309–331. https://doi.org/10.18814/epiiugs/2022/022004

Shen, S. Z., Yuan, D. X., Zhang, Y. C., Henderson, C. M., Zheng, Q. F., Zhang, H., … Mei, S. (2024). Redefinition of the Global Stratotype Section and Point (GSSP) and new Standard Auxiliary Boundary Stratotype (SABS) for the base of the Wuchiapingian Stage (Lopingian Series, Permian) in South China. *Episodes*, *47*(1), 147–177. https://doi.org/10.18814/epiiugs/2023/023023

Shergold, J. H., & Nicoll, R. S. (1992). Revised Cambrian-Ordovician boundary biostratigraphy, Black Mountain, western Queensland. In B. D. Webby, & J. R. Laurie (Eds.), *Global perspectives on Ordovician geology* (pp. 81–92). Rotterdam: Balkema.

Shohel, M., McAdams, N. E. B., Cramer, B. D., & Forbes, T. Z. (2020). Ontogenetic variability in crystallography and mosaicity of conodont apatite: Implication for microstructure, palaeothermometry and geochemistry. *Royal Society Open Science*, *7*(7), 200322. https://doi.org/10.1098/rsos.200322

Slavík, L. (2004). A new conodont zonation of the Pragian Stage (Lower Devonian) in the stratotype area (Barrandian, central Bohemia). *Newsletters on Stratigraphy*, *40* (1-2), 39–71. https://doi.org/10.1127/0078-0421/2004/0040-0039

Slavík, L., & Hladil, J. (2004). Lochkovian/Pragian GSSP revisited: Evidence about conodont taxa and their stratigraphic distributions. *Newsletters on Stratigraphy*, *40*(3), 137–153. https://doi.org/10.1127/0078-0421/2004/0040-0137

Slavík, L., & Carls, P. (2012). Post-Lau Event (late Ludfordian, Silurian) recovery of conodont faunas of Bohemia. *Bulletin of Geosciences*, *87*, 815–832. https://doi.org/10.3140/bull.geosci.1368

Slavík, L., & Hladil, J. (2020). Early Devonian (Lochkovian-early Emsian) bioevents and conodonts response in the Prague Synform (Czech Republic). *Palaeogeography, Palaeoclimatology, Palaeoecology*, *549*, 109148. https://doi.org/10.1016/j.palaeo.2019.04.004

Slavík, L., Kříž, J., & Carls, P. (2010). Reflection of the mid-Lufordian Lau Event in conodont faunas of Bohemia. *Bulletin of Geosciences*, *85*, 395–414. https://doi.org/10.3140/bull.geosci.1204

Slavík, L., Carls, P., Hladil, J., & Koptikova, L. (2012). Subdivision of the Lochkovian Stage based on conodont faunas from the stratotype area (Prague Synform, Czech

Republic). *Geological Journal*, *47*(6), 616–631. https://doi.org/10.1002/gj.2420

Slavík, L., Storch, P., Manda, S., & Fryda, J. (2014). Integrated stratigraphy of the Lufordian in the Prague Synform. *GFF*, *136*(1), 238–242. https://doi.org/10.1080/11035897.2013.851733

Spalletta, C., & Perri, M. C. (1993). Associazioni rimaneggiate a conodonti nei calcari micritici del Tournaisiano superiore (Alpi Carniche): Implicazioni sedimentologiche e paleoambientali. *Paleopelagos*, *3*, 141–153.

Spalletta, C., Perri, M. C., Over, D. J., & Corradini, C. (2017). Famennian (Upper Devonian) conodont zonation: Revised global standard. *Bulletin of Geosciences*, *92*, 31–57. https://doi.org/10.3140/bull.geosci.1623

Spalletta, C., Corradini, C., Feist, R., Korn, D., Kumpan, T., Perri, M. C., … Venturini, C. (2021). The Devonian/Carboniferous Boundary in the Carnic Alps (Austria and Italy). *Palaeobiodiversity and Palaeoenvironments*, *101*(2), 487–505. https://doi.org/10.1007/s12549-019-00413-3

Spiridonov, A., Brazauskas, A., & Radzevičius, S. (2016). Dynamics of abundance of the mid- to late Přídolí conodonts from the eastern part of the Silurian Baltic Basin: Multifractal, state shifts, and oscillations. *American Journal of Science*, *316*(4), 363–400. https://doi.org/10.2475/04.2016.03

Sun, Y. D., Liu, X. T., Yan, J. X., Li, B., Chen, B., Bond, D. P. G., … Lai, X. L. (2017). Permian (Artinskian to Wuchiapingian) conodont biostratigraphy in the Tieqiao section, Laibin area, South China. *Palaeogeography, Palaeoclimatology, Palaeoecology, 465(Part A)*, 42–63. https://doi.org/10.1016/j.palaeo.2016.10.013

Swade, J. W. (1985). Conodont distribution, paleoecology, and preliminary biostratigraphy of the upper Cherokee and Marmaton groups (upper Desmoinesian, middle Pennsylvanian) from two cores in south-central Iowa. *Iowa Geological Survey Technical Information Series*, *14*, 1–71. https://doi.org/10.17077/rep.006529

Sweet, W. C. (1970). Uppermost Permian and Lower Triassic Conodonts of the Salt Range and Trans-Indus Ranges, West Pakistan. In B. Kummel, & C. Teichert (Eds.), *Stratigraphic boundary problems: Permian and Triassic of West Pakistan* (pp. 207–275). Lawrence: University of Kansas.

Sweet, W. C. (1984). Graphic correlation of upper Middle and Upper Ordovician rocks, North American Midcontinent Province, U. S.A. In D. L. Bruton (Ed.), *Aspects of the Ordovician System* (pp. 23–35). Oslo: University of Oslo.

Sweet, W. C. (1988). *The Conodonta: morphology, taxonomy, paleoecology, and evolutionary history of a long-extinct animal phylum*. New York: Oxford University Press.

Sweet, W. C., & Bergström, S. M. (1984). Conodont provinces and biofacies of the Late Ordovician. *Geological Society of America. Special Paper*, *196*, 69–87. https://doi.org/10.1130/SPE196-p69

Sweet, W. C., & Donoghue, P. C. J. (2001). Conodonts: Past, present and future. *Journal of Paleontology*, *75*(6), 1174–1184. https://doi.org/10.1666/0022-3360(2001)075<1174:CPPF>2.0.CO;2

Sweet, W. C., Turco, C. A., Warner, E., Jr.,, & Wilkie, L. D. (1959). The American Upper Ordovician Standard. I. Eden Conodonts from the Cincinnati Region of Ohio and Kentucky. *Journal of Paleontology*, *33*, 1029–1068.

Sweet, W. C., Ethington, R. L., & Barnes, C. R. (1970). North American Middle and Upper Ordovician conodont faunas. *Geological Society of America Memoirs*, *127*, 163–193. https://doi.org/10.1130/MEM127-p163

Terrill, D. F., Jarochowska, E., Henderson, C. M., Shirley, B., & Bremer, O. (2022). Sr/Ca and Ba/Ca ratios support tropic partitioning within a Silurian conodont community from Gotland, Sweden. *Paleobiology*, *48*(4), 601–621. https://doi.org/10.1017/pab.2022.9

Thompson, T. L. (1993). *Paleozoic succession in Missouri, Part 3, Silurian and Devonian Systems* (pp. 1–214). Rolla, MO: Missouri Department of Natural Resources.

Tjernvik, T. (1952). Om de lägsta ordoviciska lagren i Närke. *Geologiska Föreningens i Stockholm Förhandlingar*, *74* (1), 51–70. https://doi.org/10.1080/11035895209454161

Trotter, J. A., & Eggins, S. M. (2006). Chemical systematics of conodont apatite determined by laser ablation ICPMS. *Chemical Geology*, *233*(3-4), 196–216. https://doi.org/10.1016/j.chemgeo.2006.03.004

Trotter, J. A., Korsch, M. J., Nicoll, R. S., & Whitford, D. J. (1999). Sr isotopic variation in single conodont elements: Implications for defining the Sr seawater curve. *Bollettino della Società Paleontologica Italiana*, *37*, 507–514.

Trotter, J. A., Williams, I. S., Barnes, C. R., Lécuyer, C., & Nicoll, R. S. (2008). Did cooling oceans trigger Ordovician biodiversification? Evidence from conodont thermometry. *Science*, *321*(5888), 550–554. https://doi.org/10.1126/science.1155814

Vacek, F., Slavík, L., Sobień, K., & Čáp, P. (2018). Refining the late Silurian sea–level history of the Prague Syncline – a case study based on the Přídolí GSSP (Czech Republic). *Facies*, *64*(4), 30. https://doi.org/10.1007/s10347-018-0542-3

Valenzuela-Ríos, J. I., & Murphy, M. A. (1997). A new zonation of middle Lochkovian (Lower Devonian) conodonts and evolution of *Flajsella* n. gen. (Conodonta). *Geological Society of America. Special Paper*, *321*, 131–144.

Valenzuela-Ríos, J. I., Slavík, L., Liao, J., Calvo, H., Husková, A., & Chadimová, L. (2015). The middle and upper Lochkovian (Lower Devonian) conodont successions in key peri-Gondwana localities (Spanish Central Pyrenees and Prague Synform) and their relevance for global correlations. *Terra Nova*, *27*(6), 409–415. https://doi.org/10.1111/ter.12172

Voges, A. (1959). Conodonten aus dem Unterkarbon I und II (*Gattendorfia*- und *Pericyclus*-Stufe) des Sauerlandes. *Paläontologische Zeitschrift*, *33*(4), 266–314. https://doi.org/10.1007/BF02987939

Voges, A. (1960). Die Bedeutung der Conodonten für die Stratigraphie des Unterkarbons I und II (Gattendorfia- und Pericyclus-Stufe) im Sauerland. *Fortschritte in der Geologie von Rheinland und Westfalen*, *3*(1), 197–228.

von Bitter, P. H., & Purnell, M. A. (2005). An experimental investigation of postdepositional taphonomic bias in conodonts. *Special Papers in Palaeontology*, *73*, 39–56.

von Bitter, P. H., Sandberg, C. A., & Orchard, M. J. (1986). Phylogeny, speciation, and palaeoecology of the Early Carboniferous (Mississippian) conodont genus *Mestognathus. Royal Ontario Museum Life Sciences Contributions*, *143*, 1–115. https://doi.org/10.5962/bhl.title.52223

Walliser, O. H. (1964). Conodonten des Silurs. *Abhandlungen der Hessischen Landesamtes Bodenforschung*, *41*, 1–106.

Wardlaw, B. R. (2000). Guadalupian conodont biostratigraphy of the Glass and Del Norte Mountains. *Smithsonian Contributions to the Earth Sciences*, *22*, 37–87.

Webers, G. F. (1966). The Middle and Upper Ordovician conodont fauna of Minnesota. *Minnesota Geological Survey Special Publication*, *4*, 1–123.

Wenzel, B., Lécuyer, C., & Joachimski, M. M. (2000). Comparing oxygen isotope records of Silurian calcite and phosphate–δ^{18}O compositions of brachiopods and conodonts. *Geochimica et Cosmochimica Acta*, *64*(11), 1859–1872. https://doi.org/10.1016/S0016-7037(00)00337-9

Wu, K., Tong, J., Metcalfe, I., Liang, L., Xiao, Y., & Tian, L. (2020). Quantitative stratigraphic correlation of the Lower Triassic in South China based on conodont unitary associations. *Earth-Science Reviews*, *200*, 102997. https://doi.org/10.1016/j.earscirev.2019.102997

Yin, H. F., Zhang, K. X., Tong, J. N., Yang, Z. Y., & Wu, S. B. (2001). The Global Stratotype Section and Point (GSSP) of the Permian-Triassic boundary. *Episodes*, *24*(2), 102–114. https://doi.org/10.18814/epiiugs/2001/v24i2/004

Yolkin, E. A., Weddige, K., Izokh, N. G., & Erina, M. V. (1994). New Emsian conodont zonation (Lower Devonian). *Courier Forschungsinstitut Senckenberg*, *168*, 139–157.

Yuan, D., Shen, S. Z., Henderson, C. M., Chen, J., Zhang, H., & Feng, H. Z. (2014). Revised conodont-based integrated high-resolution timescale for the Changhsingian Stage and end-Permian extinction interval at the Meishan sections, South China. *Lithos*, *204*, 220–245. https://doi.org/10.1016/j.lithos.2014.03.026

Yuan, D., Shen, S., & Henderson, C. M. (2017). Revised Wuchiapingian conodont taxonomy and succession of South China. *Journal of Paleontology*, *91*(6), 1199–1219. https://doi.org/10.1017/jpa.2017.71

Zhang, K. (1987). The Permo-Triassic conodont fauna in Changxing area, Zhejiang Province and its stratigraphic significance. *Earth Science Journal of Wuhan College of Geology*, *12*, 193–200.

Zhang, S., & Barnes, C. R. (2002). Paleoecology of Llandovery conodonts, Anticosti Island, Québec. *Palaeogeography, Palaeoclimatology, Palaeoecology*, *180*(1-3), 33–55. https://doi.org/10.1016/S0031-0182(01)00422-9

Zhang, S., & Barnes, C. R. (2004). Conodont bio-events, cladistics and response to glacio-eustasy, Ordovician-Silurian boundary through Llandovery, Anticosti Basin, Québec. *Geological Society of London Special Publications*, *230*(1), 73–104. https://doi.org/10.1144/GSL.SP.2004.230.01.05

Zhang, S., & Barnes, C. R. (2022). Late Ordovician (Katian) conodont community analysis and anoxic shallow water origin of organic-rich black shales, Red Head Rapids Formation, Southampton Island, Canadian Arctic. *Palaeogeography, Palaeoclimatology, Palaeoecology*, *592*, 110896. https://doi.org/10.1016/j.palaeo.2022.110896

Zhang, S., Mirza, K., & Barnes, C. R. (2016). Upper Ordovician – Upper Silurian conodont biostratigraphy, Devon Island and southern Ellesmere Island, Canadian Arctic Islands, with implications for regional stratigraphy, eustasy, and thermal maturation. *Canadian Journal of Earth Sciences*, *53*(9), 931–949. https://doi.org/10.1139/cjes-2016-0002

Zhao, L. S., Tong, J. N., & Orchard, M. J. (2005). *Study on the Lower Triassic conodont sequence and the Induan-Olenekian Boundary in Chaohu, Anhui Province* (pp. 58–80). Wuhan: China University of Geosciences Press.

Zhuravlev, A. V., Plotitsyn, A. N., Cigler, V., & Kumpan, T. (2021). Taxonomic notes on some advanced Tournaisian (Mississippian) siphonodellids (Conodonta). *Geobios*, *64*, 93–101. https://doi.org/10.1016/j.geobios.2020.12.001

Ziegler, W. (1962). Taxonomie und Phylogenie Oberdevonischer Conodonten und ihre stratigraphische Bedeutung. *Abhandlungen des Hessischen Landesamtes für Bodenforschung*, *38*, 1–166.

Ziegler, W. (1969). Eine neue Conodontenfauna aus dem höichsten Oberdevon. *Fortschritte in der Geologie von Rheinland und Westfalen*, *17*, 343–360.

Ziegler, W., & Sandberg, C. A. (1984). *Palmatolepis*–based revision of upper part of standard Late Devonian conodont zonation. *Geological Society of America. Special Paper*, *196*, 179–194.

Ziegler, W., & Sandberg, C. A. (1990). The Late Devonian Standard Conodont Zonation. *Courier Forschungsinstitut Senckenberg*, *121*, 1–115.

Manuscript received: December 01, 2023
Revisions required: January 31, 2024
Revised version received: March 11, 2024
Manuscript accepted: March 12, 2024